DESIGNING THE DYNAMICS OF COUPLED OSCILLATORS

Submitted by Bonnie Liefting, to the University of Exeter as a thesis for the degree of Doctor of Philosophy in Mathematics, December 2023.

I certify that all material in this thesis which is not my own work has been identified and that any material that has previously been submitted and approved for the award of a degree by this or any other University has been acknowledged.

Abstract

By designing coupling to control populations of oscillators, we can control their synchonisation behaviour. Oscillators (e.g. neurons) can be coupled on different levels. The most basic level is through links between pairs of oscillators. However, using graphs with only pairwise links is not necessarily a satisfactory approximation of reality as nonpairwise interactions can be found in many dynamical systems including social networks and the human brain. Even though the effects of these nonpairwise interactions have been observed, described and modeled in a wide range of oscillatory systems, controlling nonpairwise interactions in arbitrary populations of oscillators has remained a relatively unexplored area. In this thesis we generalise synchronisation engineering to control nonpairwise interactions in arbitrary systems. We designed a nonlinear time-delayed coupling that can be used to match the phase reduction of a system of oscillators to a target phase model. The contribution of this thesis is allowing for nonpairwise interactions in the target phase model. We used an optimisation proceidure to find coupling parameters to match a nonpairwise target phase model that has the collective behaviour we aim to introduce to the system We found that we need one additional filter to find the parameter sets that match the bifurcation of both in-phase and splay configuration in to the nonpairwise target phase model.

Acknowledgements

Five years ago on a sunny spring afternoon my train arrived in Exeter and I got to climb up a hill. On a terrace on top of the hill Christian Bick was waiting for me. We were having the first of many chats in which Chris' enthusiasm for nonpairwise interactions got a chance to spread. Kyle Wedgwood soon joined all of our meetings, adding some strong nonpairwise interactions to the collaboration that became this thesis. I'm thankful for having had such dedicated supervisors.

During the final stages of my project I was welcomed by Kristian Debrabant at SDU. I'm thankful for Kristian being an invaluable mentor once again.

I'm thankful for my colleagues in Exeter and Odense. In particular I appreciate the guidance and support from Peter Aswhin and Paul Ritchie.

It took some time for me to appreciate the beauty of nonpairwiseness. I remember thinking during those first chats with Kyle and Chris that it seemed strange that they were talking so passionately about something that surely was not much more than a change of notation. I'm thankful to have had the opportunity to find out how wrong I was.

It remains for me to thank my family, friends and others I met along the way. I thank Anders, Stan and Ella in particular for their curiosity, support and for just being there.

Contents

Nomenclature

δ	Right hand side of inequality constraints for the optimisation ($\delta \ll 1$)
$\Delta\tau$	General delay bifurcation parameter in the target phase models
ϵ	Coupling / perturbation strength
κ_s	Gain coupling parameters for pairwise target models
κ_{pq}	Gain coupling parameters for nonpairwise target models
ω	Natural frequency of an oscillator
ψ_ℓ	Phase difference $\theta_\ell - \theta_N$
τ_s	Delay coupling parameters for pairwise models
τ_{pq}	Delay coupling parameters for nonpairwise models
θ_ℓ	Phase of oscillator ℓ
A, B	Parameters in the Brusselator model
a_l	Fourier coefficients of the waveform $x(\theta_j)$
F	A function in the Brusselator model
f	Nonlinear function defining the vector field of an oscillator
g	Pairwise or nonpairwise coupling function
g_l	Fourier coefficient of the pairwise coupling function
g_{lm}	Fourier coefficient of the nonpairwise coupling function

H Pairwise or nonpairwise target interaction function

H_l Fourier coefficient of the pairwise target interaction function

H_{lm} Fourier coefficient of the nonpairwise target interaction function

i Imaginary unit ($\sqrt{i} = -1$)

j, k, ℓ Indices of (phase) oscillators (j being the current oscillator)

l, m Indices of Fourier coefficients

N Number of oscillators in the population

P A perturbation / coupling function

p, q Powers in the coupling function g for nonpairwise models

S Overall order of the (pairwise and nonpairwise) coupling

s Power in the coupling function g for pairwise models

$x(\theta_j)$ Waveform in the first variable at phase θ_j of oscillator j

X, Y Concentrations of species in the chemical model of the Brusselator

Z Phase response curve in the first variable of a nonlinear oscillator

Z_l Fourier coefficient of the phase response curve Z

$\mathbf{x}$ Nonlinear oscillator variables

$\mathbf{x}_1^j$ (and $\mathbf{x}_2^j$) First (and second) variable of the Brusselator j

$\mathbf{Z}$ Phase response curve of a nonlinear oscillator

Code Availability

As part of this thesis, a significant amount of Matlab code was created. We included some details and instructions to run the code in Appendix C. We made the code available for the sake of future research here:

https://github.com/liefting/sync_engineering

List of Figures

Introduction

Many living systems consist of rhythmically moving elements and require the presence of synchronisation to maintain vital biological functions [Kiss, 2018]. Examples of such biological functions in mammals are the sleep/wake cycle [Winfree, 2002], neuronal information processing in the brain [Pikovsky et al., 2001], the waves of muscular contraction in the intestines [Pikovsky et al., 2001] and the heart beating [Boyett et al., 2000]. When the amount or type of synchronisation in such living systems is suboptimal, interventions might be required to maintain the affected biological functions [Kiss, 2018].

In this thesis, we control the collective behaviour of a type of rhythmic element known as oscillators. An oscillator has the property that it sustains its movement, a movement that keeps following and repeating the same path when undisturbed. When weak disturbances are coming from the control we apply, then the oscillator follows and keeps repeating a similar path.

In this thesis, we propose a method to design nonpairwise interactions to control the collective behaviour of a population of arbitrary oscillators. We generalise an existing method known as synchronisation engineering [Kori et al., 2008, Kiss, 2018]. Synchronisation engineering has so far only been used to design coupling where the interaction between the oscillators is a summation of sinusoids of pairwise differences [Kori et al., 2008, Rusin et al., 2009, Rusin et al., 2010, Kiss et al., 2007a, Kiss, 2018].

We conjecture that controlling nonpairwise interactions may advance the design of minimum-power stimuli for the treatments using neurostimulation. [Battiston et al., 2020].

Examples of interventions to control the collective behaviour of living systems

are sleep medication, electronic heart pacemakers, and neurostimulation [Rusin et al., 2010]. In neurostimulation, it remains a challenge to determine the necessary stimuli to reduce symptoms of for example Parkinsons disease [Schiff, 2010], epilepsy and essential tremours [Rusin et al., 2010].

We are interested in designing weak coupling to adjust the frequencies of the oscillations. By doing so, we can introduce synchrony and other types of collective behaviour to populations of oscillators that otherwise would not admit this behaviour, or apply the control to sustain a collective behaviour that broke down by error. An example of applying control to populations of oscillators that failed to produce the desired synchronous behaviour is using neurostimulation in the treatment of Parkinsons disease [Schuepbach et al., 2013].

A convenient property of the synchronisation engineering method is that it is not specific to a particular type of oscillator. We use some already widely used properties of oscillators as an input to the method. There are different ways to derive these properties (waveform and phase response curve) for different types of oscillators.

The first step in applying our method is to decide what collective behaviour we want to introduce to the system of oscillators. Then we need to choose a phase model that admits this behaviour. Phase models are often used to study different types of collective behaviour. We could for example study the stability of in-phase synchronisation in a particular phase model, and find out under which conditions in-phase synchronisation loses its stability.

The next step in designing the coupling uses a phase reduction of the system of oscillators that we want to control. A phase reduction is similar to a phase model, but it is derived from a system of nonlinear oscillators. Phase reductions can also be used to study the stability of in-phase synchronisation and other types of collective behaviour. Findings on the collective behaviour of a phase reduction can then be used to understand the specific behaviour of the original system. We are interested in going one step further and using the phase reduction to design the coupling to control the collective behaviour of the original system.

We decided on a form of coupling that includes several parameters. The values of those coupling parameters are decided by scaling the parameterised coupling using a phase response curve and then comparing it to the target phase model we chose previously.

Recall that the goal is to introduce a type of collective behaviour to the system of oscillators and that we chose a nonpairwise target phase model that has this desired collective behaviour. In the process, we used the waveform and the phase response curve of the oscillators we want to control. Now we need to find the coupling parameters such that the phase reduction matches the target phase model. We do this by matching the Fourier coefficients of the target phase model and the phase reduction. Then we use the coupling parameters we found and apply the coupling to the original system.

This thesis is organised as follows. Chapter 1 is a collection of preliminaries including definitions of oscillators, (asymptotic) phase and phase response curves. In Chapter 1 we also introduce the chemical oscillator and the phase interaction functions that we will use when we demonstrate the control in Chapters 2, 3 and 4. In Chapter 2 we reproduce some results on classical pairwise synchronisation engineering.

Chapters 3 and 4 contain novel material describing and demonstrating the nonpairwise coupling that we propose. In Chapter 3 we introduce the form of the nonpairwise coupling and derive the constraints needed to find coupling parameter sets. In Chapter 4 we find coupling parameter sets for a specific target interaction function and type of chemical oscillator, and then run simulations using these parameters. We used a target collective behaviour using a nonpairwise target phase model (1.32,1.33), whose bifurcation points for in-phase and splay configuration in a system of Brusselators correspond to the bifurcation points for the controlled Brusselators. In Chapter 5 we discuss and speculate about directions to continue this research.

Chapter 1

Interacting oscillators and synchronisation

In this chapter, we go over a variety of preliminaries. We give some mathematical background on oscillators in Section 1.1, and define how to describe an oscillator by a single phase variable in Section 1.2. In Section 1.3 we introduce the more general concept of asymptotic phase, which is used to describe perturbed oscillators in terms of a single (asymptotic phase) variable. In Section 1.4 we look at interacting oscillators and their phase reduction. In Section 1.5 we discuss different types of synchronisation, and in Section 1.6 we introduce order parameters to analyse different types of collective behaviour. In Section 1.7 we discuss interaction functions. We introduce a pairwise interaction function in Section 1.8, and a nonpairwise interaction function in Section 1.9 that we will use to demonstrate our method. In Section 1.10 we give some background on the chemical oscillator model that we will apply the control to in our demonstration, and in Section 1.11 we calculate its phase response curve. We conclude this chapter with an overview of control approaches in Section 1.12.

1.1 Oscillators

Many physical, chemical and biological systems exhibit rhythmic oscillatory behaviour. When external perturbations do not influence such a system, it behaves

periodically and keeps repeating itself. This periodicity can be found in nature in the beating of hearts, in gait patterns, in planets and other bodies rotating around each other or their own axis [Strogatz, 2003, Winfree, 2002, Pikovsky et al., 2001].

We consider systems that evolve in time in a deterministic manner [Broer and Takens, 2011]. We use differential equations to describe these dynamical systems. We consider (deterministic) dynamical systems of the form

$$\frac{d\mathbf{x}}{dt} = \mathbf{f}(\mathbf{x}), \qquad \mathbf{x} \in \mathbb{R}^n \qquad \text{where } n \geq 2, \tag{1.1}$$

where $\mathbf{f} : V \to \mathbb{R}^n$ is a smooth function defined on a subset $V \subseteq \mathbb{R}^n$. Note that the dynamical system is autonomous, e.g. $\mathbf{f}$ does not explicitly depend on time t. In this thesis, we only consider $n = 2$ dimensional dynamical systems, but the theory below holds for general $n \geq 2$ [Moehlis et al., 2006].

When a solution to Equation 1.1 is constant in time, this is a stationary solution of the dynamical system. Another possible type of solution to Equation 1.1 is a periodic solution.

Definition 1. (Periodic solution / closed orbit) A *periodic solution* (or *closed orbit*) is a solution $\gamma \in \mathbb{R}^n$ of a dynamical system (1.1) such that $\gamma(t) = \gamma(t + T)$ for any $t \in \mathbb{R}$, for some $0 < T < \infty$ [Guckenheimer and Holmes, 1983].

This is a function that after a fixed period returns to the same state and keeps repeating the same trajectory.

When talking about periodic solutions, it is convenient to consider the time it takes before the solutions repeat themselves again.

Definition 2. (Period) The *period* of a periodic solution is the minimal $T > 0$ such that $\gamma(t) = \gamma(t + T)$.

We are often interested in looking at one repetition of the periodic solution in state space.

Definition 3. (Cycle / periodic orbit) The *cycle* (or *periodic orbit*) is the trajectory of a periodic solutions of (1.1) in state space ($\mathbb{R}^n$) at $[0, T]$ [Moehlis et al., 2006].

It is possible for a periodic solution γ to attract other solutions [Hirsch et al., 2013]. This means that in the limit of $t \to \infty$, a solution of (1.1) approaches the periodic solution γ.

Definition 4. (ω-limit set) For a system of differential equations, a point $\mathbf{y} \in \mathbb{R}^n$ is an ω-limit point for the solution through $\mathbf{x}$ if the solution curve through $\mathbf{x}$ accumulates on the point $\mathbf{y}$ as $t \to \infty$. The *ω-limit set* $\omega(\mathbf{x})$ is the set of all ω-limit points [Hirsch et al., 2013].

The α-limit set of $\mathbf{x}$, $\alpha(\mathbf{x})$, is defined similar to the ω-limit set, but instead going backwards in time (e.g. replacing $t \to \infty$ by $t \to -\infty$ in the definition above).

Definition 5. (Limit cycle) [Hirsch et al., 2013] A *limit cycle* is a periodic solution (or periodic orbit) $\gamma \in \mathbb{R}^n$ such that $\gamma \subset \omega(\mathbf{x})$ or $\gamma \subset \alpha(\mathbf{x})$ for some $\mathbf{x} \notin \gamma$.

A periodic solution is not necessarily a limit cycle. A property of a limit cycle is that it is an isolated closed orbit [Strogatz, 1994]. This means that neighbouring orbits either spiral towards or away from the limit cycle. A limit cycle is stable when all neighbouring orbits approach the limit cycle [Strogatz, 1994].

We require a stronger type of stability known as asymptotic stability. To determine the stability of a point, we linearise the system and find the eigenvalues of the Jacobian at this point [Holmes and Shea-Brown, 2006]. If its eigenvalues have strictly negative real parts, then the point is asymptotically stable. For a periodic orbit, if the Poincaré map of a point on the periodic orbit is asymptotically stable, then the periodic orbit is asymptotically stable [Moehlis et al., 2006].

For autonomous dynamical systems (1.1), an oscillator is defined as follows.

Definition 6. (Oscillator) An *oscillator* is an n-dimensional ($n \geq 2$) dynamical system (1.1) that has an asymptotically stable limit cycle.

1.2 Phase

The state of oscillation can be characterised by a phase that describes where the oscillator is on the limit cycle. A common use of phase descriptions to describe

the state of a system with oscillatory behaviour is the 24-hour clock. The earth takes about 24 hours to rotate around its own axis, e.g. it has a period T of 24 hours. How far along the earth is in this rotation can be described by stating the time on your clock.

Definition 7. (**Phase**) A *phase* of a point $\mathbf{x}_0$ on the periodic orbit γ is the time θ since the last passing of an arbitrarily chosen point $\bar{\mathbf{x}}_0 \in \gamma$ on the periodic orbit.

We will normalize the phase by $T/2\pi$. The arbitrarily chosen point $\bar{\mathbf{x}}_0 \in \gamma$ corresponds to zero phase. The choice of this initial point results in different parametrizations that are equivalent up to a constant phase shift. Choosing $\bar{\mathbf{x}}_0$ would correspond to choosing which timezone to use in our 24-hour clock analogy. A common choice for $\bar{\mathbf{x}}_0$ in oscillations involving a pronounced peak such as regularly spiking neurons is take a maximum as the zero phase point $\bar{\mathbf{x}}_0$.

Definition 8. (**Phase representation**) The *phase representation* of (1.1), where the phase evolves uniformly on cycle, is given by

$$\frac{d\theta}{dt} = \omega, \qquad \theta \in \mathbb{S}^1, \tag{1.2}$$

where $\omega = 2\pi/T$ is called the *natural frequency* of the oscillator, and $\mathbb{S}^1$ is the unit circle.

1.3 Phase reduction

A phase reduction is a phase description of an oscillator that takes into account how the particular oscillator responds to other external perturbations. Consider regularly spiking neurons, a type of oscillator that has spikes in its membrane potential at regular time intervals. If the neuron is close enough to spiking when receives an external perturbation, then this perturbation could make the neuron spike earlier. However, that same perturbation to the same neuron, but at a different time during its cycle (e.g. right after it spiked) could instead not have any effect on the timing of the next spike.

Thus depending on where it is in its cycle, a (neuronal) oscillator can respond differently to a perturbation. To define more precisely what we mean with phrases such as “is about to spike” and “has just spiked”, we use the concept of phase as described in Section 1.1. A phase response curve captures these differences in response depending on the phase at which the perturbation is applied.

Different types of oscillators respond differently to external perturbations. One oscillator might respond more strongly to a perturbation at a certain phase than another oscillator would. However, in this thesis, we consider populations of oscillators that are identical, and thus we scale the perturbations in the same way for all oscillators when we write the populations in terms of the oscillators' phases.

We now add a perturbation term to the dynamical system defined by Equation 1.1

$$\frac{d\mathbf{x}}{dt} = \mathbf{f}(\mathbf{x}) + \varepsilon\, \mathbf{P}(\mathbf{x}, t), \qquad \mathbf{x} \in \mathbb{R}^n, \tag{1.3}$$

where the perturbation $\varepsilon\, \mathbf{P}(\mathbf{x}, t)$ is scaled by a small strength parameter $0 < \varepsilon \ll 1$. We assume that the unperturbed system (1.1), e.g. (1.3) with $\varepsilon = 0$, has an asymptotically stable limit cycle.

The perturbation moves the trajectory away from the limit cycle γ of the unperturbed system (1.1). However, because the perturbation is small, and the limit cycle is stable, the trajectory only slightly deviates from the limit cycle.

To include the effect of external perturbations in the phase representation of the oscillator, we will extend the definition of phase to points close to the limit cycle γ of the unperturbed oscillator (1.1). Let $\mathbf{y}_0 = \mathbf{y}(0)$ be a point in $\mathbb{R}^n$, and $\mathbf{y}(t)$ its trajectory according to (1.1). If this trajectory $\mathbf{y}(t)$ approaches the limit cycle as $t \to \infty$, then the initial point $\mathbf{y}_0$ is said to be in the *basin of attraction* of the limit cycle. To all points in the basin of attraction we can assign an asymptotic phase.

To introduce the concept of phase for points that are not on the limit cycle $\mathbf{y}_0 \notin \gamma$, we find the point on the limit cycle $\mathbf{x}_0 \in \gamma$ for which the asymptotic behaviour of its trajectory $\mathbf{x}(t)$ is indistinguishable from that of $\mathbf{y}(t)$.

Definition 9. (Asymptotic phase) The *asymptotic phase* θ of a point $\mathbf{y}_0$ in the basin of attraction of a limit cycle γ is the phase of the point $\mathbf{x}_0 \in \gamma$ for which

$$\mathbf{y}(t) \to \mathbf{x}(t), \qquad \text{as } t \to \infty. \tag{1.4}$$

For every point $\mathbf{x}_0 \in \gamma$, we can find all the points $\mathbf{y}_0 \notin \gamma$ in the basin of attraction that have the same asymptotic phase as $\mathbf{x}_0$.

Definition 10. (Isochrones) An *isochron* is a set of points $\mathbf{y}_0$ that have the same asymptotic phase.

The isochron of $\mathbf{x}_0$ is the *stable manifold* of $\mathbf{x}_0$. The concept of asymptotic phase allows us to reduce the weakly perturbed system (1.3) in terms of a single phase variable. To do this, we need a way to scale the perturbation $\mathbf{P}(\mathbf{x}, t)$ in (1.3) to obtain the corresponding change in the (asymptotic) phase. The size of the phase shift resulting from a perturbation depends on the amplitude of the perturbation as well as the timing of the perturbation. A perturbation that moves the trajectory from one isochron to another, changes the (asymptotic) phase.

Definition 11. (Phase response curve in the first component) [Brown et al., 2004] A *phase response curve* $\hat{Z}_a(\theta)$ of an oscillator (1.1) for perturbation in the first component is given by

$$\hat{Z}_a(\theta) = \frac{\Delta\theta}{a}, \tag{1.5}$$

where $\Delta\theta = [\theta(\mathbf{x}^\lambda + (a, 0, 0, \ldots, 0) - \theta(\mathbf{x}^\lambda)]$ is the change in asymptotic phase $\theta(\mathbf{x})$ after applying a perturbation a to the first coordinate $\mathbf{x}_1$ of a point $\mathbf{x}^\lambda$ on limit cycle λ of oscillator (1.1).

Definition 12. (Infinitesimal phase response curve in the first component) An *infinitesimal phase response curve* is given by

$$Z(\theta) = \lim_{a \to 0} Z_a(\theta). \tag{1.6}$$

Phase response curves are used to reduce a perturbed oscillator described by the rate of change of $n \geq 2$ variables (1.3) to a representation of the oscillator by the rate of change in its (asymptotic) phase. We will only consider oscillators that are perturbed in their first variable. Phase reduction theory holds however more generally.

Definition 13. (Infinitesimal phase response curve) For an n dimensional oscillator (1.1) we can find its phase response curves using perturbations in separately in all variables rather than just to x_1 in Definition 11 to obtain the $\mathbf{Z}(\theta) \in \mathbb{R}^n$.

Definition 14. (**Phase reduction**) The (first order) *phase reduction* of a weakly perturbed oscillator (1.3) is given by

$$\frac{d\theta}{dt} = \omega + \varepsilon\, \mathbf{Z}(\theta)\mathbf{P}(\mathbf{x}(\theta), t). \tag{1.7}$$

Recall that $\frac{d\theta}{dt} = \omega$ is the phase representation of the unperturbed oscillator (1.1). The phase response curve $\mathbf{Z}(\theta)$ is used to scale the perturbations $\varepsilon\mathbf{P}(\mathbf{x}, t)$.

We will show how to obtain approximations of an *infinitesimal phase response curves* for different types of oscillators. Note that when we consider *phase response curves*, we are referring to infinitesimal phase response curves. Depending on the type of oscillator different methods might be necessary to obtain approximations to their phase response curves. The *direct method* [Izhikevich, 2005] that we will use for example, requires that we can perturb the oscillator at specific times in its cycle and wait each time to observe its asymptotic behaviour. When it is not possible to isolate and perturb an oscillator in this way, one can instead consider methods that derive phase response curves by observing oscillators in its natural environment [Cestnik and Rosenblum, 2018, Galán et al., 2010, Mori and Kori, 2022, Ota et al., 2009].

1.4 Phase interacting oscillators

The interactions between periodically moving systems can lead to different types of synchronisation in their periodic movements. Synchronisation happens at many scales and there is a wide variety in the way that different oscillators and other periodically moving systems interact. Our moon for example has synchronised the rotation around its axis with its rotation around the earth [Strogatz, 2003]. This can be seen from Earth in that we always see only one side of the moon.

Natural systems on Earth have synchronised to the different periodic movements of the Earth as well. The periodicity with which the Earth is rotating around its axis as well as around the sun can be observed from Earth. On most of the surface of the Earth, the rotation around the Earth's axis leads to periods of light (during the day) as well as periods of darkness (at night). Many species on earth (including most people) have synchronised their internal clock to these light and darkness periods in terms of their sleep-wake cycle. Similarly, many species (excluding humans) have synchronised their breeding cycles to the rotation of the Earth around the sun. For example, leading vertebrates to produce offspring during certain yearly seasons [Winfree, 2002, Chapter 19].

We defined an oscillator (Definition 1.1) and defined the phase reduction both for an unperturbed (Definition 1.2) and a weakly perturbed 1.3 oscillator. Now we look into populations of interacting oscillators. We consider a population of N oscillators of the form (1.3) with phase reduction (1.7) where the perturbation $\epsilon \mathbf{P}(\mathbf{x}, t)$ defines the interaction between oscillators $j = 1, 2, \ldots, N$. We can write the phase reduction of a population of N interacting oscillators as follows:

$$\frac{d\theta_j}{dt} = \omega_j + \varepsilon\, \mathbf{Z}(\theta) \cdot \mathbf{P}(\mathbf{x}^1(\theta_1), \mathbf{x}^2(\theta_2), \ldots, \mathbf{x}^N(\theta_N), t), \tag{1.8}$$

where $\mathbf{x}_j(\theta_j)$ are the waveforms of oscillator j at the phase θ_j.

We can imagine phase oscillators as joggers running on a track [Strogatz,

2003]. Each of them is running at their own natural frequency ω_j in the absence of interaction. Suppose that some of the joggers have a faster pace than the others, then the faster joggers will keep overtaking the slower ones as they run around the track.

Alternatively, we could model a more friendly group of joggers who instead of just running at their own pace, will try to run together. In that case, we need the faster joggers to slow down a bit instead of overtaking the others, and perhaps the slower joggers should speed up a bit. We want them to interact and adapt their pace depending on where the other joggers are.

When the jogger (or oscillators in general) start interacting with each other, their collective behaviour becomes interesting. Friendly joggers often end up in some sort of synchronised rhythm.

1.5 Types of synchronisation

When describing synchronous behaviour, we distinguish between phase and frequency synchronisation. When we say oscillators are synchronised in phase, we mean that the phases and frequencies of those oscillators are the same and remain the same over time. Your sleep-wake rhythm, for example, is most likely approximately synchronised in phase with the people around you (who are awake around the same times as you). Around the world, people tend to have a 24-hour sleep-wake cycle and are thus synchronised in frequency. However, there would for example be a phase difference (of approximately 1 hour) between the sleep-wake cycles of people living in Amsterdam and those living in Exeter.

The synchronisation can be global or local. Global synchronisation is over the entire network meaning that all oscillators in the system synchronise. Local synchronisation means that only a subset of the oscillators are synchronised to each other, while the other oscillators are not synchronised to the oscillators from that subset.

Apart from global phase and frequency synchronisation, many more types

of synchronous behaviour have been observed in natural systems as well as in mathematical models. Localised synchronisation includes collective behaviour like clustering [Okuda, 1993], Chimera states [Abrams and Strogatz, 2004] and travelling waves [Lanford and Mintchev, 2015].

A population of oscillators is (phase) clustered when it is divided into two or more (phase) synchronised groups. A Chimera state appears when some of the oscillators are synchronised while the others are not synchronised.

Research into phase models [Strogatz, 2000, Kuramoto, 1984, Acebrón et al., 2005] helps determine what properties of the interaction (or "coupling") between the oscillators are responsible for different types of synchronisation.

1.6 The order parameter

When we have access to the (asymptotic) phases of a system of oscillators, we can use a measure of phase (cluster) synchronisation called the Kuramoto-Daido order parameters [Kuramoto, 1984, Daido, 1993]. The order parameters are given by

$$R_c(t) = \left| \frac{1}{N} \sum_{n=1}^{N} e^{ic\theta_n(t)} \right|, \qquad , \tag{1.9}$$

where $c \geq 1$ is integer.

When considering the oscillators as points on the unit circle with angles equal to their phases θ, each oscillator at time t is represented by the point $e^{-i\theta_n(t)}$ in the complex plane.

Kuramoto's original order parameter $R_1(t)$ measures how close the population is to in-phase synchronisation. Taking the average $\frac{1}{N}\sum_{n=1}^{N} e^{-i\theta_n(t)}$, can give an idea of the degree of in-phase synchronisation between the oscillators $n = 1, 2, \ldots, N$ [Strogatz, 2003]. The quantity $\frac{1}{N}\sum_{n=1}^{N} e^{-i\theta_n(t)}$ is also referred to as the complex Kuramoto order parameter [Pietras and Daffertshofer, 2019], but here we refer to the amplitude $R_c(t)$ when we talk about the order parameter.

In Figure 1.1 we show 10 possible configurations (labelled A to J) of $N = 4$

Figure 1.1: Different configurations (labelled A-J) of $N = 4$ phase oscillators (filled circles) on a unit cycle together. A line between the origin of the unit circle represents the first order parameter R_1. The absolute values of the order parameters R_c for $c = 1, 2, 3, 4$ are shown to the right of each configuration.

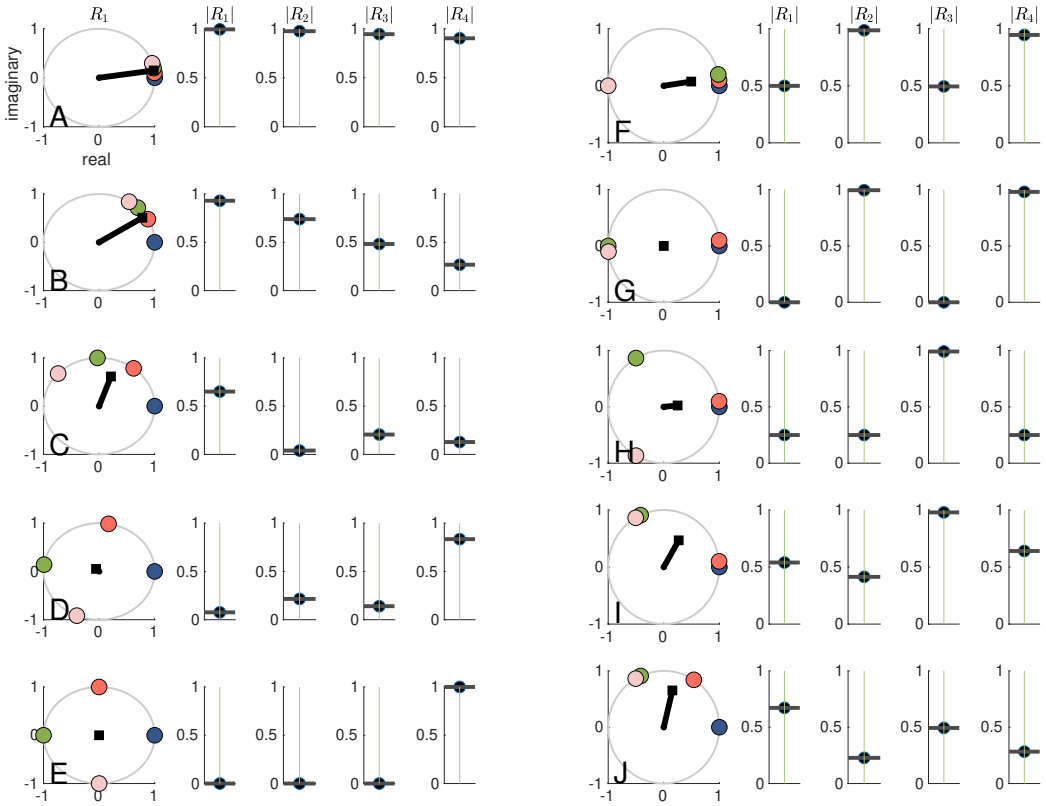

phase oscillators using coloured circles on top of the unit circle. The value of the first order parameter is plotted on top of the unit circle using a line from the origin to R_1. For all order parameters R_c with $c = 1, 2, 3, 4$ we also plotted the absolute values $|R_c|$.

Figure 1.1, configuration A shows a configuration close to the in-phase configuration: All oscillators have a similar phase. The absolute value of the first order parameter $|R_1| \approx 1$. Configurations B is further away from in-phase and $|R_1|$ goes further away from 1 as expected. Notice how $|R_1|$ decreases further as the oscillators spread out further over the unit circle in configurations C-D. In configuration E (called splay configuration), the oscillators are spread out evenly over the unit circle, and $|R_1| = 0$.

When the oscillators are in splay configuration, then $|R_1| = 0$, but the other

way around $|R_1| = 0$ does not imply that the oscillators are in splay configuration. For $N = 4$ oscillators, we can have for example configuration G (close to anti-phase configuration), where $|R_1| = 0$ even though the oscillators are not in splay configuration. To distinguish between anti-phase configuration and splay configuration for $N = 4$ oscillators, we can take the second order parameter into account as $|R_2|$ equals 0 for splay configuration and 0 for anti-phase configuration.

Notice how for configuration E, the corresponding absolute value of the fourth order parameter $|R_4| = 1$. For $N = 4$ oscillators, splay configuration implies $|R_4| = 1$. However, the other way around $|R_4| = 1$ does not imply that the oscillators are in splay configuration. Figure 1.1, configuration F also has a corresponding absolute value of the fourth order parameter $|R_4| \approx 1$ even though this is not slay configuration. When we compare configuration E and F, we notice that for splay configuration (E), $|R_1| = |R_2| = |R_3| = 0$ while for configuration F $|R_1| \approx 0.5$, $|R_2| \approx 1$, and $|R_3| = 0.5$. Similarly, we can use the value of $|R_2|$ to distinguish between anti-phase configuration (G) and splay configuration (E).

The order parameter $R_1(t)$of a system of oscillators equals 1 if and only if the phases of all oscillators are equal. If the order parameter has a value of 1 for all t, this implies that the oscillators are in-phase synchronised. When the order parameter $R_1(t)$ approaches 1, then this indicates that the oscillators are approaching the state of in-phase synchronisation. The general order parameter $R_c(t)$ can be used to study the stability of balanced c-cluster states. To study the stability of splay configuration, we use that when 4 oscillators are divided into 4 clusters with phases spread uniformly, then for the fourth order parameter $|R_4(t)| = 1$ while $R_c = 0$ for $c < 4$.

We will be interested in shifting the stability of in-phase synchronisation in Chapter 3. We apply our control on a system of oscillators starting close to in-phase synchronisation and use the order parameter $R_1(t)$ converging or not converging to 1 as a measure of in-phase synchronisation being stable or not. Similarly, we study the stability of the splay configuration (or 4-cluster state) of 4 oscillators using $R_4(t)$. Since in-phase synchrony as well as anti-phase configu-

ration would also give an $R_4(t)$ order parameter of 1, we rule those two configurations out by checking that $R_1(t)$ and $R_2(t)$ are small.

1.7 Interaction functions

The rate of change of phase $\dot{\theta}_\ell$ in a phase model is a sum of the oscillators' natural frequencies ω_ℓ and a coupling term. We consider phase models for which the coupling term is made up of phase interaction functions H that take one or more phase differences as their input. We scale by the number of oscillators N in the population such that systems with different N are comparable. We assume that the (pairwise) phase interactions sum linearly:

$$\frac{d\theta_j}{dt} = \omega_j + \frac{\epsilon}{N}\sum_{\ell=1}^{N} H(\theta_\ell - \theta_j) \qquad \text{for } j = 1, 2, \ldots, N. \tag{1.10}$$

Increasing the coupling strength ϵ from 0 can lead to interesting changes in the collective behaviour. In the Kuramoto model for example, where the interaction function $H(\theta_\ell - \theta_j) = \sin(\theta_\ell - \theta_j$ and the frequencies ω_j are unimodally distributed, increasing the coupling strength ϵ leads to a sudden change in collective behaviour [Kuramoto, 1984, Acebrón et al., 2005, Strogatz, 2000].

When the coupling strength ϵ is increased past the critical coupling the oscillators suddenly all move around the circle with the same frequency and in the limit of time $t \to \infty$ with the same phase as well.

Such a sudden change in collective behaviour that happens while changing a parameter is an example of a bifurcation. In the case of the Kuramoto model, the critical value of ϵ at which this bifurcation occurs can be found exactly when we look at the limit of infinitely many oscillators, $N \to \infty$. When considering other distributions of the natural frequencies of the oscillators, the critical coupling can be different. In contrast to Kuramoto's analysis, we will consider a finite number of oscillators, fixed coupling strength ϵ and identical oscillators.

Another important difference with the Kuramoto model is that we consider non-

pairwise interaction functions which take more than one phase difference as their input. An interaction function $H(\theta_\ell - \theta_j)$ describes the impact of each pair, each triplet, etc. on the instantaneous frequency. When we consider a phase model with an interaction function $H(\theta_\ell - \theta_j, \theta_k - \theta_j)$ that takes two phase differences as its input, it can be written as follows.

$$\frac{d\theta_j}{dt} = \omega_j + \frac{\epsilon}{N^2} \sum_{\ell=1}^{N} \sum_{k=1}^{N} H(\theta_\ell - \theta_j, \theta_k - \theta_j) \qquad \text{for } j = 1, 2, \ldots, N. \tag{1.11}$$

When the interaction function is positive, this increases the frequency with which the phase oscillator is moving. If it is negative, it will slow the oscillator down. And if it is zero, then that particular phase difference does not affect the oscillator's frequency.

An interaction function can be oscillator dependent and define the interaction for each pair or group using for example adjacency matrices. In our joggers example, this could mean that joggers Kyle and Chris are more motivated to run together than the other joggers are. We however consider global isotropic coupling, modelling i.e. joggers who all are equally motivated to run together with each of the other joggers.

A common modelling decision is to choose the interaction function such that it is zero when the oscillators have the same phase. In our joggers example, this would mean that if two of the joggers are already at the same place on the track, then their interaction does not make them change their frequency. If there are more joggers on the track, those other joggers can of course still influence the frequencies of the two joggers that happened to already be at the same place on the track. Recall that ω_j is the natural frequency of the oscillator and that its frequency is also affected by the interactions.

Note that two oscillators having the same phase (e.g. "being in the same place on the track") does not imply that they are moving with the same frequency. Two oscillators also briefly have the same phase when one of them is overtaking the other one. In that case, the faster oscillator is first sped up by the one in front and

then slowed down by the other oscillator after it has overtaken it.

1.8 A pairwise interaction function

In this section, we introduce a phase model with only pairwise interactions. We will use this model as a target phase model to determine the coupling. In Section 1.9 we will use an adaptation of this phase model that includes nonpairwise interactions.

The phase model we introduce here has an interaction function with a first harmonic and a second harmonic:

$$H(\theta_\ell - \theta_j) = \sin(\theta_\ell - \theta_j + \Delta\tau) + 0.5\sin(2(\theta_\ell - \theta_j + \Delta\tau)), \tag{1.12}$$

with the general phase delay bifurcation parameter $\Delta\tau$.

We denote the phase difference as $\psi_j = \theta_j - \theta_N$ for oscillators $j = 1, 2, \ldots, N-1$. We write this interaction function as follows, and will consider (1.12) with $N = 2$ oscillators in the following [Rusin et al., 2010].

$$H(\psi_\ell) = \sin(\psi_\ell + \Delta\tau) + 0.5\sin(2(\psi_\ell + \Delta\tau)) \tag{1.13}$$

There exists a range of $\Delta\tau$ that result in stable solutions with a phase difference that is not 0 or π. For $N = 2$ oscillators, a pairwise phase difference of 0 means that both oscillators are at the same location, while a phase difference of π corresponds to the two oscillators being at opposite locations, or in splay configuration. We look at the relation between $\Delta\tau$ and the resulting pairwise phase difference.

Since nonpairwise interactions will require more than $N = 2$ oscillators if we do not want them to be reduced to pairwise interactions, we find the values of $\Delta\tau$ again for $N = 4$ in Section 1.9.

We write Equations 1.10 for $N = 2$ oscillators in terms of the phase difference

$\psi_1 = \theta_1 - \theta_2$ and follow the bifurcation analysis from [Rusin et al., 2010]:

$$\frac{d\psi_1}{dt} = \omega_1 - \omega_2 + \frac{\epsilon}{2}[H(-\psi_1) - H(\psi_1)]. \tag{1.14}$$

Defining the odd part H^- of the interaction function as

$$2H^-(\psi_1) = H(\psi_1) - H(-\psi_1), \tag{1.15}$$

we can rewrite Equation 1.14 to

$$\frac{d\psi_1}{dt} = \omega_1 - \omega_2 - KH^-(\psi_1). \tag{1.16}$$

Figure 1.2: Convergence of $R_1(t)$ to 1 (in-phase configuration). We plot $\log(1 - R_1)$ for different overall delays $\Delta\tau$.

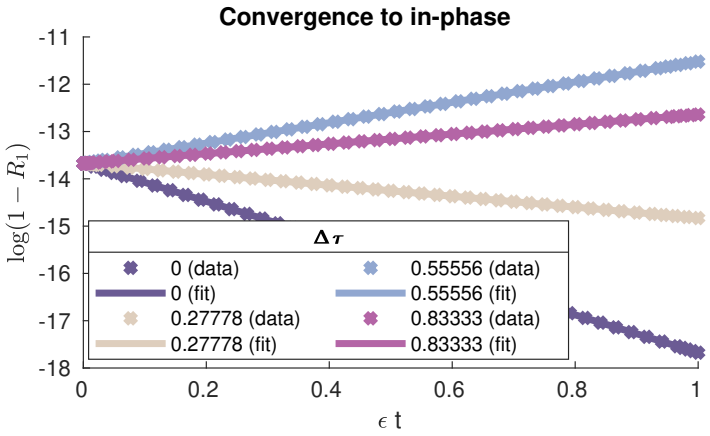

We can find the stability of the in-phase solutions by calculating the Jacobian of

$$\frac{d\theta_j}{dt} = \omega + \frac{\epsilon}{N}\sum_{\ell=1}^{2} H(\theta_\ell - \theta_j) \qquad \text{for } j = 1, 2 \tag{1.17}$$

at $\theta \in \mathbb{R}^2$ such that $\theta_1 = \theta_2$.

This Jacobian is given by

$$J = \begin{pmatrix} -H'(\theta_2 - \theta_1 + \Delta\tau) & H'(\theta_1 - \theta_2 + \Delta\tau) \\ H'(\theta_2 - \theta_1 + \Delta\tau) & -H'(\theta_1 - \theta_2 + \Delta\tau) \end{pmatrix} \tag{1.18}$$

Figure 1.3: Convergence of $R_1(t)$ to 1 (in-phase configuration). We plot the slopes of $\log(1 - R_1(t))$ for a range of different $\Delta\tau$'s (green line) to confirm the in-phase bifurcation. The dots correspond to the data shown in Figure 1.2.

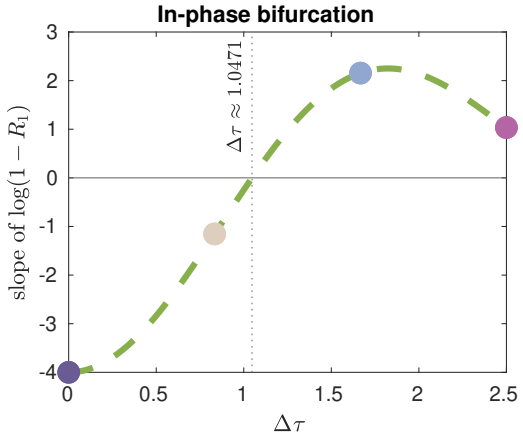

and at $\theta = (\theta_1, \theta_1)$:

$$J_{\theta_{\text{in-phase}}} = \begin{pmatrix} -H'(\Delta\tau) & H'(\Delta\tau) \\ H'(\Delta\tau) & -H'(\Delta\tau) \end{pmatrix}. \tag{1.19}$$

Obtaining the characteristic (with λ the eigenvalue and I the identity matrix)equation:

$$\det(J_{\theta_{\text{in-phase}}} - \lambda I) = 0 \tag{1.20}$$

$$2\lambda H'(\Delta\tau) + \lambda^2 = 0. \tag{1.21}$$

Thus $\lambda = 0$ or $\lambda = -2H'(\Delta\tau)$. Hence the in-phase solution is stable for $H'(\Delta\tau) > 0$ [Rusin et al., 2010], though not hyperbolic.

Calculating the actual value for (1.12), we find:

$$H'(\Delta\tau) > 0 \tag{1.22}$$

$$\cos(\Delta\tau) + \cos(2\Delta\tau) > 0, \tag{1.23}$$

such that on the interval $0 < \Delta\tau < \pi$, in-phase will be stable for

$$0 < \Delta\tau < \frac{\pi}{3} \approx 1.0471. \tag{1.24}$$

We can confirm this bifurcation by simulating the phase model (1.10) with target interaction function (1.12) using e.g. Matlabs *ode45*. We run simulations for different $\Delta\tau$ and calculate the order parameter $R_1(t)$. Figure 1.2 shows a plot of $\log(1 - R_1(t)$ versus scaled time ϵt for 4 different values of $\Delta\tau$ as well as a line fitted to the data for each simulation. When we plot the slopes of these lines for a range of $\Delta\tau$, we obtain the curve shown in Figure 1.3. The slopes of the 4 lines shown in Figure 1.2 are plotted in Figure 1.3 as dots.

Negative slopes indicate convergence of the order parameter $R_1(t)$ towards 1, while a positive slope indicates divergence. At the point where the curve crosses the horizontal axis, the stability of in-phase (with $R_1(t) \approx 1$) changes. Figure 1.3 confirms that the in-phase configuration for simulated phase oscillators with interaction function given by (1.12 loses stability around $\Delta\tau = \frac{\pi}{3} \approx 1.0471$ as found using the Jacobian above.

Figure 1.4: Convergence of R_2 to 1 (splay configuration). We plot the slopes of $\log(1 - R_2(t))$ to confirm the splay bifurcation.

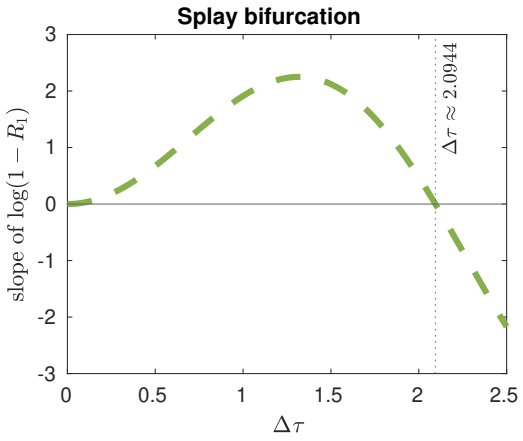

To study the stability of splay configuration, we check the conditions for pitchfork bifurcations [Strogatz, 1994].

We check the following list of conditions:

$$-\epsilon H^-(\Delta\theta) = KH^-(-\Delta\theta) \Rightarrow \text{ odd} \tag{1.25}$$

$$-\epsilon\frac{dH^-}{d\Delta\theta}(\pi, 2\pi/3) = 0 \tag{1.26}$$

$$-\epsilon\frac{d^2H^-}{d\Delta\theta^2}(\pi, 2\pi/3) = 0 \tag{1.27}$$

$$-\epsilon\frac{d^3H^-}{d\Delta\theta^3}(\pi, 2\pi/3) = -1.5\epsilon \neq 0 \tag{1.28}$$

$$-\epsilon\frac{dH^-}{d\Delta\tau}(\pi, 2\pi/3) = 0 \tag{1.29}$$

$$-\epsilon\frac{d^2H^-}{d\Delta\theta\Delta\tau}(\pi, 2\pi/3) = \frac{3}{2}\sqrt{3} \neq 0 \tag{1.30}$$

We confirm a supercritical pitchfork bifurcation at $(\psi_1, \Delta\tau) = (\pi, 2\pi/3)$. It followed from condition (1.28) that the pitchfork bifurcation is supercritical as the right-hand side is negative for coupling strengths $\epsilon > 0$. Thus at $\Delta\tau = \frac{2\pi}{3} \approx 2.0944$ splay configuration (or antiphase for $N = 2$) becomes stable through a pitchfork bifurcation. On the interval $0 < \Delta\tau < \pi$, splay configuration will be stable for

$$2.0944 \approx \frac{2\pi}{3} < \Delta\tau < \pi. \tag{1.31}$$

Similar to the in-phase bifurcation, we confirm the bifurcation of splay configuration at $\Delta\tau \approx 2.0944$ by running simulations of the phase model with interaction function 1.12 for $N = 2$ oscillators for a range of $\Delta\tau$'s around the expected bifurcation. We use the second order parameter $R_2(t)$ as we expect this order parameter to approach 1 for the splay configuration of two oscillators. Figure 1.4 shows the slopes of the lines fitted to $\log(1 - R_2(t))$ from simulations starting close to splay configuration for different $\Delta\tau$'s. We observe that the slope changes from negative to positive around $\Delta\tau = \frac{2\pi}{3} \approx 2.0944$, confirming the analytic result.

Choosing $\Delta\tau$ as a parameter will be convenient since in the classical synchronisation (see Chapter 2) as well as in our generalisation (see Chapter 3) the coupling will be designed in such a way that we can vary a general delay like $\Delta\tau$ after having found the coupling parameters. This means that we find the coupling parameters for one specific $\Delta\tau$ (we chose $\Delta\tau = 0$ for convenience). Changing the

general delay $\Delta\tau$ in the designed coupling afterwards corresponds to changing the $\Delta\tau$ in the target phase model (though scaled by the natural frequency ω).

1.9 A nonpairwise interaction function

Instead of only considering interactions that take information from only two oscillators, we could consider a connection that takes information from three or more oscillators to determine its strength. This type of nonpairwise interaction also appears in real-world systems [Bick et al., 2023b]. We call these types of interactions *nonpairwise*. In nonpairwise interactions, information from three or more oscillators is combined in a not necessarily additive manner. Even though pairwisely coupled oscillators can also receive information from three or more oscillators, that information was always combined in an additive manner.

When studying and controlling complex systems it is crucial to understand the interactions between the many individual components that make up the system. Traditionally, complex systems have been understood as networks that represent interactions as coupling between pairs of components. To describe biological, social, ecological and other real-world systems, many have added different types of details to these pairwise couplings. The coupling can for example be weighted, directed, or even changing over time [Battiston et al., 2020, Porter, 2020].

Even though many propositions have been made to add more details to the components as well as the pairwise coupling between them, there's a fundamental limitation in trying to describe complex systems using only pairwise coupling. In terms of networks, group interactions can partly be represented by using multiple layers to describe different types of interactions [Porter, 2020], or by using bipartite graphs that allow only for interactions between nodes of different "types" [Newman et al., 2001]. More natural ways have been developed to describe connections between more than two components, for example in terms of simplicial complexes and hypergraphs [Battiston et al., 2020, Porter, 2020, Torres et al., 2021]. As we will only consider global isotropic interactions, we are not es-

Figure 1.5: Examples of networks described with nodes, edges and hyperedges. (a) A network with strictly pairwise coupling is represented by edges. (b) A similar network to (a), but now including a three-way connection represented by a hyperedge. (c) A network with all possible pairwise and three-way connections.

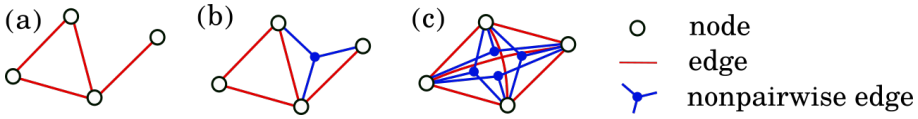

pecially interested in using hypergraphs or simplicial complexes to describe the interactions. Hypergraphs can be used to visualise networks in which not certain pairs, triplets, etc. of oscillators interact, while other pairs triplets, etc. of oscillators do not interact. Simplicial complexes can also be used to visualise which oscillators interact with each other and have the additional property that a nonpairwise interaction between certain oscillators implies that all other possible (non)pairwise configurations of interactions are also present between these oscillators.

We visualise $N = 4$ interacting oscillators using (hyper)graph theory in Figure 1.5 to show what we mean by global isotropic interactions. Nodes are depicted by open circles. A pairwise coupling between two oscillators is represented by an edge depicted by a line between two nodes. Figure 1.5(a) is a visual representation of a set of nodes that are connected by (pairwise) edges. In Figure 1.5(b) there is a 3-way nonpairwise interaction present. In this section (and in Chapter 3) we will consider network structures of the type shown in Figure 1.5(c), where all possible combinations of pairwise and three-way nonpairwise interactions are present.

This section introduces a nonpairwise interaction function that we will use as a target phase model. We choose the target phase model such that it (1) has a tunable overall delay $\Delta\tau$, (2) has the same pairwise terms as the pairwise interaction function (1.12), and (3) has different collective behaviour after including the nonpairwise term.

This third point means that we need to make sure that we have a way to measure the effects of the nonpairwise behaviour. We decided on adding a nonpair-

Figure 1.6: A shift in the bifurcation of in-phase configuration for 4 phase oscillators with target the nonpairwise (1.32 and pairwise (1.12) functions. A negative slope of $\log(1 - R_1)$ indicates convergence to in-phase.

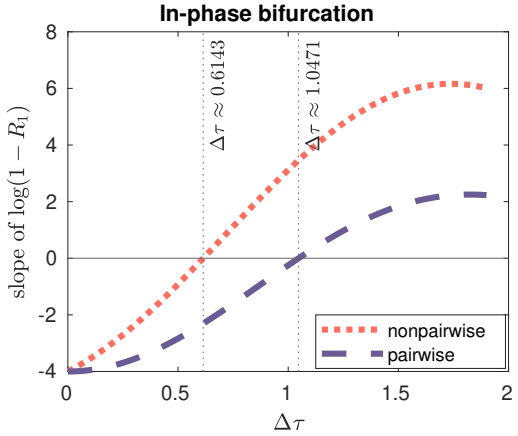

Figure 1.7: No shift in the bifurcation of in-phase configuration for 4 phase oscillators with target the nonpairwise (1.32 and pairwise (1.12) functions. A negative slope of $\log(1 - R_4)$ can indicate convergence to splay.

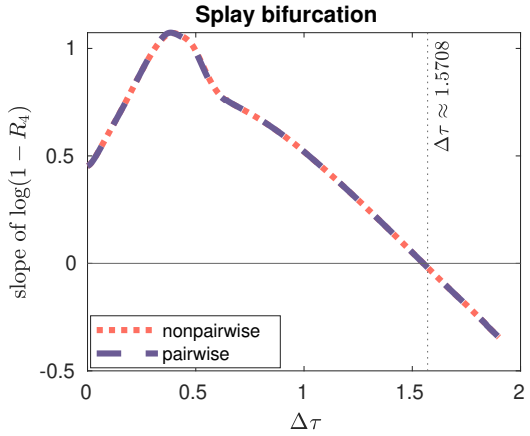

wise term that makes the system less synchronisable, i.e. makes the in-phase synchronisation lose stability at a smaller value of $\Delta\tau$ than for the pairwise target interaction function.

Our aim is to find a target phase model for which we can observe a change in collective behaviour when we add the nonpairwise interactions, and observe the same change when we use it as a target model. We consider the nonpairwise

interaction function

$$H(\theta_\ell - \theta_j, \theta_k - \theta_j) = \overbrace{\sin(\theta_\ell - \theta_j + \Delta\tau) + 0.5\sin(2(\theta_\ell - \theta_j + \Delta\tau))}^{\text{pairwise}} \underbrace{+ \cos(\theta_\ell + \theta_k - 2\theta_j + \Delta\tau)}_{\text{nonpairwise}}. \tag{1.32}$$

To find out how this nonpairwise cosine term changes the stability of the in-phase solution, we consider the population of $N = 4$ oscillators

$$\frac{d\theta_j}{dt} = \omega + \frac{\epsilon}{16}\sum_{\ell=1}^{4}\sum_{m=1}^{4} H(\theta_\ell - \theta_j, \theta_m - \theta_j) \qquad \text{for } j = 1, 2, \ldots, 4. \tag{1.33}$$

with the nonpairwise interaction function H given by 1.32.

The eigenvalues of the Jacobian of this system for the in-phase solution (e.g. where $\theta_1 = \theta_2 = \theta_3 = \theta_4$) were computed by Bick, Ashwin and Rodrigues [Bick et al., 2016]. We find[1] that in-phase oscillations bifurcate at

$$2\sin(\Delta\tau) - \cos(\Delta\tau) - \cos(2\Delta\tau) = 0. \tag{1.34}$$

This equation has solutions $\Delta\tau \approx 0.6142904 + 2\pi n$ and $\Delta\tau \approx \pi + 2\pi n$ for any integer n. We are interested in the bifurcation around $\Delta\tau \approx 0.6142904$. On the interval $0 < \Delta\tau$, in-phase synchronisation is stable for

$$0 < \Delta\tau \lessapprox 0.6142904, \tag{1.35}$$

while for $0.6142904 \lessapprox \Delta\tau < \pi$ it is unstable (see Figure 1.6).

When considering only the pairwise terms that appear in the interaction function (1.32), then the in-phase oscillations lose stability when:

$$\cos(\Delta\tau) + \cos(2\Delta\tau) = 0. \tag{1.36}$$

And on the interval $0 < \Delta\tau < \pi$ in-phase oscillations in the pairwise case are

[1] In the notation from [Bick et al., 2016], the target phase model described by (1.32) is given by taking $\xi = (1, \frac{1}{2}, 1, 0, 0)$, $\chi = (-\frac{\pi}{2} + \Delta\tau, -\frac{\pi}{2} + \Delta\tau, \Delta\tau, 0, 0)$. We use their "Equation 15" (for the stability of in-phase configuration) and their "Equation 19" (for the stability of splay configuration).

stable for

$$0 < \Delta\tau < \frac{\pi}{3} \approx 1.0472 \tag{1.37}$$

and unstable for $\frac{\pi}{3} < \Delta\tau < \pi$ (see Figure 1.6). Note that the values of $\Delta\tau$ at which these bifurcations for the pairwise model occur differ from those found in Section 1.8. This change in collective behaviour is due to increasing the number of oscillators from $N = 2$ to $N = 4$.

When we compare the pairwise and the nonpairwise interaction function discussed above, then the range of $\Delta\tau$ for which the in-phase oscillations are stable differs. For the phase model with only pairwise terms, in-phase configuration loses stability at $\Delta\tau \approx 1.05$, while for the model with interaction function (1.32) that also includes nonpairwise terms, in-phase configuration already loses stability at $\Delta\tau \approx 0.61$.

We also find that the phase model (1.33) with interaction function (1.32) has a steady bifurcation of splay configuration at

$$-\cos(\Delta\tau) = 0 \tag{1.38}$$

which does not depend on the nonpairwise term in (1.32) [Bick et al., 2016]. This means that both the nonpairwise (1.32) and the pairwise (1.12) interaction functions produce target phase models with a bifurcation of splay configuration at (1.38). From equation 1.38 we find the relevant solution to be $\Delta\tau = \frac{\pi}{2} \approx 1.5708$. On the interval $0 < \Delta\tau < \pi$, splay configuration for $N = 4$ oscillators is stable for

$$1.5708 \approx \frac{\pi}{2} < \Delta\tau < \pi \tag{1.39}$$

for the pairwise and nonpairwise target phase models (see Figure 1.7) discussed in the current and the previous section.

We would like the coupling to introduce the above bifurcations for in-phase and splay to a system of nonlinear oscillators to the system of oscillators. In Section 1.10 we introduce the nonlinear oscillator that we will use to demonstrate

our control design on in this thesis.

1.10 A chemical oscillator

This section gives some background on the Brusselator and the chemical reaction that forms the basis for the model. We demonstrate how to obtain a phase response curve by finding a Brusselators PRC in Section 1.11. We will use this model throughout to demonstrate the coupling control we design later on as well.

For a long time it was thought that chemical reactions would monotonically approach an equilibrium state [Strogatz, 1994]. Therefore oscillating reactions discovered by Belousov did not get much attention at first. He had problems with getting such unexpected and unbelievable results published. When Zhabotinsky reproduced the results years later and started to again communicate the results, it was finally believed and picked up by other scientists that chemical reactions can approach equilibrium in an oscillatory manner [Strogatz, 2003].

The Belousov-Zhabotingsky (BZ) reaction is a family of related oscillatory chemical reactions that are commonly used to study collective behaviour, e.g. pattern formation, of coupled oscillatory systems [Epstein, 2014]. Usually, the BZ reaction consists of a malonic acid (an acid naturally found in many fruits) that is oxidated using a strong oxidising agent (such as bromide) and a catalyst (a metal) in a solution of a strong acid (such as sulphuric or nitric acid) [Epstein, 2014]. The concentrations of several species in the BZ reaction then increase and decrease (almost) periodically. These oscillations can continue for hundreds of cycles, where each cycle lasts a few minutes [Epstein, 2014]. Even though the oscillatory behaviour dies out eventually, the BZ reaction having nearly oscillatory behaviour for a relatively long time makes it an attractive chemical reaction for studying synchronisation patterns. This reaction is also the subject of many popular science videos which is probably due to its colourful oscillation (patterns) that change the liquid from orange to blue, back to orange and so on.

The actual BZ reaction consists of many different species having periodically

varying concentrations of species. We consider an idealised oscillatory chemical reaction called the Brusselator that has the chemical reactions

$$A \to X \tag{1.40}$$

$$2X + Y \to 3X \tag{1.41}$$

$$B + X \to Y + C \tag{1.42}$$

$$X \to D, \tag{1.43}$$

between chemical species A, B, C, D, X, and Y. It is assumed that all rate constants are 1, meaning that all reactions occur at the same rate. We are interested in the change of the concentrations of X and Y. These concentrations are denoted as $[X]$ and $[Y]$, and the change of concentrations by $\frac{d}{dt}[X]$ and $\frac{d}{dt}[Y]$.

To find the equation for the total rate of change $\frac{d}{dt}[X]$, we first look at each of the chemical reactions (1.40-1.43) where X occurs either on the left-hand side (causing a decrease in $[X]$), or on the right-hand side (causing an increase in $[X]$). Assuming that A and B are held constant, chemical reaction (1.40) implies that species X increases with constant rate depending on the concentration of $[A]$ of species A. By the Law of Mass Action, this gives the differential equation $\frac{d}{dt}[X] = [A]$, or in the dimensionless form:

$$\frac{d}{dt}X = A. \tag{1.44}$$

Similarly, chemical reaction 1.41 causes an increase in concentration of X described by $\frac{d}{dt}[X] = 3[X]^2[Y]$, or in dimensionless form:

$$\frac{d}{dt}X = 3X^2Y. \tag{1.45}$$

Chemical reaction 1.41 also causes a decrease the concentration of X since X appears on the left-hand side as well. This decrease is described by $\frac{d}{dt}[X] =$

$-2[X]^2[Y]$, or in dimensionless form:

$$\frac{d}{dt}X = -2X^2Y. \tag{1.46}$$

All of these changes in concentration of X can be added up to obtain the total rate of change of concentration of X due to chemical reactions (1.40-1.43). Adding the right hand sides of (1.44), (1.45), and (1.46):

$$\frac{d}{dt}X = A + 3X^2Y - 2X^2Y - BX - X \tag{1.47}$$

$$= A + X^2Y - (B+1)X. \tag{1.48}$$

Similarly, from chemical reactions 1.41 and 1.42, we obtain the dimensionless differential equation for the rate of change of concentration of species Y:

$$\frac{d}{dt}Y = BX - X^2Y. \tag{1.49}$$

Equations 1.47 and 1.49 together describe the oscillatory chemical reaction of the Brusselator for certain constants A and B.

The system (1.47-1.49) has a fixed point (found by setting $\frac{d}{dt}X = 0$, $\frac{d}{dt}Y = 0$) at $(X, Y) = (A, \frac{B}{A})$. This fixed point becomes unstable at the critical concentration of B, $B_c = 1 + A^2$. When the concentration of B becomes larger than $1 + A^2$, this causes the birth of a periodic orbit through a supercritical Hopf bifurcation. That means that the concentrations of X and Y start oscillating around the (now unstable) fixed point.

1.11 Deriving a phase response curve

In the previous section we introduced the Brusselator, which is an oscillator that for certain parameter values takes on a limit-cycle oscillation. We derived its equations in terms of concentrations X and Y. Changing notation to x_1 and x_2 for

the remainder of this thesis, the equations for the Brusselator oscillator are

$$\frac{dx_1}{dt} = (B-1)x_1 + A^2 x_2 + F(x_1, x_2) \tag{1.50}$$
$$\frac{dx_2}{dt} = -Bx_1 - A^2 x_2 - F(x_1, x_2), \tag{1.51}$$

where $F(x,y) = \frac{B}{A}x^2 + 2Axy + x^2 y$. Setting parameters $A = 1.0$, $B = 2.3$ results in the oscillator admitting a limit-cycle oscillation since $B = 2.3 > 1 + A^2 = B_c$ (see Section 1.10). We only use these parameters in this thesis.

In this section we derive the phase reduction (see Definition 1.3) of a population of interacting Brusselators. Recall that this requires deriving the phase response curve of the oscillator. We are interested in applying perturbations only to the x_1 variable of the Brusselator (1.50,1.51). Thus we need to find its phase response curve Z in the x_1-direction.

A Brusselator (1.50,1.51) with a perturbation applied to its x-variable can be written as

$$\frac{dx_1}{dt} = (B-1)x_1 + A^2 x_2 + F(x_1, x_2) + \epsilon P(t) \tag{1.52}$$
$$\frac{dx_2}{dt} = -Bx_1 - A^2 x_2 - F(x_1, x_2), \tag{1.53}$$

where $0 < \epsilon \ll 1$ is the perturbation strength (or coupling strength when the perturbations come from other oscillators in the population). Recall that the phase reduction (see Definition 1.3) of this system is given by

$$\frac{d\theta}{dt} = \omega + \epsilon Z(\theta) P(t). \tag{1.54}$$

When considering oscillators such as the Brusselator that can easily be modelled and simulated many times, a phase response curve can be obtained using the direct method. The direct method is based on perturbing the oscillator many times at different phases in its cycle. For a range of phases between 0 and 2π we run simulations and measure how much the oscillator has gone forward (or backwards) in phase compared to the unperturbed oscillator. We do this by taking the

difference in time between the third maxima after the time of perturbation of the perturbed and unperturbed trajectory and scaling by the perturbation size.

In Figure 1.9 a perturbation is applied at $t = 10$ and the third peak of the unperturbed trajectory is marked with a red circle, while the third peak of the perturbed trajectory is marked with a blue circle. An approximation for a phase response curve is obtained by scaling each difference (between the perturbed and unperturbed oscillator) by the size of the perturbations. By decreasing the size of the perturbation, and repeating this for phases $[0, 2\pi]$ the curve obtained in this way converges to the phase response curve. The phase response curve (in the x_1-direction) $Z(\theta)$ that we obtained for the Brusselator oscillator is shown in Figure 1.10.

When the model of the oscillator is available, then an alternative method to find the PRC is by solving the linear adjoint equation [Izhikevich, 2005]. The program XPPAUT implements computation of the adjoint of the linearisation around a stable limit cycle [Ermentrout, 2007]. To find the adjoint using XPPAUT we first find the periodic orbit and set the integration time to one period. XPPAUT can then compute the adjoint-based on the periodic data. Figure 1.10 compares the PRCs or the Brusselator obtained using the direct method and the adjoint method. There also exist methods to infer phase response curves from noisy data such as in [Cestnik and Rosenblum, 2018].

We now consider a population of $N = 4$ identical Brusselators that are coupled through a perturbation function $P(x_1^1, x_1^2, x_1^3, x_1^4, , t)$ that is applied to and takes information from the first variable x_1^j of each of the Brusselator oscillators $j = 1, 2, 3, 4$. We write this population of oscillators as

$$\frac{dx_1^j}{dt} = (B-1)x_1^j + A^2 x_2^j + F(x_1^j, x_2^j) + \epsilon P(x_1^1, x_1^2, x_1^3, x_1^4, t) \tag{1.55}$$

$$\frac{dx_2^j}{dt} = -Bx_1^j - A^2 x_2^j - F(x_1^j, x_2^j), \qquad \text{for } j = 1, 2, 3, 4. \tag{1.56}$$

The population of Brusselators (1.55,1.56) has the phase reduction

$$\frac{d\theta_j}{dt} = \omega + \epsilon Z(\theta_j) \cdot P(x(\theta_1), x(\theta_2), x(\theta_3), x(\theta_4), t), \qquad \text{for } i = 1, 2, 3, 4, \tag{1.57}$$

where $x(.)$ is the waveform of the first variable x_1^j of the unperturbed Brusselator oscillator (1.50,1.51) shown in Figure (1.10 (left)) and the phase response curve $Z(\theta)$ is shown in Figure 1.10 (right). Figure 1.8 shows the limit cycle together with several equally spaced isochrons (see Definition 10) of the Brusselator. Restricting our description of a nonlinear oscillator by using its phase as the only variable, implies that we are losing some of the systems information.

It is important to realise that the collective dynamics of a phase reduction are not necessarily equivalent to the dynamics of the system of weakly coupled nonlinear oscillators. However, the dynamics of phase reductions can be analytically tractable. It can be used as a tool to understand the behaviour of a system that can otherwise not be studied in a straightforward manner.

Phase response curves can be used in different ways to control collective behaviour. In Section 1.12 we discuss some control methods that use phase response curves to put synchronisation engineering into perspective.

Figure 1.8: Isochrons and limit cycle of a Brusselator oscillator.

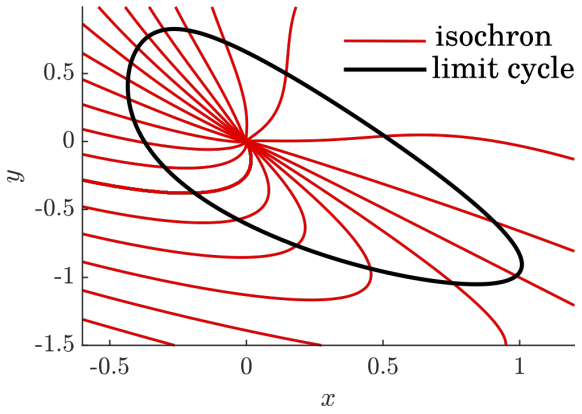

Figure 1.9: Demonstration of the direct method to obtain a phase response curve of a Brusselator oscillator. The red trajectory shows the x_1 variable of a few periods of a Brusselator oscillator. The blue trajectory shows the same oscillator, but after a perturbation at $t = 10$. We use the difference in time of the third maxima after the perturbation (marked with circles) to calculate each point of the PRC. For illustrative purposes the perturbation here is quite large, but we decreased the size of the perturbation to better approximate the infinitesimal PRC (1.6)

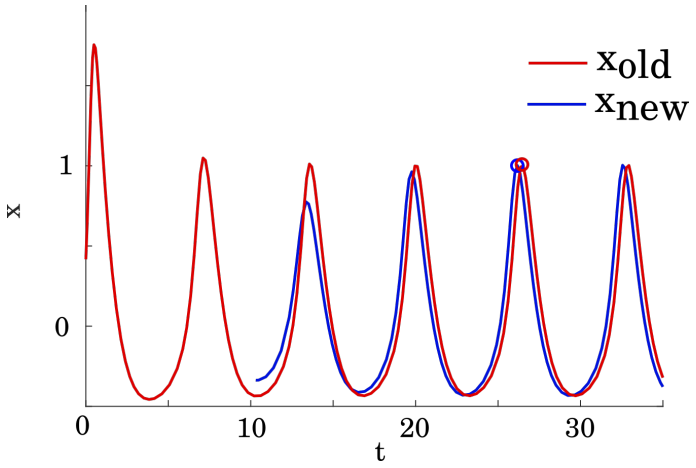

1.12 Controlling synchronisation

There are different approaches to controlling networks of oscillators. A common approach in engineering applications is based on the ability to change how the oscillators in the system respond to external impulses, including impulses from other oscillators [Gao and Wang, 2017, Wang et al., 2013, Proskurnikov and Cao, 2017, Wang and Doyle, 2012, Li et al., 2013]. Particularly for applications concerning biological and chemical oscillators, controlling how the oscillator responds to external perturbations might be difficult as we cannot easily manipulate intracellular processes. An alternative approach is to control the connections between the oscillators themselves instead.

To illustrate the difference, consider the following two examples. Our first example is on controlling the synchronisation between power plants that are connected in a utility power grid [Rohden et al., 2012]. In such a system the power plants correspond to the oscillators and they should be synchronised to the same frequency to avoid blackouts occurring. In such a system it is more convenient to engineer the way in which the power plant adjust its frequency than to add,

Figure 1.10: A waveform and phase response curve of a Brusselator oscillator. They are derived using different methods, and there is a difference in phase resulting in two approximations of different phase response curves for the same Brusselator oscillator. Waveform in the x-direction (left) and a phase response curve in the x-direction (right) of a Brussalator oscillator (1.50,1.51) with $A = 1.0$, $B = 2.3$.

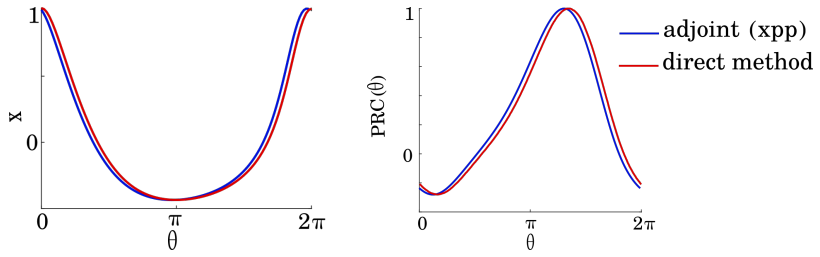

remove or change transmission lines.

Our second example concerns pacemaker cells in the heart [Boyett et al., 2000]. In this case, we again would like the oscillators (the pacemaker cells) to synchronise their phase and frequency. When the pacemaker cells synchronise, they give a unified signal to the muscles in the heart to contract. When the synchronisation fails, then this signal is not strong enough and the muscles do not contract sufficiently strong to pump enough blood around. The most convenient way to get these oscillators (pacemaker cells) to synchronise again is to introduce an external signal (in the form of an electronic pacemaker).

We are interested in designing what signals such a pacemaker would have to give to control collective behaviour. Although we are not designing control specific to the rhythmic cells in the heart, this is one of the motivations for designing this type of control. In biological applications, it is an advantage to use types of control that are weak because it is desirable to destroy individual biological elements. We will use properties of the rhythmic elements that only hold when the control we apply to them is weak.

Controlling synchronisation is a problem in many disciplines, and different methods have been developed depending on the application. The synchronisation engineering method [Kori et al., 2008] that we are generalising has been shown to work using electrochemical experiments [Rusin et al., 2010]. Therefore we look into some different control methods for chemical systems to put synchro-

nisation engineering into perspective.

One control problem is that of stabilising synchronisation (patterns) in systems where they are unstable in the absence of control. One approach to control such behaviour is to design coupling to increase the excitability of the system. This can be done locally as shown experimentally by for example [Sakurai et al., 2002], who measure the excitability in their medium using image processing and then, at each time step, determine and introduce the desired excitability at each pixel to guide the travelling waves. Another approach is to stabilise unstable waves using global feedback to reach a minimal excitability in the medium, and then apply a second feedback loop to control the motion of the travelling wave [Mihaliuk et al., 2002]. Another approach to stabilise unstable synchronisation (patterns) in subexcitable media is through stochastic resonance [Wiesenfeld and Moss, 1995]. Waves that would otherwise die out in chemical media are shown to propagate under the effect of noise applied to the whole system, indicating noise plays a role in wave propagation in chemical and biological systems [Mikhailov and Showalter, 2006].

Another problem is the control of synchronisation (patterns) in media that already exhibit stable oscillatory behaviour. Phase reduction techniques have been used before to control the behaviour of the original oscillatory system. The next spiking time of neurons in vitro can be controlled by writing the phase reduction as a Hamiltonian system and applying optimal control theory techniques [Nabi et al., 2013]. Particular properties of phase response curves have been used to determine the optimal phases to apply bursts of stimuli to control beta oscillations for the treatment of Parkinsons disease: The phase for which according to the PRC gives the largest perturbation [Azodi-Avval and Gharabaghi, 2015], and the phase(s) for which the positive slope of the PRC is the largest [Holt et al., 2016].

These control methods focus on changing the timing of the spiking of a single neuron or a single cluster of neurons. Their goal is to introduce behaviour which is not full synchrony, and their approach is to focus on a particular part of the system (a neuron or a cluster of neurons) to change the phase of that part such

that it is not synchronised with the rest anymore. The synchronisation engineering approach [Kori et al., 2008] we generalise, takes a particular different type of collective behaviour and introduces that to the system, rather than only breaking up a behaviour without having a specific target behaviour in mind.

Chapter 2

Synchronisation engineering

In this chapter we review results on synchronisation [Kori et al., 2008, Rusin et al., 2010] and introduce the concept of synchronisation engineering. Thus far we looking at how to describe a population of weakly coupled nonlinear oscillators (1.55,1.56) by its phase reduction (Equation 1.57). If we now change the coupling function $P(t)$ in the original system, this of course changes the behaviour of its phase reduction. We can try to pick the coupling function in such a way that the systems phase reduction has some particularly interesting behaviour. We consider a method to find the desired coupling function $P(t)$ in a structured manner [Kori et al., 2008, Rusin et al., 2016, Bick et al., 2017] in the next Section.

Synchronisation engineering is a method to control the synchronisation of a population of oscillators by introducing a global delayed coupling signal to the population [Kori et al., 2008, Rusin et al., 2010, Kiss, 2018]. It uses the way in which oscillators respond to external perturbations (including perturbations coming from other oscillators in the system), but it does not attempt to change how the oscillators respond. It is important to ensure that the coupling we introduce is sufficiently weak.

2.1 Relation between phase model and coupling

If we suppose that the coupling has the form $P(t) = \frac{1}{N}\sum_\ell g(\mathbf{x}_1^\ell(t)))$, then a population of identical oscillators with this coupling is written as

$$\frac{d\mathbf{x}^j}{dt} = \mathbf{f}(\mathbf{x}^j) + \frac{\epsilon}{N}\sum_\ell g(\mathbf{x}_1^\ell(t))) \qquad \text{for } j = 1, 2, \ldots, N. \tag{2.1}$$

Its phase reduction (see Definition 1.3) is given by

$$\frac{d\phi_j}{dt} = \omega + \frac{\epsilon}{N} Z(\theta_j) \cdot \sum_\ell g(x(\theta_\ell)), \qquad \text{for } j = 1, \ldots, N, \tag{2.2}$$

where Z is the phase response curve and $x(\theta)$ is the waveform in the first variable $x\mathbf{x}_1^j$ of the unperturbed identical oscillators (1.1). We consider the phase deviation $\hat{\theta}_j = \omega t + \theta_j$ and rewrite Equation 2.2, dropping hats again, to

$$\frac{d\theta_j}{dt} = \frac{\epsilon}{N} Z(\omega t + \theta_j) \cdot \sum_\ell g(x(\omega t + \theta_\ell)), \qquad \text{for } j = 1, \ldots, N, \tag{2.3}$$

which can be averaged to

$$\frac{d\theta_j}{dt} = \frac{\epsilon}{N}\sum_\ell H(\theta_\ell - \theta_j), \qquad \text{for } j = 1, \ldots, N, \tag{2.4}$$

with the interaction functions computed as [Izhikevich and Kuramoto, 2006]:

$$H(\theta_\ell - \theta_j) = \frac{1}{2\pi}\int_{\theta_j}^{\theta_j + 2\pi} Z(\theta_j + \rho) g(\theta_\ell + \rho) d\rho \tag{2.5}$$

$$= \frac{1}{2\pi}\int_0^{2\pi} Z(\rho) g(\theta_\ell - \theta_j + \rho) d\rho. \tag{2.6}$$

We assume that averaging over time results in a good approximation of the original system. It can be proven that the solutions of the original system and the averaged system remain order ϵ close for time of order $\frac{1}{\epsilon}$ [Sanders et al., 2007]. This means that if the coupling strength ϵ is too large compared to the time interval of interest, then we cannot be sure that the averaged system is a good approximation any more.

We write H, Z and g in terms of their exponential Fourier series ($H(\phi) = \sum_l H_l e^{-il\phi}$, $Z(\phi) = \sum_l Z_l e^{-il\phi}$, $g(\phi) = \sum_l g_l e^{-il\phi}$), since solving the relation between the Fourier coefficients H_l, Z_l and g_l, will be more convenient than trying to solve Equation 2.6. The relation between the Fourier coefficients is:

$$H_l = g_l Z_{-l}, \qquad \text{for } l = 1, 2, \ldots, S, \tag{2.7}$$

where the overall coupling order S is chosen according to the order of the nonzero harmonics appearing in the target phase model. The details of obtaining (2.7) are left out as we will present the derivation of the more general case in Chapter 3. In practice, we will aim to satisfy the corresponding inequality constraints

$$|g_l Z_{-l} - H_l| < \delta. \tag{2.8}$$

for some $\delta \ll 1$.

Rather than trying to solve (2.7) or satisfy (2.8) for general coupling g, we assume that g has a certain form, depending on gain κ_s and delay τ_s parameters. By deciding on a form of coupling g beforehand, we can design coupling for different types of soscillators and different desired collective behaviours without having to design the coupling from scratch each time. We choose the type(s) of oscillators and a target phase model describing the desired behaviour. We then determine for which of the coupling parameters κ_s, τ_s the inequalities (Equations 2.8 for $l = 1, 2, \ldots, S < \infty$) hold.

2.2 The form of the coupling

We consider coupling that only takes input from the x_1^j-variables. The coupling is then applied to that same state variable. It is common that only the first coordinate of an oscillator is observed, and that this is also the coordinate to which the coupling is applied. This is for example the case in many models of coupled neurons where the first coordinate represents the voltage. The S-dimensional

function P is set to zero for all other state variables:

$$P(t) = \frac{1}{N}\sum_{\ell=1}^{N}[g(\mathbf{x}_1^{\ell}), 0, \ldots, 0]. \tag{2.9}$$

We assume $g(x_\ell)$ has the following form:

$$g(x(\theta_\ell)) = \sum_{s=0}^{S} \kappa_s [x(\theta_\ell - \omega\tau_s) - a_0]^s, \tag{2.10}$$

where κ_n is the coupling gain, and a_0 is the time average of the waveform $x(\theta)$. The coupling (2.10) is time delayed in that uses states of the oscillators calculated at S different times $t-\tau_1, t-\tau_2, \ldots, t-\tau_S$, where S is the degree of the coupling. Based on those past states of the (other) oscillators, its own rate of change at the current time t is adjusted.

Which past states are used is determined by the parameters τ_n, and it is the same for all oscillators. (The coupling $P(t)$ equals a sum over all oscillators j, and we assumed that g is independent of ℓ and j.) This does not imply that all the terms in the sum are the same, but they are based only on the states of the other oscillators at one certain point in past, and not on the particular oscillators involved.

The coupling (Equation 2.10) is nonlinear as it also considers squared and higher order terms, i.e. the coupling has a polynomial form. For each of the terms in its sum, the state is considered at a different time lag. The linear term corresponds to the state at $t-\tau_1$, the quadratic term corresponds to the state at $t-\tau_2$, the cubic one at $t-\tau_3$ and so on. Each of the terms is scaled by the gains κ_s that determine the influence of each of the terms in the coupling.

Expanding the waveform in its complex Fourier series $x(\theta) = \sum_l a_l e^{-il\theta}$, the coupling function becomes

$$g(\theta_\ell) = \sum_{s=0}^{S} \kappa_s \left[\sum_{l\neq 0} a_l e^{-il\theta_\ell} e^{il\omega\tau_s}\right]^s. \tag{2.11}$$

Recall that we needed to solve Equations 2.7 for the Fourier coefficients of the

coupling g_l. From Equation 2.11 it follows that those Fourier coefficients will depend on the parameters κ_s and τ_s, and the Fourier coefficients a_l of the waveform. For given interaction function H, phase response curve Z and waveform x, we can consider Equation 2.11 at the needed order S, and expand the sum and start to compare coefficients of $e^{-il\theta_\ell}$ to find expressions for the nontrivial g_l in terms of κ_s and τ_s for $s = 1, 2, \ldots, S$. Using those expressions, Equations 2.7 can be solved analytically for a strictly harmonic waveform $x(\theta) = e^{-il\theta} + e^{il\theta}$ (see Appendix B.3), as one might expect from systems near a supercritical Hopf bifurcation.

Which target interaction functions we can choose depends on which harmonics of the phase response curve are nonzero. We can namely only control the harmonics of target interaction functions that correspond to nonzero harmonics in the phase response curve of the oscillators. In the classical synchronisation engineering approach, having a second harmonic in the phase response curve means we can control the second harmonic in the target interaction function.

2.3 Designing coupling for Brusselators

In this section we reproduce the results from [Rusin et al., 2010] to design the coupling for a population of $N = 2$ Brusselator oscillators.

Figure 2.1: Reproduction of "Figure 3" in [Rusin et al., 2010]. For $N = 2$ Brusselators, coupling strength $\epsilon = 10^{-3}$, using parameter set 1 of 2, using *dde23* with reltol $= 10^{-5}$, abstol $= 10^{-8}$, endtime = 170100. Starting close to in-phase sync.

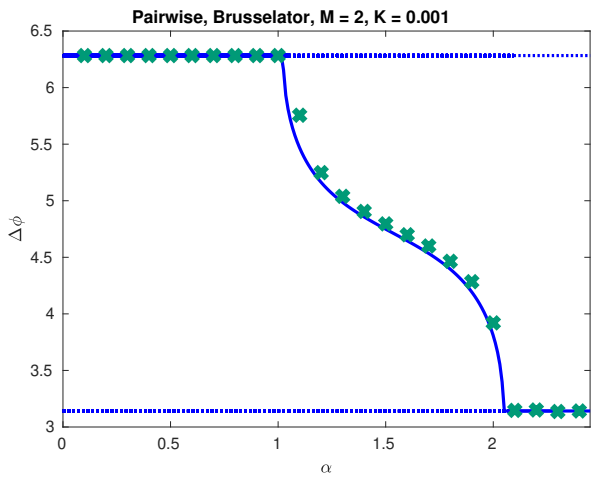

Figure 2.2: More general version of Figure 2.1 using the order parameter $R_1(t)$ instead of the phase difference to compare different phase lags $\alpha = \omega\Delta\tau$.

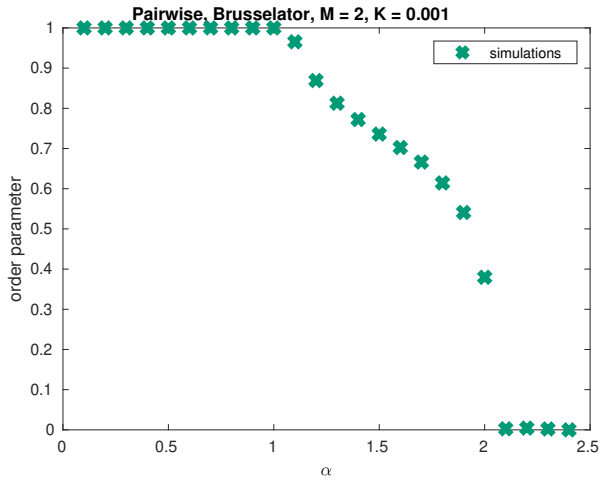

We used an optimisation algorithm implemented in Matlabs fmincon method to minimize $\sum \kappa_s$ starting at a set of random vectors with values between 0 and T using the additional constraints that $0 \leq \tau_s \leq T$. The optimisation finds the coupling parameters that satisfy the constraints for Fourier parameters H_l, g_l and Z_l (2.8 for $l = 1, 2$) with $\delta = 10^{-2}$ for the pairwise phase model (1.10) with interaction function H as in Equation 1.12 to control a population of $N = 2$ Brusselators (1.55,1.56). We chose to minimise over $\sum \kappa_s$ because we want the overall coupling to be weak due to the weak coupling assumptions we made in the averaging and phase reduction steps.

We then calculate the phases of the two oscillators at the endpoint and plot this for each $\alpha = \omega\Delta\tau$ in Figure 2.1. This is a reproduction of "Figure 3" in [Rusin et al., 2010], and is a convenient measure of synchronisation when simulating only two oscillators. By changing $\Delta\tau$, the phase difference between the two oscillators can be controlled to take on a value between π and 2π.

Nonpairwise interactions reduce to pairwise interactions when the number of oscillators is less than three. We produce a Figure similar to Figure 2.1, but using the order parameter $R_1(t)$ instead as this figure can be produced for $N = 4$ oscillators as well for comparison. Figure 2.2 plots the order parameter against the general delay $\alpha = \omega\Delta\tau$. Recall that a value of $R_1(t)$ close to 1 indicates

full in-phase synchrony. For more than two oscillators, values close to 0 can mean full incoherence, antiphase state, or some kind of clustering. We are mainly interested in finding out if the stability of the in-phase synchronisation shifts as expected when we introduce nonpairwise interactions to the pairwise target phase model we have studied so far.

Figure 2.3: The slopes of $\log(1 - R_1(t))$ for $N = 2$ Brusselators with coupling. For reference, we plotted the slopes for the target interaction function that was used as well (see Section 1.8.)

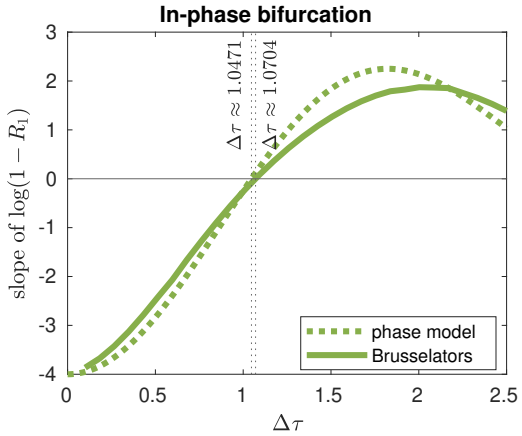

To study the stability of in-phase and splay configuration, we pick initial conditions close to in-phase orientation and calculate the rate of convergence of the order parameters $R_1(t)$ and $R_N(t)$ to 1 (where N is the numberof oscillators in the population). Thus we are not interested in controlling phase differences, but want to only confirm that the convergence to in-phase and splay configuration matches the target phase models.

We do this by plotting $\log(1 - R_1(t))$ for different values of $\Delta\tau$ as we did in Section 1.8 for the target phase model (with interaction function H given by Equation 1.12). We run the simulations (using Matlabs *dde23*) for the two Brusselators with coupling as described above for a range of $\Delta\tau$'s. We fit a line to $\log(1-R_1(t))$for each $\Delta\tau$ and plot the slope of this line versus $\Delta\tau$ (see Figure 2.3).

Recall that negative slopes indicate convergence to in-phase while positive slopes indicate divergence. Where the curve crosses the horizontal axis, the stability of the in-phase configuration changes. To compare the target phase model to the controlled Brusselators, we plot the curve from Figure 1.3 again (dashed)

and plot the curve for the controlled Brusselators on top (solid). For the target phase model, we found (analytically and confirmed by simulations) that the in-phase configuration loses stability at $\Delta\tau \approx 1.0471$. For the controlled Brusselators we found (using simulations) that the in-phase configuration loses stability at $\Delta\tau \approx 1.0704$. Thus the coupled system of oscillators has approximately the same bifurcation point of in-phase stability as the target phase model.

Synchronisation engineering has previously been used with various target interaction phase models [Kiss, 2018]. In this Chapter we reproduced the results from [Rusin et al., 2010] where the phase difference between two oscillators could be controlled. Other demonstrations of synchronisation engineering include the clustering of both periodic and chaotic oscillators [Kori et al., 2008, Rusin et al., 2009, Rusin et al., 2011], chimera states [Bick et al., 2017], and desynchronisation [Kiss et al., 2007b].

Chapter 3

Higher order synchronisation engineering

This Chapter contains novel theory and experiments to introduce our generalisation of the classical synchronisation engineering method [Rusin et al., 2010]) that we discussed in Chapter 2. We demonstrate that we are able to control nonpairwise interactions in weakly coupled populations of oscillators using phase reduction as in the synchronisation engineering framework. To our knowledge, this nonpairwise form of the coupling has not been considered before. Figure 3.1 gives a schematic overview of our suggested methodology to contol non-pairwise interactions using a synchronisation engineering approach.

Classical synchronisation engineering of the type presented in Chapter 2 allows for a range of possible target phase models, that do not include nonpairwise terms. If we would like to use synchronisation engineering to introduce the collective behaviour exhibited by a nonpairwise target phase model, we need to rewrite the parameter dependent coupling accordingly. In order to do so, we introduce more gain and delay parameters. We index these parameters according to which phase differences they control input for as discussed below.

Figure 3.1: Schematic illustrating the main stages of the methodology developed in this thesis.

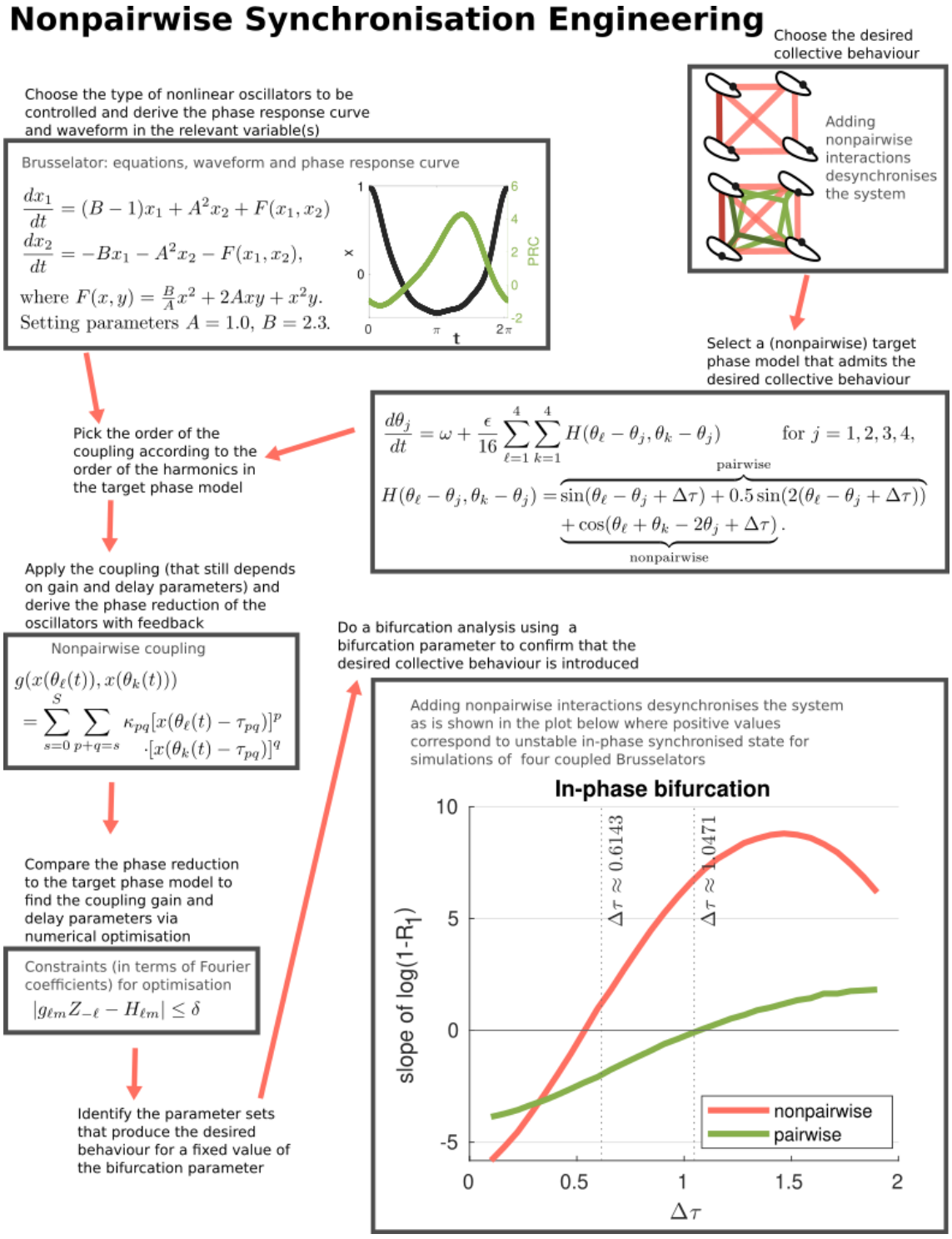

3.1 Relation between phase model and coupling

We consider a target phase model of identical oscillators with general coupling of the form (1.33). In this thesis we consider $N = 4$ oscillators:

$$\frac{d\theta_j}{dt} = \omega + \frac{\epsilon}{16}\sum_{\ell=1}^{4}\sum_{k=1}^{4} H(\theta_\ell - \theta_j, \theta_k - \theta_j) \qquad \text{for } j = 1,2,3,4, \tag{3.1}$$

though comment that extensions to networks with more oscillators follow in a straightforward manner.

We want to design the interactions $\mathbf{P}(\mathbf{x}^1, \mathbf{x}^2, \mathbf{x}^3, \mathbf{x}^4, t)$ for a population of $N = 4$ Brusselators (1.55,1.56) where $\mathbf{x}_1^j$ are the first variable of Brusselator oscillators $j = 1,2,3,4$. In particular, we want the nonpairwise phase model (1.33) with interaction function (1.32) to match the phase reduction of (1.55,1.56) that is given by Equation 1.57.

The coupling $\mathbf{P}(.)$ takes as its input the first coordinates $\mathbf{x}_1^j$ of all oscillators j in the population, but effectively it only uses this value at particular times $t - \tau_{pq}$.

We designed a form of the coupling $P(.)$ for general N. For $N = 4$ oscillators, it looks as follows:

$$\mathbf{P}(\mathbf{x}^1(t), \mathbf{x}^2(t), \mathbf{x}^3(t), \mathbf{x}^4(t), t) = \sum_{\ell=1}^{4}\sum_{k=1}^{4} g(\mathbf{x}_1^\ell(t), \mathbf{x}_1^k(t)), \tag{3.2}$$

where $g(.,.)$ is given by

$$g(\mathbf{x}_1^\ell(t), \mathbf{x}_1^k(t)) = g(x(\theta_\ell(t)), x(\theta_k(t))) \tag{3.3}$$

$$= \sum_{s=0}^{S}\sum_{p+q=s} \kappa_{pq}[x(\theta_\ell(t) - \tau_{pq})]^p [x(\theta_k(t) - \tau_{pq})]^q, \tag{3.4}$$

where $x(\theta)$ is the waveform of the first variable $\mathbf{x}_1^j$. We assume that the unperturbed oscillators $j = 1,2,3,4$ are identical, i.e. $\mathbf{x}_1^j(t) = x(\theta_j(t))$ for $j = 1,2,3,4$.

Recall that in classical synchronisation engineering, we used gain parameters κ_s and delay parameters τ_s for $s = 1,2,\ldots,S$ where S is the overall order of the coupling.

Note that some of the terms in this double sum do not actually represent three-way interactions as they can concern the same oscillator twice, representing pairwise interactions. Or they can take information from the oscillator j to which the coupling is applied (which is of course still at a delay τ_{pq} compared to the current time t). Thus we do not need to write a separate coupling to control the pairwise interactions as they are included in this general form of coupling as well.

For nonzero coupling $\epsilon > 0$ it can be proven that the phase reduction explicitly depends on the delay τ_{pq} if the delay term large enough, e.g. when it is of order $\frac{1}{\epsilon}$ periods [Izhikevich, 1998]. However, for weak coupling ϵ the effect of the delay τ_{pq} is reduced to a phase shift $\omega\tau_{pq}$ as follows [Kori and Kuramoto, 2001]. Similar to how we obtained Equation 2.3 in Chapter 2, when there is no interaction between the oscillators, then [Kori et al., 2008]

$$\theta(t - \tau_{pq}) = \theta(t) - \omega\tau_{pq}, \tag{3.5}$$

where ω is the natural frequency of the oscillators. This means we can write $x(\theta(t - \tau_{pq})) = x(\theta(t) - \omega\tau_{pq})$ when $\epsilon \ll 1$.

Similar to in Section 2.2, we want to find the relation between the nonpairwise target interaction function (1.32), the phase response curve $Z(\theta)$, and the phase reduction 1.57 with coupling $P(.)$ as in Equation 3.2 and nonpairwise target coupling $g(.)$ given by Equation 3.4 that depends on coupling parameters κ_{pq} and τ_{pq}.

Following a similar procedure as in [Kori et al., 2008] and Section 2.2 now for 2-dimensional Fourier series of $H(.)$ and $g(.)$,

$$g(\theta_\ell, \theta_k) = \sum_l \sum_m g_{lm} e^{-il\theta_\ell} e^{-im\theta_k} \tag{3.6}$$

$$H(\theta_\ell, \theta_k) = \sum_l \sum_m H_{lm} e^{-il\theta_\ell} e^{-im\theta_k} \tag{3.7}$$

Written in terms of the Fourier series of the waveform, $x(\theta) = \sum_l a_l e^{-il\theta}$, the

coupling as in Equation 3.4 becomes

$$g(\theta_\ell, \theta_k) = \sum_{s=0}^{S} \sum_{p+q=s} \kappa_{pq} \left[\sum_{l \neq 0} a_l e^{-il(\theta_\ell - \omega\tau_{pq})} \right]^p \cdot \left[\sum_{l \neq 0} a_l e^{-il(\theta_k - \omega\tau_{pq})} \right]^q . \tag{3.8}$$

We can express the target nonpairwise interaction function $H(.,.)$ in terms of the phase response curve $Z(\theta)$ and the target coupling $g(.)$ as follows

$$\begin{aligned}
H(.) &= H(\theta_\ell - \theta_j, \theta_k - \theta_j) && (3.9)\\
&= \frac{1}{2\pi} \int_0^{2\pi} Z(\rho + \theta_j) g(\rho + \theta_\ell, \rho + \theta_k) d\rho && (3.10)\\
&= \frac{1}{2\pi} \int_0^{2\pi} Z(\rho) g(\rho + \theta_\ell - \theta_j, \rho + \theta_k - \theta_j) d\rho && (3.11)\\
&= \frac{1}{2\pi} \int_0^{2\pi} \sum_n Z_n e^{-il\rho} \cdot \sum_l \sum_m g_{lm} e^{-i(l+m)\rho} e^{-i(l(\theta_\ell - \theta_j)_1 + m(\theta_k - \theta_j))} d\rho && (3.12)\\
&= \frac{1}{2\pi} \int_0^{2\pi} \sum_l \sum_m \sum_n g_{lm} Z_n e^{-i(l+m+n)\rho} e^{-i(l(\theta_\ell - \theta_j) + m(\theta_\ell - \theta_j)} d\rho && (3.13)\\
&= \frac{1}{2\pi} 2\pi \sum_{l+m+n=0} g_{lm} Z_n e^{-i(l(\theta_\ell - \theta_j) + m(\theta_\ell - \theta_j)} && (3.14)\\
&= \sum_l \sum_m g_{lm} Z_{-l-m} e^{-i(l(\theta_\ell - \theta_j) + m(\theta_\ell - \theta_j)} && (3.15)
\end{aligned}$$

By comparing terms with Equation 3.7, we obtain the following relation between the Fourier coefficients:

$$H_{lm} = g_{lm} Z_{-l-m} \qquad \text{for } l + m \leq S, \tag{3.16}$$

where S is the overall order of the coupling. These are the equations that we need to solve for the coupling delay τ_{pq} and gain κ_{pq} parameters for $p, q \geq 0$, $p + q \leq S$, which appear in the coupling $g(.)$.

3.2 Deriving the coupling constraints

From the relation between the Fourier coefficients 3.16 we can draw some conclusions on the type of oscillators and target phase models that we can design coupling for using our generalised synchronisation engineering method. Suppose

that we want to use a target interaction function $H(.,.)$ for which H_{lm} is nonzero for some $l, m \geq 1$. Then that interaction function has a nonpairwise term. To satisfy Equation 3.16 with a nonzero left-hand side, it is necessary to have that Z_{-l-m} is nonzero. The Fourier coefficient $-l - m \leq -1 - 1 = -2$ should be nonzero. Thus we should have at least one second or higher order harmonic in the phase response curve $Z(\theta)$ if we want to use a target interaction function with nonpairwise interactions. Which order harmonics of the phase response curve $Z(\theta)$ should be nonzero can be determined as soon as it is decided what target interaction function is used.

The nonpairwise target interaction function we use in this thesis (given by Equations 1.33,1.32), has nonzero Fourier coefficients in its interaction function $H(.)$ for H_{10}, H_{20} and H_{11}. Looking at Equations 3.16, we can see that if we want to include only the constraints in which H_{10}, H_{20} and H_{11} appear, then an overall order of the coupling $S = 2$ would be enough. We want to make sure that all terms up to third order terms H_{30} and H_{03} are zero, as well as other terms of overall third order H_{21} and H_{12}. If the interaction function contains higher-order nonzero terms, then we might need to include more constraints here. However, for the nonpairwise interaction function given by Equations 1.33,1.32 we assume that controlling terms up to order $S = 3$ is sufficient.

Thus we use all Equations 3.16 such that $l + m \leq S = 3$. Thus we decided to

use the following constraints for $\delta \ll 1$:

$$|g_{10}Z_{-1} - H_{10}| \leq \delta \tag{3.17}$$

$$|g_{20}Z_{-2} - H_{20}| \leq \delta \tag{3.18}$$

$$|g_{30}Z_{-3} - H_{30}| \leq \delta \tag{3.19}$$

$$|g_{01}Z_{-1} - H_{01}| \leq \delta \tag{3.20}$$

$$|g_{02}Z_{-1} - H_{02}| \leq \delta \tag{3.21}$$

$$|g_{03}Z_{-3} - H_{03}| \leq \delta \tag{3.22}$$

$$|g_{11}Z_{-2} - H_{11}| \leq \delta \tag{3.23}$$

$$|g_{21}Z_{-3} - H_{21}| \leq \delta \tag{3.24}$$

$$|g_{12}Z_{-3} - H_{12}| \leq \delta \tag{3.25}$$

We now derive the expressions for the Fourier coefficients g_{lm} of the coupling $g(.,.)$ that appear in the constraints (3.18-3.25).

For overall order $S = 3$, the coupling becomes:

$$g(\theta_\ell, \theta_k) = \sum_{s=0}^{3} \sum_{p+q=s} \kappa_{pq}[x(\theta_\ell - \omega\tau_{pq}) - a_0]^p \cdot [x(\theta_k - \omega\tau_{pq}) - a_0]^q, \tag{3.26}$$

where $p, q \geq 0$. To find the Fourier coefficients of the coupling $g(.,.)$ for overall

order $S = 3$, we start by writing out the double sum in Equation 3.26 to obtain

$$
\begin{aligned}
g(\theta_\ell, \theta_m) =& \kappa_{00} + \kappa_{10}[x(\theta_\ell - \omega\tau_{10}) - a_0] && (3.27)\\
&+ \kappa_{01}[x(\theta_k - \omega\tau_{01}) - a_0] && (3.28)\\
&+ \kappa_{11}[x(\theta_\ell - \omega\tau_{11}) - a_0] \cdot [x(\theta_k - \omega\tau_{11}) - a_0] && (3.29)\\
&+ \kappa_{20}[x(\theta_\ell - \omega\tau_{20}) - a_0]^2 && (3.30)\\
&+ \kappa_{02}[x(\theta_k - \omega\tau_{02}) - a_0]^2 && (3.31)\\
&+ \kappa_{21}[x(\theta_\ell - \omega\tau_{21}) - a_0]^2 \cdot [x(\theta_k - \omega\tau_{21}) - a_0] && (3.32)\\
&+ \kappa_{12}[x(\theta_\ell - \omega\tau_{12}) - a_0] \cdot [x(\theta_k - \omega\tau_{12}) - a_0]^2 && (3.33)\\
&+ \kappa_{30}[x(\theta_\ell - \omega\tau_{30} - a_0)]^3 && (3.34)\\
&+ \kappa_{03}[x(\theta_k - \omega\tau_{03} - a_0)]^3 && (3.35)
\end{aligned}
$$

Now expand the waveform in its fourier coefficients $x(\theta) = \sum_l a_l e^{-il\theta}$ to obtain

$$
\begin{aligned}
g(\theta_\ell, \theta_k) =& \kappa_{00} + \kappa_{10} \sum_{l\neq 0} a_l e^{-il(\theta_\ell - \omega\tau_{10})} + \kappa_{01} \sum_{l\neq 0} a_l e^{-il(\theta_k - \omega\tau_{010})}\\
&+ \kappa_{11} \sum_{l\neq 0} a_l e^{-il(\theta_\ell - \omega\tau_{11})} \cdot \sum_{l\neq 0} a_l e^{-il(\theta_k - \omega\tau_{11})}\\
&+ \kappa_{20} \left[\sum_{l\neq 0} a_l e^{-il(\theta_\ell - \omega\tau_{20})}\right]^2 + \kappa_{02} \left[\sum_{l\neq 0} a_l e^{-il(\theta_k - \omega\tau_{02})}\right]^2\\
&+ \kappa_{21} \left[\sum_{l\neq 0} a_l e^{-il(\theta_\ell - \omega\tau_{21})}\right]^2 \cdot \sum_{l\neq 0} a_l e^{-il(\theta_k - \omega\tau_{21})}\\
&+ \kappa_{12} \sum_{l\neq 0} a_l e^{-il(\theta_\ell - \omega\tau_{12})} \cdot \left[\sum_{l\neq 0} a_l e^{-il(\theta_k - \omega\tau_{12})}\right]^2\\
&+ \kappa_{30} \left[\sum_{l\neq 0} a_l e^{-il(\theta_\ell - \omega\tau_{30})}\right]^3 + \kappa_{03} \left[\sum_{l\neq 0} a_l e^{-il(\theta_k - \omega\tau_{03})}\right]^3
\end{aligned}
$$

Now we extract the Fourier coefficients corresponding to the coefficients of the coupling g_{lm} as in Equation 3.6 that are used in constraints (3.18-3.25 upto the fifth Fourier coefficient of the waveform $x(.)$.

We split the Fourier coefficients up into three types: (1) Those corresponding to pairwise interactions with phase difference $\theta_\ell - \theta_j$, (2) those corresponding

to pairwise interactions with phase difference $\theta_k - \theta_j$, and (3) those corresponding to nonpairwise interactions that use both phase difference $\theta_\ell - \theta_j$ and phase difference $\theta_k - \theta_j$.

The Fourier coefficients corresponding to the phase difference θ_ℓ (type 1) are:

$$\begin{aligned}
g_{10} &= \kappa_{10} a_1 e^{i\omega\tau_{10}} + 2\kappa_{20} e^{i\omega\tau_{20}}(a_2 a_{-1} + a_3 a_{-2} + a_4 a_{-3} + a_5 a_{-4}) \\
&\quad + 3\kappa_{30} e^{i\omega\tau_{30}}(a_1^2 a_{-1} + a_1 a_2 a_{-2} + a_1 a_3 a_{-3} + a_1 a_4 a_{-4} + a_1 a_5 a_{-5} \\
&\quad + a_3 a_{-1}^2 + a_4 a_{-1} a_{-2} + a_5 a_{-2}^2 + a_{-3} a_2^2 \\
&\quad + a_{-3} a_{-1} a_5 + a_{-4} a_2 a_3 + a_{-5} a_3^2 + a_{-5} a_2 a_4) \\
&\quad + 2\kappa_{12} e^{i\omega\tau_1 2}(a_1 a_5 a_{-5} + a_1 a_4 a_{-4} + a_1 a_3 a_{-3} + a_1 a_2 a_{-2} + a_1^2 a_{-1}) \\
g_{20} &= \kappa_{10} a_2 e^{2i\omega\tau_{10}} + 2\kappa_{20} e^{2i\omega\tau_{20}}(a_1^2/2 + a_3 a_{-1} + a_4 a_{-2} + a_5 a_{-3}) \\
&\quad + 3\kappa_{30} e^{2i\omega\tau_{30}}(a_1 a_2 a_{-1} + a_1 a_3 a_{-2} + a_1 a_4 a_{-3} + a_1 a_5 a_{-4} \\
&\quad + a_4 a_{-1}^2 + a_5 a_{-1} a_{-2} + a_{-2} a_2^2 + a_{-3} a_2 a_3 + a_{-4} a_3^2 \\
&\quad + a_{-4} a_2 a_4 + a_{-5} a_3 a_4 + a_{-5} a_2 a_5) \\
&\quad + 2\kappa_{12} e^{i\omega\tau_1 2}(a_2 a_5 a_{-5} + a_2 a_4 a_{-4} + a_2 a_3 a_{-3} + a_2 a_2 a_{-2} + a_2^2 a_{-1}) \\
g_{30} &= \kappa_{10} e^{3i\omega\tau_{10}} a_3 + 2\kappa_{20} e^{3i\omega\tau_{20}}(a_1 a_2 + a_4 a_{-1} + a_5 a_{-2}) \\
&\quad + 6\kappa_{30} e^{3i\omega\tau_{30}}(a_1^3/6 + a_2^2 a_{-1}/2 + a_3 a_2 a_{-2} + a_4 a_1 a_{-2} \\
&\quad + a_4 a_2 a_{-3} + a_4 a_3 a_{-4} + a_5 a_1 a_{-3} + a_5 a_2 a_{-4} + a_5 a_3 a_{-5} + a_5 a_{-1}^2/2)
\end{aligned} \tag{3.36}$$

(3.37)

(3.38)

These Fourier coefficients were also present in the constraints for pairwise cou-

pling. The Fourier coefficients for the phase differences θ_m (type 2) are:

$$\begin{aligned}
g_{01} &= \kappa_{01}a_1e^{i\omega\tau_{01}} + 2k_{02}e^{i\omega\tau_{02}}(a_2a_{-1} + a_3a_{-2} + a_4a_{-3} + a_5a_{-4}) \\
&\quad + 3\kappa_{03}e^{i\omega\tau_{03}}(a_1^2a_{-1} + a_1a_2a_{-2} + a_1a_3a_{-3} + a_1a_4a_{-4} + a_1a_5a_{-5} \\
&\quad + a_3a_{-1}^2 + a_4a_{-1}a_{-2} + a_5a_{-2}^2 + a_{-3}a_2^2 \\
&\quad + a_{-3}a_{-1}a_5 + a_{-4}a_2a_3 + a_{-5}a_3^2 + a_{-5}a_2a_4) \\
&\quad + 2\kappa_{21}e^{i\omega\tau_2 1}(a_1a_5a_{-5} + a_1a_4a_{-4} + a_1a_3a_{-3} + a_1a_2a_{-2} + a_1^2a_{-1})
\end{aligned} \tag{3.39}$$

$$\begin{aligned}
g_{02} &= \kappa_{01}a_2e^{2i\omega\tau_{01}} + 2k_{02}e^{2i\omega\tau_{02}}(a_1^2/2 + a_3a_{-1} + a_4a_{-2} + a_5a_{-3}) \\
&\quad + 3\kappa_{03}e^{2i\omega\tau_{03}}(a_1a_2a_{-1} + a_1a_3a_{-2} + a_1a_4a_{-3} + a_1a_5a_{-4} \\
&\quad + a_4a_{-1}^2 + a_5a_{-1}a_{-2} + a_{-2}a_2^2 + a_{-3}a_2a_3 + a_{-4}a_3^2 \\
&\quad + a_{-4}a_2a_4 + a_{-5}a_3a_4 + a_{-5}a_2a_5) \\
&\quad + 2\kappa_{21}e^{i\omega\tau_2 1}(a_2a_5a_{-5} + a_2a_4a_{-4} + a_2a_3a_{-3} + a_2a_2a_{-2} + a_2^2a_{-1})
\end{aligned} \tag{3.40}$$

$$\begin{aligned}
g_{03} &= \kappa_{01}e^{3i\omega\tau_{01}}a_3 + 2\kappa_{02}e^{3i\omega\tau_{02}}(a_1a_2 + a_4a_{-1} + a_5a_{-2}) \\
&\quad + 6\kappa_{03}e^{3i\omega\tau_{03}}(a_1^3/6 + a_2^2a_{-1}/2 + a_3a_2a_{-2} + a_4a_1a_{-2} \\
&\quad + a_4a_2a_{-3} + a_4a_3a_{-4} + a_5a_1a_{-3} + a_5a_2a_{-4} + a_5a_3a_{-5} + a_5a_{-1}^2/2)
\end{aligned} \tag{3.41}$$

These Fourier coefficients were not present in the constraints for the pairwise coupling, but they still represent pairwise interactions. The Fourier coefficients that appear in the constraints for the nonpairwise coupling, and correspond to nonpairwise interactions that use both phase differences θ_ℓ and θ_m (type 3) are:

$$\begin{aligned}
g_{11} &= \kappa_{11}a_1^2e^{2i\omega\tau_{11}} \\
&\quad + 2\left(\kappa_{21}e^{2i\omega\tau_{21}} + \kappa_{12}e^{2i\omega\tau_{12}}\right)\cdot a_1(a_2a_{-1} + a_3a_{-2} + a4a_{-3} + a_5a_{-4})
\end{aligned} \tag{3.42}$$

$$\begin{aligned}
g_{21} &= 2\kappa_{110}e^{3i\omega\tau_{21}}a_2a_1 + 2\kappa_{21}e^{3i\omega\tau_{21}}a_1(a_1^2/2 + a_3a_{-1} + a_4a_{-2} + a_5a_{-3}) \\
&\quad + 2\kappa_{12}e^{3i\omega\tau_{12}}a_2(a_2a_{-1} + a_3a_{-2} + a_4a_{-2} + a_5a_{-4})
\end{aligned} \tag{3.43}$$

$$\begin{aligned}
g_{12} &= 2\kappa_{110}e^{3i\omega\tau_{12}}a_2a_1 + 2\kappa_{21}e^{3i\omega\tau_{12}}a_1(a_1^2/2 + a_3a_{-1} + a_4a_{-2} + a_5a_{-3}) \\
&\quad + 2\kappa_{21}e^{3i\omega\tau_{21}}a_2(a_2a_{-1} + a_3a_{-2} + a_4a_{-2} + a_5a_{-4}).
\end{aligned} \tag{3.44}$$

3.3 Finding coupling parameters

Now we want to find the parameters τ_{pq} and κ_{pq} such that the constraints (3.18-3.25) are satisfied for some δ. We first need to pick our interaction function H and choose Equation 1.32. Secondly, we need to find the waveform x and Z for the Brusselator as shown in Figure 1.10 and calculate their Fourier coefficients. We also need to set a bound for the constraints: $\delta = 10^{-2}$ (and decide on an optimisation algorithm). Then we are ready to find the coupling parameters τ_{pq}, κ_{pq} and subsequently run simulations using those coupling parameters.

Using the direct method to find the PRC for the Brusselator as described in Section 1.11, we found the Fourier coefficients $Z_{-1} \approx -0.8761 + 0.9535i$, $Z_{-2} \approx -0.2358 - 0.1576i$, and $Z_{-3} \approx 0.0361 - 0.0215i$.

The H_{lm} are given by the target phase model that we choose and described in Section 1.9. Recall that this interaction function is given by:

$$H(\theta_\ell - \theta_j, \theta_k - \theta_j) = \overbrace{\sin(\theta_\ell - \theta_j + \Delta\tau) + 0.5\sin(2(\theta_\ell - \theta_j + \Delta\tau))}^{\text{pairwise}} \underbrace{+ \cos(\theta_\ell + \theta_k - 2\theta_j + \Delta\tau)}_{\text{nonpairwise}}. \tag{3.45}$$

The nonzero Fourier coefficients are $H_{10} = 0.5i$, $H_{11} = 0.5$, $H_{20} = 0.25i$ and we also use the coefficients $H_{01} = H_{02} = H_{03} = H_{30} = H_{21} = H_{12} = 0$

We find the following Fourier coefficients for the waveform $x(\theta)$ of the Brusselator (1.50,1.51): $a_1 \approx 0.2993 + 0.0315i$, $a_2 \approx 0.1159 + 0.0220i$, $a_3 \approx 0.0489 + 0.0031i$, $a_4 \approx 0.0223 - 0.0030i$, and $a_5 \approx 0.0102 - 0.0036i$.

We use the constraints (3.18-3.25) with the expressions for g_{lm} (3.36-3.44) and the values for H_{lm}, Z_l and a_l given above to find the relevant gain k_{pq} and delay τ_{pq} parameters.

A good check for the validity of our control algorithm is to find out if the stability of the in-phase configuration as well as splay configuration matches that of the original target phase model. So we want to know if the phase lags $\Delta\tau$ for which in-phase/splay configuration in the target phase model becomes unstable (see Section 1.9) , coincide with the phase lags for which the in-phase/splay configu-

ration in the simulated coupled Brusselators becomes unstable.

We expect that the bifurcation point at which in-phase synchronisation solution loses stability shifts when we include nonpairwise interactions in the target phase model (1.32,1.33). The inclusion of such nonpairwise terms should not change the value of $\Delta\tau$ at which the splay state loses stability (see Section 1.9). Thus when we find that the $\Delta\tau$'s for which trajectories starting close to full synchronisation converge to synchronisation match up between the phase model and the simulations, then we could do the same to test if the stability of splay matches. If the stability of splay matches as well, that would be strong evidence that the shift in stability of in-phase synchronisation is due to the successful matching of the nonpairwise target interaction function to the phase reduction.

Table 3.1: The stability behaviour of the pairwise and nonpairwise target interaction functions H for $N = 4$ oscillators at in-phase and splay configurations.

	in-phase stable	splay stable	
pairwise H	$\Delta\tau < 1.0472\ldots$	$\Delta\tau > 1.5708\ldots$	(Equation 1.32)
nonpairwise H	$\Delta\tau < 0.6142\ldots$	$\Delta\tau > 1.5708\ldots$	(Equation 1.12)

In the following chapter, we use a Matlab optimisation algorithm[1] to find the gain κ_{pq} and delay τ_{pq} coupling parameters that satisfy the constraints (3.18-3.25) for $\delta = 10^{-2}$.

An example of an interaction function that can not be realised using coupling of the form 3.4 is a phase model with interaction function [Bick et al., 2016]

$$\begin{aligned} H(\theta_\ell - \theta_j, \theta_k - \theta_j) = &\cos(\theta_\ell + \theta_k - 2\theta_j + \Delta\tau) \\ &+ \cos(2\theta_\ell - \theta_k - \theta_j + \Delta\tau). \end{aligned} \tag{3.46}$$

The problem with Equation 3.46 is that the phase differences $\theta_\ell + \theta_k - 2\theta_j$ and $2\theta_\ell - \theta_k - \theta_j$ use the same three phases, and thus the same coupling parameters.

[1] We used Matlab's `fmincon` method to minimize $\sum \kappa_{pq}$ starting at a set of random vectors with values between 0 and T using the additional constraints that $0 \leq \tau_{pq} \leq T$.

Chapter 4

Experimental results

In this chapter, we apply the coupling we designed and introduced in Chapter 3 to four Brusselators. In Section 4.1 we find coupling parameter sets that satisfy the constraints derived in Section 3.2. We then present the data resulting from simulations using two of the coupling parameter sets we found, and describe how we made the bifurcation plots in Section 4.2. These bifurcation plots show at which delays $\Delta\tau$ the splay and in-phase configurations become unstable. We also derived these bifurcation plots for the target interaction functions in Sections 1.8 and 1.9. In Section 4.3 we compare the resulting bifurcation plots from Section 4.2 to the bifurcation plots for the target phase models.

4.1 coupling parameter sets

Using our optimisation algorithm we find several coupling parameter sets that satisfy the constraints. For the pairwise target interaction function (1.12) we found two sets of coupling parameters using this routine. For the nonpairwise target interaction function (1.32) we found 19 parameter sets. They can be found in Table A.1 in Appendix A. The two parameter sets we found for the pairwise target model are shown in Table 4.1.

We have to pick one coupling parameter set at the time and run simulations where we apply the coupling (3.2) with (3.4) using those parameters to control a population of $N = 4$ Brusselator oscillators. Our optimisation method finds several

Table 4.1: The coupling parameters found using the constraints found above. Parameter set 2 is similar to the set found by [Rusin et al., 2010].

set	τ_{10}	τ_{20}	κ_{10}	κ_{20}
1	1.4823	5.3072	0.706	6.4606
2	5.3409	1.9873	2.4955	4.5012

coupling parameter sets that result in convergence to in-phase oscillations at the expected overall delays. However, the optimisation also finds coupling parameter sets that do not result in the expected convergence. Thus we can find coupling parameter sets that satisfy the constraints, and produce the desired collective behaviour in the Brusselators. But we also find coupling parameter sets that satisfy the constraints, but do not produce the desired collective behaviour in the Brusselators when we use them to run the simulations instead.

We simulate each of the nonpairwise coupling parameter sets found to make sure that at an overall delay $0 < \alpha \ll 1$, we observe convergence towards in-phase synchronisation. We apply the coupling to $N = 4$ Brusselators, calculate their phases using isochron data (see Figure 1.8), and from this calculate the order parameter $R_1(t)$ (given by Equation 1.9). Then we check the convergence to in-phase synchronisation where $R_1(t) = 1$.

We pick the nonpairwise parameter sets that have stronger convergence to in-phase for $\alpha = 10^{-8}$ and use those in our further analysis below. These sets are enumerated 2, 3, 5, 7, 9, 10, 11, 12, 13, and 18. Of these sets, we found that sets 2, 3, 7, 12, 13, and 18 have a bifurcation of in-phase close to the expected bifurcation value of $\Delta\tau \approx 0.6143$ (see Section 1.9). In addition to this, we checked the bifurcation value of splay configuration and found that sets 2, 3, 7, 12, and 13 have a bifurcation value close to the expected bifurcation value of splay of $\Delta\tau \approx 1.5708$ (see Section 1.9). Thus 5 out of the 19 coupling parameter sets that satisfied the constraints (3.18-3.25) result in approximately the same bifurcations in in-phase and splay configuration as the target phase model. In the following section, we show these results for two of these coupling parameter sets, namely, coupling parameter sets 1 and 2 (see Table A.1).

Figure 4.1: These figures have many data points, which makes it difficult to analyse convergence from them. The plots show the order parameter R_1 for different overall delays $\Delta\tau$ using coupling parameter sets 1 (top) and 2 (bottom) as in Table A.1 for the nonpairwise target interaction function (3.45), for 4 Brusselators starting close to in-phase configuration.

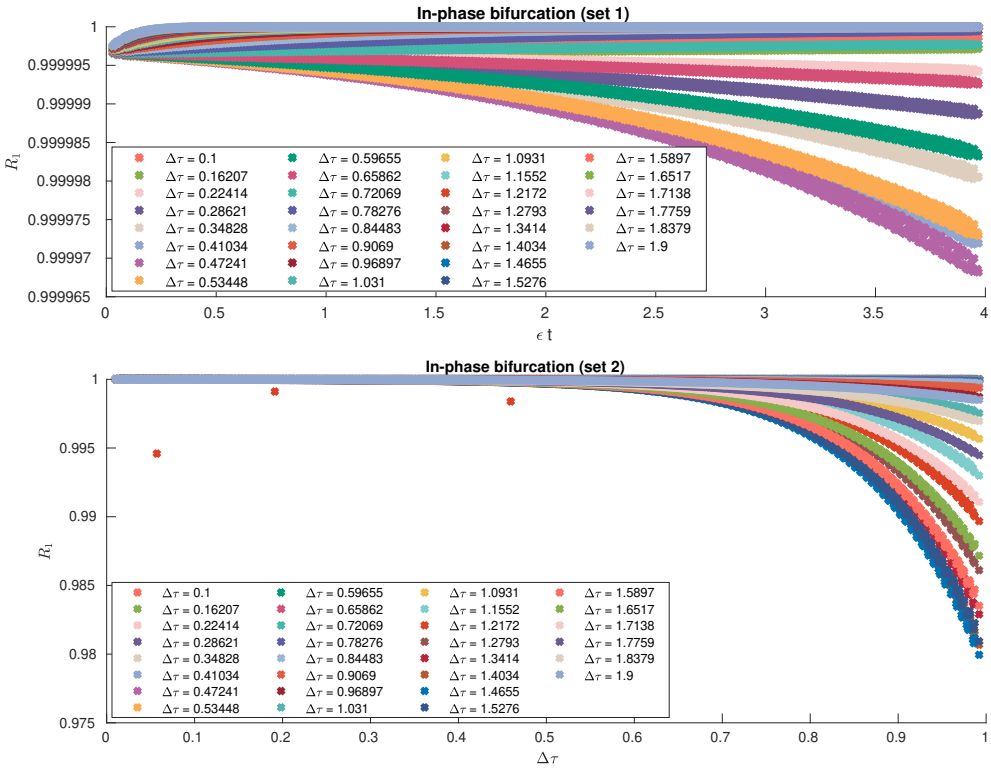

4.2 Results of simulating controlled Brusselators

In this Section we give the results using coupling parameter sets 1 and 2 (see Table A.1), for which the bifurcation looks very different. Each Figure in this section contains plots for both coupling parameter sets. One of these two coupling parameter sets has bifurcations for both in-phase bifurcation and splay bifurcation as expected from the target phase model.

In this section, we include Figures showing the data used to produce the bifurcation plots in Chapter 3. We also include bifurcation plots for a set of coupling parameters that satisfies the constraints we introduced in Chapter 3 (given by Equations 3.18-3.25) but do not result in controlled Brusselators showing bifurcations similar to what we expect from studying the target phase model.

Recall that in Chapter 3, the nonpairwise coupled Brusselators use the coupling parameters from set 2 in Table A.1. We now show data for parameter set 1

Figure 4.2: We use the slopes of these lines to analyse convergence to in-phase. Plots of $\log(1 - R_1)$ showing the convergence of order parameter R_1 for different overall delays $\Delta\tau$. The colours match Figure 4.1, and represent the different overall delays $\Delta\tau$. Dashed black lines are the fitted lines for each $\Delta\tau$.

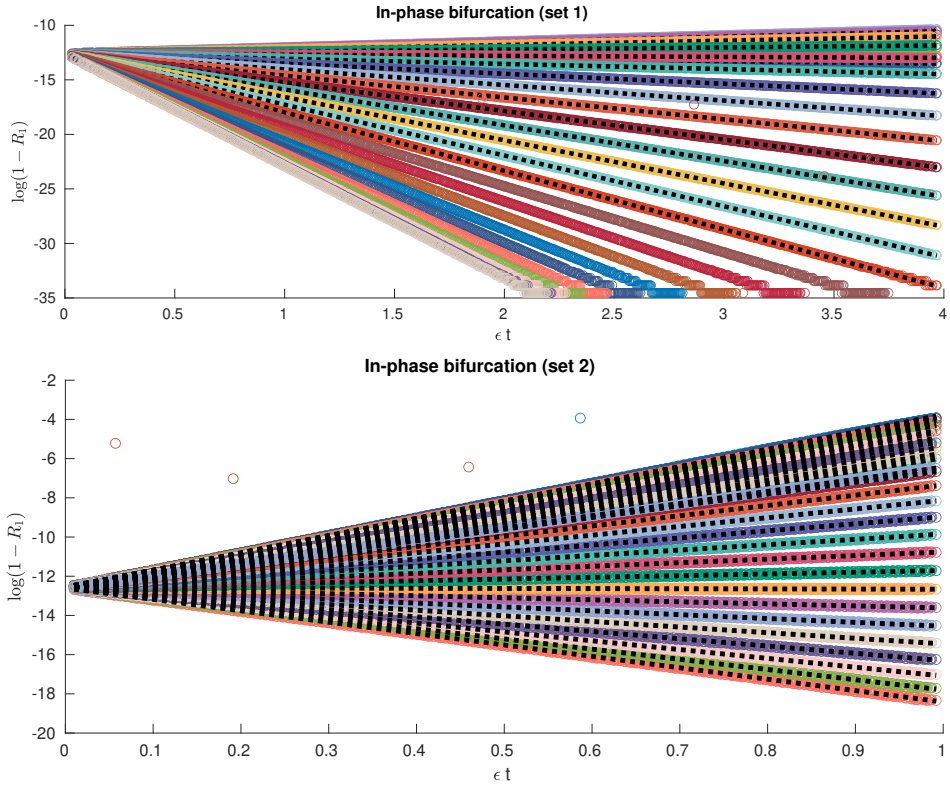

Figure 4.3: Negative values indicate convergence towards in-phase configuration. Bifurcation plot showing the slope of the fitted lines in Figure 4.2 versus the overall delay $\Delta\tau$. Dotted lines are plotted where the curves cross the horizontal axis.

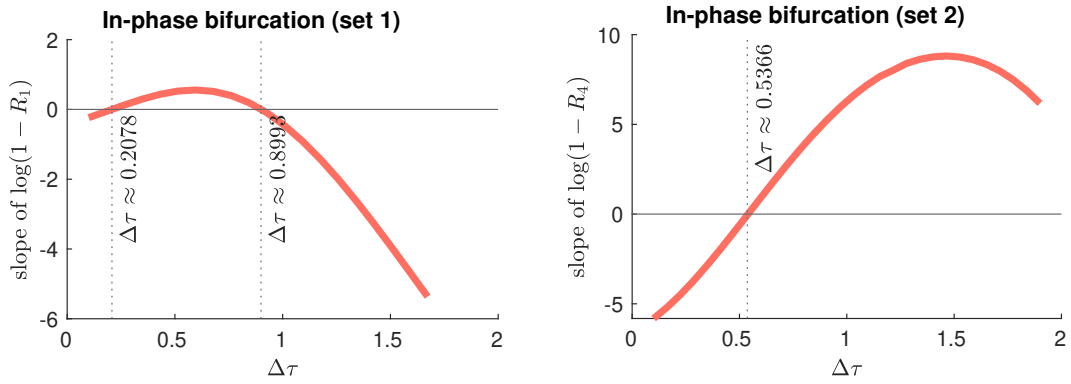

Figure 4.4: These figures have many data points, which makes it difficult to analyse convergence from them. Order parameter R_4 for different overall delays $\Delta\tau$ using parameter set 1 (top) and 2 (bottom) as in Table A.1 for the nonpairwise target interaction function (1.32), controlling $N = 4$ Brusselators starting close to splay configuration.

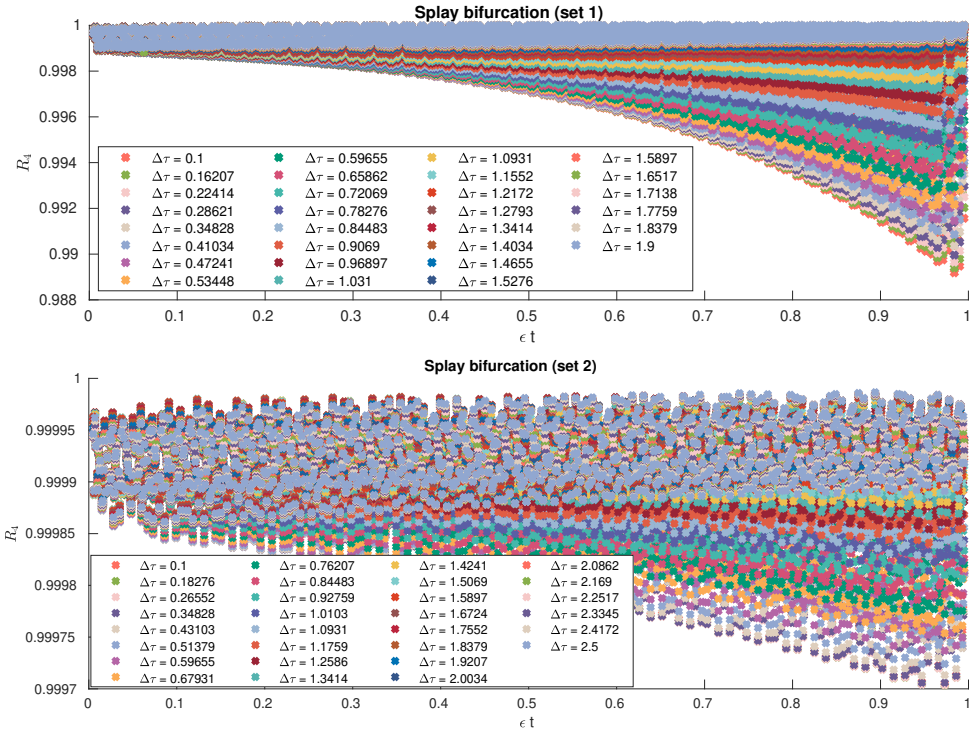

Figure 4.5: Plots of $\log(1 - R_1)$ showing the convergence of order parameter R_4 for different overall delays $\Delta\tau$. The colours match Figure 4.4, and represent the different overall delays $\Delta\tau$. Dashed black lines are the fitted lines for each $\Delta\tau$. The bottom plots show the first and last trajectory and fitted lines for clarity.

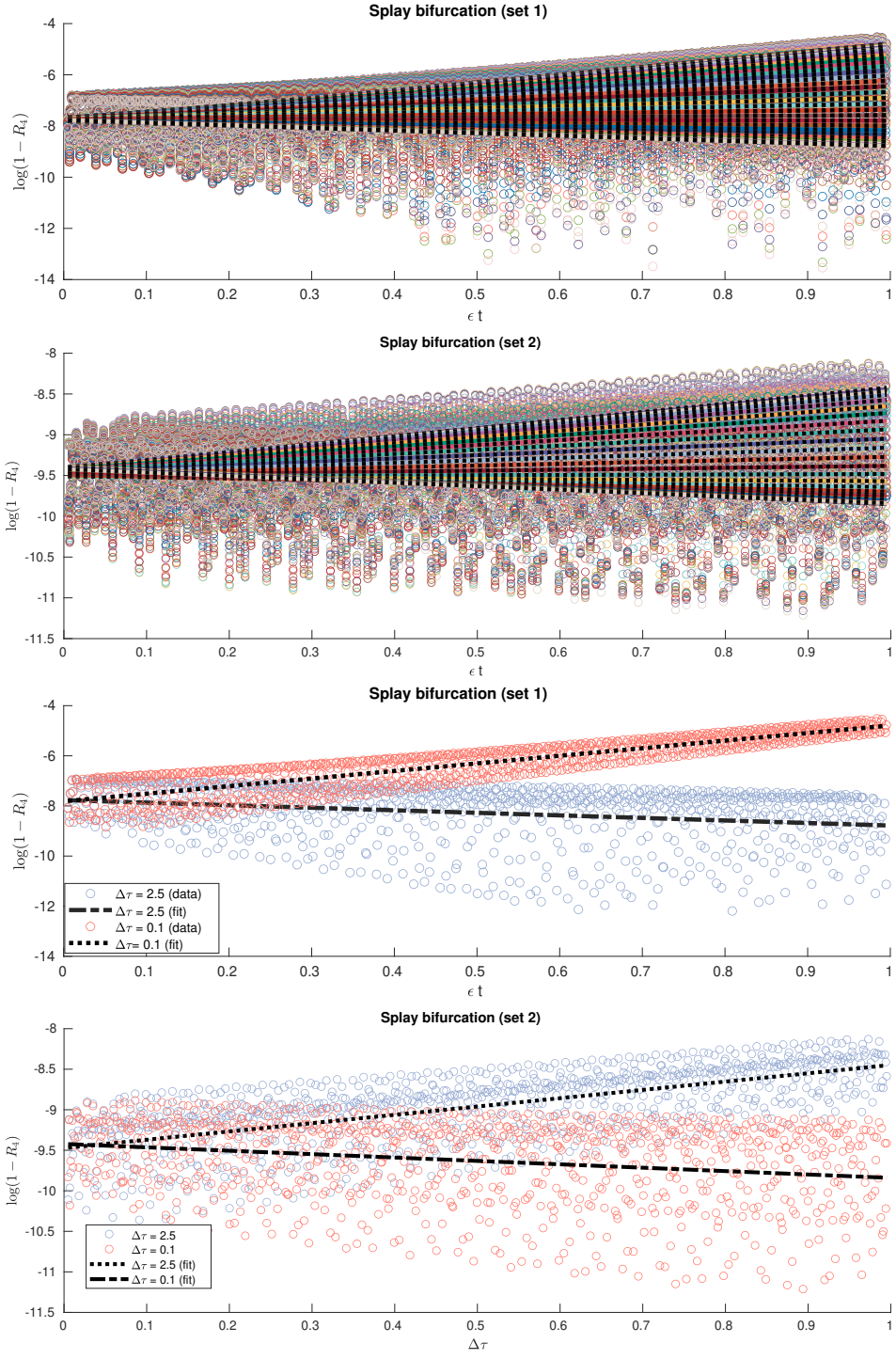

Figure 4.6: Negative values indicate convergence towards splay configuration. Bifurcation plot showing the slope of the fitted lines in Figure 4.5 versus the overall delay $\Delta\tau$. Dotted lines are plotted where the curves cross the horizontal axis.

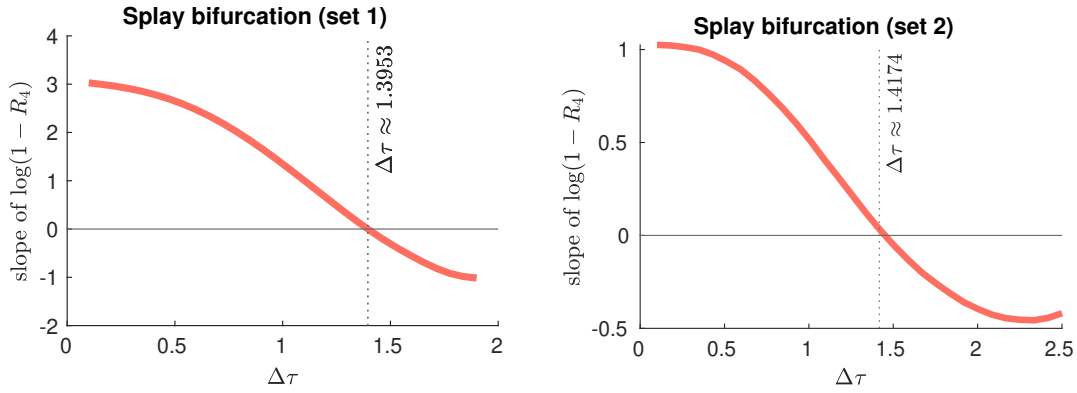

in Table A.1.

Figure 4.1 shows the order parameter $R_1(t)$ versus time ϵt for different overall delays $\Delta\tau$ for $N = 4$ Brusselators controlled using coupling parameter set 1 from Table A.1 and coupling form (3.4). We used initial conditions close to in-phase solutions, e.g. where $R_1(0)$ is close to 1. We then simulate the delayed differential equations using Matlabs *dde23* for 30 equally distributed delays between 0.1 and 1.9. Figure 4.1 shows that some of the trajectories move away from $R_1 = 1$, while others seem to move towards R_1.

To show this more clearly, we calculate $\log(1 - R_1)$ and plot this in Figure 4.2. On top of the data in Figure 4.2, we plotted dashed lines representing lines fitted to the data. We use the slopes of these lines to produce a bifurcation diagram in Figure 4.3. From the bifurcation analysis of the target phase model (see Section 1.9 used to find the coupling, we expect that the in-phase solution is stable for $0 < \Delta\tau \lessapprox 0.6143$ and stable for $0.6143 \lessapprox \Delta\tau < \pi$. However, Figure 4.3 shows that the stability of the in-phase solution looks very different for the controlled oscillators when using coupling parameter set 1 (from Table A.1). Figure 4.3 implies that in-phase configuration is stable for $0 < \Delta\tau \lessapprox 0.2078$, and for $0.8993 \lessapprox \Delta\tau < \pi$, while it is unstable in between. Comparing this to the behaviour of the trajectory starting close to in-phase configuration in the target phase model to Figure 1.6 indicates that the collective behaviour does not match close to in-phase configuration.

We applied the same analysis to the order parameter R_4 after running simulations starting close to splay configuration, e.g. with $R_4(0)$ close to 1, for coupling parameter set 1 (from Table A.1). Thus Figure 4.4 shows the order parameter $R_4(t)$ versus scaled time ϵt, Figure 4.5 shows the closeness to 1 of R_4 on a log scale, and Figure 4.6 shows the slopes of the lines fitted to the data in Figure 4.5.

We conclude that the bifurcation of splay configuration is similar to those where we used coupling parameter set 2 from Table A.1.

4.3 Comparing simulations to bifurcation analysis

In this section, we compare the bifurcations of the Brusselators that we controlled using a nonpairwise target interaction function to the bifurcations in the target phase model. There are several steps in obtaining the bifurcation diagrams in this section, which we explained in more detail in Section 1.8. The basic idea is that we first calculate the order parameters R_1 (for in-phase) and R_4 (for splay) as described in Section 1.6 for trajectories corresponding to a range of overall delays $\Delta\tau$. Secondly, we calculate how close these order parameters are to 1, e.g. how close R_1 is to 1 to confirm convergence to in-phase and how close R_4 to 1 to confirm convergence to splay. We consider the rate of convergence given by the slope of $\log(1-R_1)$ and $\log(1-R_4)$. Thus we get a value for each delay $\Delta\tau$ that can be interpreted as follows. A negative value of the slope means that trajectories converge to a configuration with $R_1 = 1$, respectively $R_4 = 1$. A positive value of the slope means that trajectories do not converge to a configuration with $R_1 = 1$, respectively $R_4 = 1$.

For the pairwise and nonpairwise target phase models, we reproduce the plots obtained in Section 1.9 and combine them with plots similar to those in Section 1.8, but now for $N = 4$ oscillators. These plots show that when adding the nonpairwise interaction term as described in Section 1.9, there is a shift in the stability of in-phase configuration (left figure) from $\Delta\tau \approx 1.0471$ to $\Delta\tau \approx 0.6143$. The bifurcation of splay configuration (right figure) does not shift when we add the

Figure 4.7: Phase model simulations showing the bifurcation points of in-phase (left) and splay (right) configuration for the pairwise and nonpairwise target phase models (1.32,1.33). Negative values correspond to stability of in-phase (left) or splay (right) configuration.

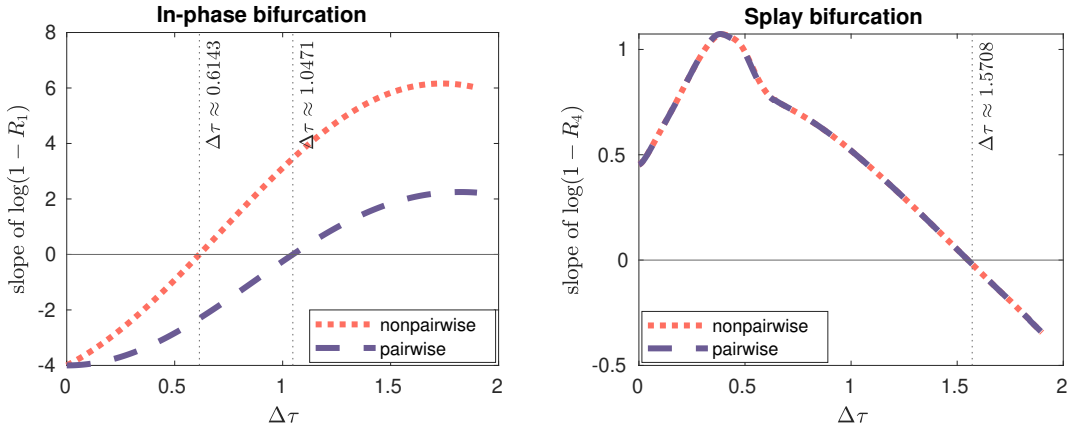

Figure 4.8: Brusselator simulations showing the bifurcation points of in-phase (left) and splay (right) configuration for $N = 4$ Brusselators with coupling designed using the pairwise and nonpairwise target phase models (1.32,1.33). We compare the zeroes (e.g. the bifurcation points) to those in Figure 4.7.

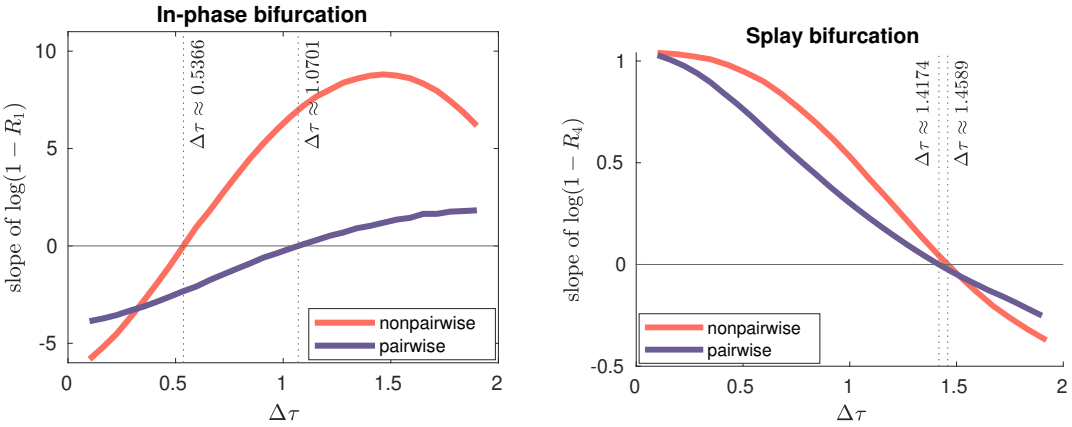

nonpairwise term and stays at $\Delta\tau \approx 1.5708$.

For the controlled Brusselators, we produced plots similar to Figure 2.3 to show the convergence to in-phase (left) and splay (right) configurations. We compare the Brusselators that used coupling parameters fitted to the pairwise target phase model, to the Brusselators that used coupling fitted to the nonpairwise target phase model. We are interested in the bifurcation points, that is, the value of $\Delta\tau$ where the curves cross the horizontal axis. These bifurcation points should shift (in-phase) or not shift (splay) similar to the target interaction function used. We observe that the bifurcation points (indicated by vertical lines) are similar to

those in Figure 4.7.

We conclude that our optimisation finds coupling parameter sets that show that our nonpairwise synchronisation engineering works according to the metrics we used. The bifurcation of the in-phase configuration shifted in the right direction when adding nonpairwise terms, as expected. The bifurcation of the splay configuration does not shift when adding nonpairwise terms, as expected.

Chapter 5

Discussion

There are different ways to control the collective behaviour of oscillatory networks, including distributed control [Gambuzza et al., 2019], model predictive control [Bagheri et al., 2007]. The advantage of phase reduction-based methods [Monga et al., 2019, Efimov et al., 2009, Kiss, 2018] compared to other types of control for the collective behaviour of oscillatory networks, is that the theory to design the coupling is developed independently of what type of oscillator is controlled. The aim is to match the population's phase reduction to a phase model that has the desired collective behaviour. The coupling given by Equation 3.4 (nonpairwise) or Equation 2.10 (pairwise), is designed in such a way that several parameters allow for tuning the coupling to a pairwise coupled phase model. Finding the coupling to control the oscillators is reduced to an optimisation problem. A phase response curve and a waveform are the only inputs that are particular to the oscillators for this optimisation problem. Phase response curves and waveforms can typically be derived or computed from data.

Reducing an oscillator to its phase representation holds for isolated limit cycle oscillators, and is only an approximation when we instead consider a system of coupled oscillators. As long as the coupling between the oscillators is weak enough in comparison to the rate of attraction to the cycle, then the phase reduction should be a good approximation for the collective behaviour of the system [Izhikevich and Kuramoto, 2006]. We thus need to make sure that we are actually in the "weak enough" regime when we apply our coupling. The different

terms in our designed coupling (3.4) contribute with varying gains to the coupling, and we use a coupling strength parameter to control the overall coupling strength. What we can do to check if the coupling is weak enough, is to first of all check that all oscillators have trajectories close to their original limit cycles in phase space.

If their trajectories are far away from the original limit cycles, then the phase reduction might not be valid anymore, and we can systematically decrease the coupling strength. We then choose the overall coupling strength ϵ such that when decreasing the coupling strength further we do not observe a change in the collective behaviour we study. Changing ϵ should only have the effect that it takes $\epsilon_{old}/\epsilon_{new}$ times longer, but the oscillators should follow the same trajectories along scaled time ϵt.

Alternatives to first-order phase reduction that allow for non-weak coupling include control using isostable reduction [Wilson, 2022, Wilson and Moehlis, 2016], local orthogonal rectification [Letson and Rubin, 2018, Letson and Rubin, 2020, Letson and E. Rubin, 2020], phase-amplitude description [Wedgwood et al., 2013].

There are many extensions of the Kuramoto model [Rodrigues et al., 2016] that could be considered as target phase models. In biological applications, purely deterministic models have limited applicability. Thus it is often important to include the effects of noise within or added to the system. It will be a challenge to design coupling for the stochastic Kuramoto model [Pikovsky, 2015, Pérez-Cervera et al., 2023].

5.1 Type of oscillators

We can clearly try the method on different classes of oscillators [Bick et al., 2020], for example, relaxation oscillators [Izhikevich, 2005]. The type of oscillator can have an effect on which (non)pairwise terms in the target interaction function we can control. Applying the method to different types of oscillators We expect that as long as we can find a phase reduction, we can apply the synchronisation engineering method. From a practical point of view, the coupling has to be weak

enough for the phase reduction to be a valid approximation, yet strong enough to observe the changes in collective behaviour in for example the lifetime of a biological oscillator. These two conditions might be hard to balance for certain combinations of oscillator type and desired collective behaviour.

There are some limitations that make the nonpairwise synchronisation engineering unsuitable to control oscillators whose phase response curve does not have a second or higher harmonic, but for example controlling FitzHugh-Nagumo [Nagumo et al., 1962] oscillators, which is an example of a relaxation oscillator, would be an interesting next step. There is no requirement for the coupling to be applied to a system of identical oscillators. Thus possible future research could include controlling a population comprising different types of oscillators, or oscillators that are nonidentical in that they have slightly different natural frequencies. It could be interesting to look into if (nonpairwise) synchronisation engineering can be applied to chaotic or noisy oscillators as well. Notions of phase [Pikovsky et al., 2001] and phase reduction [Schwabedal and Pikovsky, 2010] exist for these types of oscillators, but challenges remain [Thomas and Lindner, 2014, Pikovsky, 2015] and further research is required before applying synchronisation engineering to this type of oscillators.

5.2 Accuracy of the phase response curve

To find the coupling parameters, we use the phase response curve of the oscillators [Smeal et al., 2010, Cestnik and Rosenblum, 2018, Cestnik et al., 2022]. It would be interesting to find out how sensitive our method is to find a good approximation of the phase response curve. It might be the case that only particular properties of the phase response curve are important when it comes to introducing the collective behaviour from the target interaction function. Knowing how accurate the phase response curve needs to be would be an advantage in experiments where there are limited possibilities to calculate an accurate phase response curve, or where the calculation is time-consuming.

5.3 Stronger coupling

The phase reduction techniques used for synchronisation engineering so far are only valid when the coupling is weak. In order to apply synchronisation engineering to problems requiring stronger coupling, second (or higher) order phase reduction techniques [Gengel et al., 2021, von der Gracht et al., 2023, Bick et al., 2023a] may be appropriate. These higher-order phase reductions are difficult to compute explicitly even for relatively simple oscillators. Although designing coupling using these higher-order phase reductions for Brusselator oscillators is unfeasible with current higher-order phase reduction methods, using (classical) synchronisation engineering on Stuart-Landau or other oscillators could be doable. Where using first-order phase reduction we had relative freedom in which oscillators we could control, we would be much more restricted in our choice of oscillator when using higher-order phase reduction techniques.

While first-order phase reductions break down when the coupling is too strong, we made another approximation that relies on the coupling being weak. We used Equation 3.5 to write $x(\theta(t-\tau_{pq})) = x(\theta(t)-\omega\tau_{pq})$ in the coupling design. While this is valid for free-running oscillators, and should be a good approximation for oscillators that are only weakly perturbed, it might not be valid for stronger coupling.

The different values of $\Delta\tau$ for the bifurcations when comparing the target phase model to the controlled Brusselators might be due to a shift in bifurcation due to the phase reduction and the free-running oscillator approximations described above. To find the locations of the bifurcations in the system of controlled Brusselators and better understand this shift in bifurcation values, we could analyse the delayed differential equations we simulated by linearising the delayed differential equations or using tools such as DDEBiftool [Engelborghs et al., 2000].

5.4 Population size

We looked at controlling the nonpairwise interactions between four oscillators to demonstrate the method, but the coupling is easily scaled to be applied to larger populations of oscillators. The coupling parameters can be found independently of the number of oscillators to which we apply the coupling. Thus before we apply coupling to large populations, we have the option to validate the choice of parameters using a smaller number of oscillators and confirm that their collective behaviour matches the target phase model for this smaller number of oscillators. Changing the (number of) nonlinear oscillators that we want to control only requires minimal adaptations as the coupling parameters do not depend on the number of oscillators we control.

5.5 Non-global coupling

There are several ways in which (classical) synchronisation engineering could be generalised. The theory of synchronisation engineering does not restrict us to using all-to-all global coupling. We could apply the method to weighted and/or directed graphs as well.

Previously Chimera states [Bick and Ashwin, 2016, Ashwin and Burylko, 2015] were controlled using synchronisation engineering using for example coupling that depends on whether or not oscillators are in the same "population' [Martens et al., 2016, Bick et al., 2017]. It would be interesting to use synchronisation engineering to control nonpairwise interactions to introduce collective behaviour with heteroclinic switching between chimeras [Bick, 2018, Bick, 2019].

This increases the number of constraints we would need to solve in order to design the coupling. The optimisation problem depends on the number of different types of coupling that we would like to introduce. We have considered only one type of coupling function $H(.)$ for each (pairwise/nonpairwise) phase model. Suppose we instead consider an interaction function that differs depending on the oscillators affected. Suppose we would consider two types of coupling, one type

of coupling for certain pairs of oscillators, and another type for all other pairs of oscillators, which we could write as

$$H(\theta_\ell - \theta_j, \theta_k - \theta_j) = \begin{cases} H^1(\theta_\ell - \theta_j, \theta_k - \theta_j) & \text{if } \ell, k, j \text{ meet some condition} \\ H^2(\theta_\ell - \theta_j, \theta_k - \theta_j) & \text{otherwise} \end{cases}, \tag{5.1}$$

where $H^1(.)$ and $H^2(.)$ are two different interaction functions. Then this results in an optimisation problem with twice as many constraints as well as twice as many parameters to satisfy those constraints. It is in principle not a problem to have more constraints since we also have more parameters to satisfy the constraints. In general, we could pick an interaction function $H^{\ell,k,j}(.)$ that gives a different value for each oscillator combination ℓ, k, j through for example a nontrivial adjacency matrix.

5.6 Type of interaction function

We considered smooth target interaction functions that are the same for all pairs/triplets of oscillators and do not vanish. However, there exist oscillators including some neuronal oscillators, that have a refractory period during which the oscillator is insensitive to external signals. Refractory mechanisms can help tune synchronisation [Wiedemann and Lüthi, 2003]. The periods of insensitivity to external signals can be described using interaction functions that vanish for certain oscillator states. Such interaction functions with “dead zones” can change the effective coupling graph depending on the state of the system [Ashwin et al., 2019].

To apply synchronisation engineering using (nonpairwise) target interaction functions with “dead zones” would require editing the form of the coupling accordingly. The interaction function would (almost) vanish in an (approximate) dead zone, which depends on the oscillator state. Having several different interaction functions does not require any redesign of synchronisation engineering and we can find the coupling parameters for each interaction function separately.

We need to however make sure that we are able to check any “are we in a dead zone” conditions in the nonlinear system to determine whether or not to apply the coupling. The relation between dead zones in nonlinear systems and phase reductions has been studied previously [Ashwin et al., 2021], giving a potential starting point in finding out if particular (approximate) dead zones can be introduced to a population of oscillators using synchronisation engineering.

Recall that to control certain harmonics using synchronisation engineering, we need corresponding harmonics in the phase response curve to be nonzero. The advantage of oscillators with dead zones is that they typically have phase response curves with many nonzero Fourier coefficients.

5.7 Measuring the collective behaviour

We used order parameters to asses whether synchronisation engineering produces the desired collective behaviour. Using simulations of the oscillators we controlled, we were able to observe all variables and find the asymptotic phase for all oscillators at all times. When this is not possible, then looking at the order parameters as a measure of the collective behaviour might not be applicable, and requires finding a way of measuring the collective behaviour specific to the type of oscillators. Regardless of the type of oscillators we want to control, we might want to study types of collective behaviour that require different measures of collective behaviour. When we for example would like to introduce collective behaviour such as Chimera states, travelling waves or chaos, we might need to look at the order parameters differently [Bayani et al., 2022].

5.8 Systems with interactions already present

Synchronisation engineering assumes that we can design all interactions in the system of oscillators. In future research, we could assume that some interactions are already present in the system, and only design additional coupling rather

than all interactions. When applying control to for example populations of biological oscillators, we might want to apply the control on top of interactions already present. A starting point could be to assume a system already has pairwise interaction present and design the coupling to add nonpairwise interactions as in the target phase model with nonpairwise interaction function (1.32).

5.9 Optimisation algorithm

We used Matlab's *fmincon* optimisation algorithm to find coupling parameters satisfying the constraints for the Fourier coefficients of the interaction function, phase response curve and the coupling. There are however other options for finding these coupling parameters. In some cases (such as when the waveform is harmonic), we were able to find coupling parameters analytically (see Appendix B.3.

To find parameters for the nonpairwise phase model, we changed to the Sequential Quadratic Programming (SQP) [Gill et al., 1997] algorithm (in Matlabs *fmincon*) as the default "interior-point" algorithm did not find any parameters for certain nonpairwise target phase models including the one discussed in this thesis. For the pairwise target phase models that we tried, we found the same coupling parameter sets for both algorithms.

Apart from finding coupling parameter sets or not, it would be interesting to look into different optimisation methods such as genetic algorithms [Whitley, 1994], simulated annealing [Gendreau and Potvin, 2019] or particle swarm optimisation [Gad, 2022] that might have better or faster performance. Faster performance would be especially relevant when using synchronisation engineering to control oscillators with a relatively short lifetime. In such systems we would need to (1) find the phase response curve, (2) calculate the coupling parameters, (3) apply the coupling and (4) observe the collective behaviour before the oscillation dies out.

Decreasing the time to find the coupling parameters would become especially relevant when considering large nontrivial adjacency matrices or many different

interaction functions. Depending on the size of the adjacency matrix or the number of interaction functions, this might greatly increase the run time, making it attractive to look for other methods. Running the optimisations for different interaction functions in parallel could be an option, as well as making more educated guesses for the initial conditions. For example by looking at similar interaction functions or similar oscillators.

Appendix A

coupling parameter sets

Table A.1 shows the coupling parameter sets for a nonpairwise target interaction function (1.32) that we found using an optimisation algorithm.

Table A.1: The coupling parameter sets found for the nonpairwise target interaction function (1.32) using constraints (3.18-3.25) with $\delta = 10^{-2}$. We found that 5 of these coupling parameter sets (enumerated 2,3,7,12,13, highlighted green) match the convergence to in-phase as well as to splay with the target interaction function. Parameter set 18 (yellow) matches the in-phase behaviour, but not that of splay. Parameter sets 5,9,10,11 converged to in-phase faster than in the pairwise case at $\Delta\tau = 10^{-8}$, but had a bifurcation for in-phase at values of $\Delta\tau$ far from the bifurcation of the target phase model. Note that only entries with nonzero corresponding κ_{pq} are shown. (See Chapter 3)

set	τ_{10}	τ_{01}	τ_{20}	τ_{02}	τ_{30}	τ_{03}	τ_{12}	τ_{21}	τ_{11}
1			5.2157		1.9993		3.8664		2.6426
2		1.5233			2.0379	2.9224	5.3795	5.4419	2.2030
3		2.7619			2.0380	1.5448	5.3794	5.4423	2.2030
4		3.4524	2.3046		5.2539	5.5903	1.3767	1.2808	2.3673
5		4.6141		3.0533	2.0306		5.3783	1.3076	2.2120
6		5.3745	2.3044		5.2537	3.4428	1.3769	1.2808	2.3673
7		6.4276	1.0572		2.0749		5.3817	3.4991	2.2078
8	1.7044		0.1543		5.3936		3.7065	5.6995	2.5769
9	1.9063	4.4121					5.3707	1.3152	2.2047
10	1.9205						5.3794	1.3069	2.2035
11	1.9240						5.3810		2.2030
12	3.2441				1.9941		5.3944		2.2075
13	3.2623				1.9973		5.3944	3.5028	2.2093
14	3.3521		2.2746		5.3697		1.3292		2.3671
15	5.0264	1.4664		5.0540	5.4876		1.9860	3.5299	2.5108
16	5.2253		2.1830		3.1501		1.3317		2.3668
17	5.2499	4.3565	3.8158		2.5366		1.3348	1.2729	2.3670
18	5.2699	0.9954		2.2890	2.0541	3.5262		5.4214	2.2162
19	5.4222	5.8491		2.2994	1.9026	1.5012	3.7117	3.7042	2.5782

set	κ_{10}	κ_{01}	κ_{20}	κ_{02}	κ_{30}	κ_{03}	κ_{12}	κ_{21}	κ_{11}
1	5.3470		9.9100		3.7961		15.4954		17.8627
2		0.1287			2.5358	0.0992	12.8918	0.6968	20.4847
3		0.1263			2.5358	0.1068	12.8925	0.6961	20.4851
4		1.4524	3.3483		2.8111	1.1458	4.4623	4.8852	16.5051
5		0.2184		0.1572	2.4620		12.6053	0.7762	20.1206
6		1.4584	3.3482		2.8117	1.2300	4.4647	4.8833	16.5051
7		0.0607	0.3581		2.6258		13.4069	0.2616	20.4759
8	7.6452		5.6236		7.1415		11.6786	0.0804	18.9612
9	3.0616	0.0798					13.2991	0.3302	20.2649
10	3.0925						13.5129	0.0804	20.4258
11	3.1186						13.5996		20.4700
12	0.2267				2.6380		13.4774		20.5351
13	0.2122				2.6289		13.4207	0.0804	20.5305
14	1.6194		3.0045		3.9931		9.2731		16.5178
15	1.5935	3.3076		6.2365	2.2266	3.7720	9.0075	16.0834	20.1416
16	5.1070		2.7287		1.6369		9.2820		16.5190
17	6.0755	0.1370	1.6694		2.7742		8.7785	0.5093	16.5184
18	3.9264	4.6584		2.9005	2.3951	3.6355		13.3385	20.6709
19	4.8768	2.1712		0.4637	3.1858	1.7029	4.3011	7.4329	18.9405

Appendix B

Nonpairwise feedback: Fourier coefficients

We derive the expressions for the nonpairwise feedback for $S = 2$, and give an example of deriving the gain and delay parameters by hand.

B.1 Finding second order Fourier coefficients

For $S = 2$ we get

$$g(\phi_g, \phi_j) = \kappa_{00} + \kappa_{01}[x(\phi_j - \omega_j\tau_{01}) - a_0] + \kappa_{10}[x(\phi_g - \omega_j\tau_{01}) - a_0] \tag{B.1}$$

$$+ \kappa_{02}[x(\phi_j - \omega_j\tau_{02}) - a_0]^2 \tag{B.2}$$

$$+ \kappa_{11}[x(\phi_g - \omega_g\tau_{11}) - a_0] \cdot [x(\phi_j - \omega_j\tau_{11}) - a_0] \tag{B.3}$$

$$+ \kappa_{20}[x(\phi_g - \omega_g\tau_{20}) - a_0]^2 \tag{B.4}$$

Now expand the waveform in its Fourier coefficients $x(\phi) = \sum_l a_l e^{-il\phi}$ to obtain

$$\begin{aligned}
g(\phi_g, \phi_j) =& \kappa_{00} + \kappa_{01} \sum_{l\neq 0} a_l e^{-il(\phi_j - \omega_j \tau_{01})} + \kappa_{10} \sum_{l\neq 0} a_l e^{-il(\phi_g - \omega_j \tau_{10})} \\
&+ \kappa_{11} \sum_{l\neq 0} a_l e^{-il(\phi_g - \omega_g \tau_{11})} \cdot \sum_{l\neq 0} a_l e^{-il(\phi_j - \omega_j \tau_{11})} \\
&+ \kappa_{02} \left[\sum_{l\neq 0} a_l e^{-il(\phi_j - \omega_j \tau_{02})}\right]^2 + \kappa_{20} \left[\sum_{l\neq 0} a_l e^{-il(\phi_g - \omega_g \tau_{20})}\right]^2 \\
=& \kappa_{00} + \kappa_{01} \left(a_1 e^{-i(\phi_j - \omega_j \tau_{01})} + a_2 e^{-2i(\phi_j - \omega_j \tau_{01})} + \text{c.c} + \mathcal{O}(3)\right) \\
&+ \kappa_{10} \left(a_1 e^{-i(\phi_g - \omega_g \tau_{10})} + a_2 e^{-2i(\phi_g - \omega_g \tau_{10})} + \text{c.c} + \mathcal{O}(3)\right) \\
&+ \kappa_{11} \left(a_1 e^{-i(\phi_g - \omega_g \tau_{11})} + a_2 e^{-2i(\phi_g - \omega_g \tau_{11})} + \text{c.c} + \mathcal{O}(3)\right) \\
&\cdot \left(a_1 e^{-i(\phi_j - \omega_j \tau_{11})} + a_2 e^{-2i(\phi_j - \omega_j \tau_{11})} + \text{c.c} + \mathcal{O}(3)\right) \\
&+ \kappa_{02} \left[a_1 e^{-i(\phi_j - \omega_j \tau_{02})} + a_2 e^{-2i(\phi_j - \omega_j \tau_{02})} + \text{c.c} + \mathcal{O}(3)\right]^2 \\
&+ \kappa_{20} \left[a_1 e^{-i(\phi_g - \omega_g \tau_{20})} + a_2 e^{-2i(\phi_g - \omega_g \tau_{02})} + \text{c.c} + \mathcal{O}(3)\right]^2,
\end{aligned}$$

where c.c denotes the complex conjugate. Assuming identical oscillators, $\omega_g = \omega_j$

$$\begin{aligned}
g(\phi_g, \phi_j) =& \kappa_{00} + \kappa_{01} \left(a_1 e^{-i(\phi_j - \omega \tau_{01})} + a_2 e^{-2i(\phi_j - \omega \tau_{01})} + \text{c.c} + \mathcal{O}(3)\right) \\
&+ \kappa_{10} \left(a_1 e^{-i(\phi_g - \omega \tau_{10})} + a_2 e^{-2i(\phi_g - \omega \tau_{10})} + \text{c.c} + \mathcal{O}(3)\right) \\
&+ \kappa_{11} \left(a_1 e^{-i(\phi_g - \omega \tau_{11})} + a_2 e^{-2i(\phi_g - \omega \tau_{11})} + \text{c.c} + \mathcal{O}(3)\right) \\
&\cdot \left(a_1 e^{-i(\phi_j - \omega \tau_{11})} + a_2 e^{-2i(\phi_j - \omega \tau_{11})} + \text{c.c} + \mathcal{O}(3)\right) \\
&+ \kappa_{02} \left[a_1 e^{-i(\phi_j - \omega \tau_{02})} + a_2 e^{-2i(\phi_j - \omega \tau_{02})} + \text{c.c} + \mathcal{O}(3)\right]^2 \\
&+ \kappa_{20} \left[a_1 e^{-i(\phi_g - \omega \tau_{20})} + a_2 e^{-2i(\phi_g - \omega \tau_{20})} + \text{c.c} + \mathcal{O}(3)\right]^2
\end{aligned}$$

Now finding the coefficients of the 2-dimensional Fourier series of $g(\phi_g, \phi_j)$. So coefficients g_{lm} of $e^{-i(l\phi_g + m\phi_j)}$.

$$
\begin{aligned}
g_{00} &= \kappa_{00} + (\kappa_{02} + \kappa_{20})(a_1 a_{-1} + a_{-1} a_1 + a_2 a_{-2} + a_{-2} a_2 + \cdots) && e^0 \\
g_{01} &= \kappa_{01} a_1 e^{i\omega\tau_{01}} + 2\kappa_{02} e^{i\omega\tau_{02}} (a_2 a_{-1} + a_3 a_{-2} + \dots) && e^{-i\phi_j} \\
g_{10} &= \kappa_{10} a_1 e^{i\omega\tau_{10}} + 2\kappa_{20} e^{i\omega\tau_{20}} (a_2 a_{-1} + a_3 a_{-2} + \dots) && e^{-i\phi_g} \\
g_{11} &= \kappa_{11} a_1^2 e^{2i\omega\tau_{11}} && e^{-i\phi_g - i\phi_j} \\
g_{02} &= \kappa_{01} a_2 e^{2i\omega\tau_{01}} + 2\kappa_{02} e^{2i\omega\tau_{02}} (a_1^2/2 + a_3 a_{-1} + a_4 a_{-2} + \dots) && e^{-2i\phi_j} \\
g_{20} &= \kappa_{10} a_2 e^{2i\omega\tau_{10}} + 2\kappa_{20} e^{2i\omega\tau_{20}} (a_1^2/2 + a_3 a_{-1} + a_4 a_{-2} + \dots) && e^{-2i\phi_g}
\end{aligned}
$$

We also find coefficients for $S = 3, 4$ to check that $|g_{12} Z_{-3}|$ etc. are small.

$$
\begin{aligned}
g_{03} &= \kappa_{01} a_3 e^{3i\omega\tau_{01}} + 2\kappa_{02} e^{3i\omega\tau_{02}} (a_4 a_{-1} + a_5 a_{-2} + \dots) && e^{-3i\phi_j} \\
g_{12} &= \kappa_{11} a_1 a_2 e^{3i\omega\tau_{11}} && e^{-i\phi_g - 2i\phi_j} \\
g_{04} &= \kappa_{01} a_4 e^{4i\omega\tau_{01}} + 2\kappa_{02} e^{4i\omega\tau_{02}} (0.5 a_2^2 + a_5 a_{-1} + a_6 a_{-2} + \dots) && e^{-4i\phi_j} \\
g_{13} &= \kappa_{11} a_1 a_3 e^{4i\omega\tau_{11}} && e^{-i\phi_g - 3i\phi_j} \\
g_{22} &= \kappa_{11} a_2^2 e^{4i\omega\tau_{11}} && e^{-2i\phi_g - 2i\phi_j}
\end{aligned}
$$

B.2 Finding Fourier coefficients, harmonic waveform

Assuming identical oscillators, $\omega_g = \omega_j$, and waveform where $a_1 = a_{-1} = 1$ and rest of coefficients zero:

$$
\begin{aligned}
g(\phi_g, \phi_j) = &\kappa_{00} + \kappa_{01} \left(e^{-i(\phi_j - \omega\tau_{01})} + \text{c.c} \right) \\
&+ \kappa_{10} \left(e^{-i(\phi_g - \omega\tau_{10})} + \text{c.c} \right) \\
&+ \kappa_{11} \left(e^{-i(\phi_g - \omega\tau_{11})} + \text{c.c} \right) \cdot \left(e^{-i(\phi_j - \omega\tau_{11})} + \text{c.c} \right) \\
&+ \kappa_{02} \left[e^{-i(\phi_j - \omega\tau_{02})} + \text{c.c} \right]^2 + \kappa_{20} \left[e^{-i(\phi_g - \omega\tau_{20})} + \text{c.c} \right]^2
\end{aligned}
$$

Now finding the coefficients of the 2-dimensional Fourier series of $g(\phi_g, \phi_j)$. So coefficients g_{lm} of $e^{-i(l\phi_g + m\phi_j)}$.

$$\begin{aligned}
g_{00} &= \kappa_{00} + 2(\kappa_{02} + \kappa_{20}), && e^0 \\
g_{01} &= \kappa_{01} e^{i\omega\tau_{01}}, && e^{-i\phi_j} \\
g_{10} &= \kappa_{10} a_1 e^{i\omega\tau_{10}}, && e^{-i\phi_g} \\
g_{11} &= \kappa_{11} e^{2i\omega\tau_{11}}, && e^{-i\phi_g - i\phi_j} \\
g_{02} &= \kappa_{02} e^{2i\omega\tau_{02}}, && e^{-2i\phi_j} \\
g_{20} &= \kappa_{20} e^{2i\omega\tau_{20}}, && e^{-2i\phi_g}
\end{aligned}$$

B.3 Parameters for a strictly harmonic waveform

Try for strictly harmonic waveform: $x(\phi) = e^{-i\phi}$ + c.c., e.g. $a_1 = 1$, $a_{-1} = 1$, $a_l = 0$ for $l \neq 1, -1$.

$$\begin{aligned}
g_{00} &= \kappa_{00} + 2\kappa_{02} + 2\kappa_{20}, & g_{11} &= \kappa_{11} e^{2i\omega\tau_{11}}, \\
g_{01} &= \kappa_{01} e^{i\omega\tau_{01}}, & g_{10} &= \kappa_{10} e^{i\omega\tau_{10}}, \\
g_{02} &= \kappa_{02} e^{2i\omega\tau_{02}}, & g_{20} &= \kappa_{20} e^{2i\omega\tau_{20}}.
\end{aligned}$$

For 2-dimensional Fourier coefficients H_{lm} of target interaction function $H(\phi_g - \phi_j, \phi_g - \phi_k)$, and Fourier coefficients Z_l of PRC $Z(\phi)$, we should satisfy the relations:

$$H_{lm} = Z_{-l-m} h_{lm} \tag{B.5}$$

Considering only $l + m \leq 2$:

$$\begin{aligned}
H_{00} &= Z_0 h_{00} & H_{11} &= Z_{-2} h_{11} \\
H_{01} &= Z_{-1} h_{01} & H_{10} &= Z_{-1} h_{10} \\
H_{02} &= Z_{-2} h_{02} & H_{20} &= Z_{-2} h_{20}
\end{aligned}$$

Inserting h_{lm}

$$H_{00} = Z_0(\kappa_{00} + 2\kappa_{02} + 2\kappa_{20}) \qquad H_{11} = Z_{-2}\kappa_{11}e^{2i\omega\tau_{11}}$$
$$H_{01} = Z_{-1}\kappa_{01}e^{i\omega\tau_{01}} \qquad H_{10} = Z_{-1}\kappa_{10}e^{i\omega\tau_{10}}$$
$$H_{02} = Z_{-2}\kappa_{02}e^{2i\omega\tau_{02}} \qquad H_{20} = Z_{-2}\kappa_{20}e^{2i\omega\tau_{20}}$$

Suppose our target interaction function is

$$H(\phi_g) = \sin(\phi_g) - r\sin(2\phi_g) = \frac{i}{2}e^{-i\phi_g} - \frac{ir}{2}e^{-2i\phi_g} + \text{c.c.} \tag{B.6}$$

Then we obtain:

$$0 = Z_0(\kappa_{00} + 2\kappa_{02} + 2\kappa_{20}) \qquad 0 = Z_{-2}\kappa_{11}e^{2i\omega\tau_{11}}$$
$$0 = Z_{-1}\kappa_{01}e^{i\omega\tau_{01}} \qquad \frac{i}{2} = Z_{-1}\kappa_{10}e^{i\omega\tau_{10}}$$
$$0 = Z_{-2}\kappa_{02}e^{2i\omega\tau_{02}} \qquad -\frac{ir}{2} = Z_{-2}\kappa_{20}e^{2i\omega\tau_{20}}$$

Assuming the Z_l is nonvanishing for $l = 0, -1, -2$, we get $\kappa_{01} = \kappa_{02} = \kappa_{11} = 0$ and $\kappa_{00} = -2\kappa_{20}$. The remaining two equations can be rewritten as:

$$\frac{1}{2}e^{\frac{\pi}{2}i} = |Z_{-1}|\kappa_{10}e^{i\omega\tau_{10}+\arg(Z_{-1})i}$$
$$\frac{r}{2}e^{-\frac{\pi}{2}i} = |Z_{-2}|\kappa_{20}e^{2i\omega\tau_{20}+\arg(Z_{-2})i}$$

So we get that

$$\kappa_{10} = \frac{1}{2|Z_{-1}|}$$
$$\kappa_{20} = \frac{r}{2|Z_{-2}|}$$
$$\tau_{10} = \frac{\pi/2 - \arg(Z_{-1})}{\omega}$$
$$\tau_{20} = \frac{-\pi/2 - \arg(Z_{-2})}{2\omega}.$$

Corrected for minus sign in rewriting of eq22, but otherwise corresponding to [Kori et al., 2008].

When taking instead

$$H(\phi_g) = \sin(\phi_g - \alpha) + r\sin(2(\phi_g - \alpha)) = \frac{i}{2}e^{-i\phi_g + i\alpha} + \frac{ir}{2}e^{-2i\phi_g + 2i\alpha} + \text{c.c.}, \quad \text{(B.7)}$$

the delay parameters become $\tau_{10} = \frac{\pi/2+\alpha-\arg(Z_{-1})}{\omega}$ and $\tau_{20} = \frac{\pi/2+2\alpha-\arg(Z_{-2})}{2\omega}$. The nonzero gain parameters: $\kappa_{10} = \frac{1}{2|Z_{-1}|}$, $\kappa_{20} = \frac{r}{2|Z_{-2}|}$ Plus in front of r taken into account in τ_{20}. Want positive delays τ_{10} and τ_{20}, so do $-\alpha$.

Suppose we instead take a target interaction function $H(\phi_g, \phi_j)$ recall that both ϕ_g and ϕ_j are some phase differences $\phi_g = \theta_g - \theta_k$ and $\phi_j = \theta_j - \theta_k$, where k is the current oscillator. So the interaction function above takes information from two oscillators to one other oscillator. Consider for example:

$$H(\phi_g, \phi_j) = \sin(\phi_g + \phi_j) \quad \text{(B.8)}$$

$$= \frac{i}{2}e^{-i\phi_g - i\phi_j} + \text{c.c.} \quad \text{(B.9)}$$

or in terms of the phases θ_g, θ_j, θ_k of oscillators g, j, k:

$$H(\theta_g - \theta_k, \theta_j - \theta_k) = \sin(\theta_g + \theta_j - 2\theta_k) \quad \text{(B.10)}$$

Again considering the waveform $x(\phi) = e^{-i\phi} + \text{c.c.}$, we get:

$$0 = Z_0(\kappa_{00} + 2\kappa_{02} + 2\kappa_{20}) \qquad \frac{i}{2} = Z_{-2}\kappa_{11}e^{2i\omega\tau_{11}}$$

$$0 = Z_{-1}\kappa_{01}e^{i\omega\tau_{01}} \qquad 0 = Z_{-1}\kappa_{10}e^{i\omega\tau_{10}}$$

$$0 = Z_{-2}\kappa_{02}e^{2i\omega\tau_{02}} \qquad 0 = Z_{-2}\kappa_{20}e^{2i\omega\tau_{20}}$$

Thus $\kappa_{01} = \kappa_{02} = \kappa_{10} = \kappa_{20} = \kappa_{00} = 0$,

$$\kappa_{11} = \frac{1}{2|Z_{-1}|} \qquad \tau_{11} = \frac{\frac{\pi}{2} - \arg(Z_{-2})}{2\omega} \quad \text{(B.11)}$$

If we want to derive the feedback by hand, choosing a harmonic waveform

would be ideal. One example of an oscillator with a harmonic waveform is the Stuart-Landau oscillator [Kuramoto, 1984]. However, this oscillator has the following problem when it comes to applying generalised sync engineering. If we want to control nonpairwise interactions, then we need the phase response curve to have at least one nonzero harmonic of second or higher order. If only the first Fourier coefficient of the phase response curve Z_{-1} is nonzero, then the right hand side of all constraints $g_{\ell m} = Z_{-\ell-m}H_{\ell m}$ for ℓ, m such that $\ell + m > 1$ will be zero, and so we cannot control these terms. This includes all nonpairwise terms as we both $\ell > 0$ and $m > 0$ for any nonpairwise Fourier coefficient of the interaction function. When we derive the phase response curve, and it (or its Fourier series approximation) only has nonzero first order terms, this means that we cannot control any nonpairwise terms. The Stuart-Landau oscillator has a phase response curve $Z^x_{SL}(\theta) = -\sin(\theta) - \beta\cos(\theta)$, where $\beta = -1$ [Nakao, 2016]. Since the phase response curve Z^x_{SL} does not have any terms containing $\sin(2\theta)$, $\cos(2\theta)$, $\sin(3\theta)$, $\cos(3\theta)$ or higher order, we cannot control corresponding harmonics in the target interaction function. Thus we are forced to consider oscillators with higher order harmonics in the phase response curve.

Appendix C

Code instructions

The Matlab code is available at https://github.com/liefting/sync_engineering, we include the text of the README file below.

This repository contains the code accompanying my thesis Designing the Dynamics of Coupled Oscillators at the University of Exeter under supervision of Kyle Wedgwood and Christian Bick. It can be used to design control oscillators using a nonpairwise target interaction function.

Running the `main.m` script will produce a `.txt` file in `/data/` with order parameters calculated after simulations of coupled Brusselators. Running the `load_data_and_plot.m` script loads data from `/data/[name].txt` and produces (bifurcation) plots.

Some of the parameters that can be changed within `main.m`: - `xis` and `chis` (parameters determining the target phase model) (in particular: `xi3=1` for nonpairwise model from thesis, and `xi3=0` for the pairwise model from the thesis) - `Dtaus` (a range of overall delay parameters) - `which_oscillator` (the type of oscillator) - `M` (the number of oscillators) - `startat` (initial configuration of the oscillators, e.g. splay configuration) - `K` ("epsilon", overall coupling strength)

Running the `load_data_and_plot.m` script loads the data produced by `main.m` (`.txt` files containing order parameters for a range of delays Dtaus), and creates plots including the bifurcation plots in the thesis that plot `Dtau` versus `log(1-R_k)`.

Below is a list of the scripts and function it calls/data it loads.

```
main.m
--->    load_isochrones.m
        --->    BrusselatorFourierAverages.dat
                FHNFourierAverages.dat
                find_prc.m
        optimisation.m
        --->    get_h_functions.m
                vector_to_taus_and_ks.m
        simulations.m
        --->    oscillators.m
                    --->    brus.m
                            fitzhughnagumo.m
        find_order_parameter.m
```

other scripts that can be called seperately after running (part of) `main.m`:

```
plot_resulting_feedback.m   (after running optimisation)
load_data_and_plot.m        (after running all of main)
--->    [name].txt file in /data/
        getcolours.m
```

Bibliography

[Abrams and Strogatz, 2004] Abrams, D. M. and Strogatz, S. H. (2004). Chimera States for Coupled Oscillators. *Physical Review Letters*, 93(17):174102.

[Acebrón et al., 2005] Acebrón, J. A., Bonilla, L. L., Vicente, C. J., Ritort, F., and Spigler, R. (2005). The Kuramoto model: A simple paradigm for synchronization phenomena. *Reviews of Modern Physics*, 77(1):137–185.

[Ashwin et al., 2019] Ashwin, P., Bick, C., and Poignard, C. (2019). State-dependent effective interactions in oscillator networks through coupling functions with dead zones. *Philosophical Transactions of the Royal Society A: Mathematical, Physical and Engineering Sciences*, 377(2160):20190042.

[Ashwin et al., 2021] Ashwin, P., Bick, C., and Poignard, C. (2021). Dead zones and phase reduction of coupled oscillators. *Chaos: An Interdisciplinary Journal of Nonlinear Science*, 31(9):093132.

[Ashwin and Burylko, 2015] Ashwin, P. and Burylko, O. (2015). Weak chimeras in minimal networks of coupled phase oscillators. *Chaos*, 25(1):013106.

[Azodi-Avval and Gharabaghi, 2015] Azodi-Avval, R. and Gharabaghi, A. (2015). Phase-dependent modulation as a novel approach for therapeutic brain stimulation. *Frontiers in Computational Neuroscience*, 9(FEB):1–7.

[Bagheri et al., 2007] Bagheri, N., Stelling, J., and Doyle, F. (2007). Circadian phase entrainment *via* nonlinear model predictive control. *International Journal of Robust and Nonlinear Control*, 17(17):1555–1571.

[Battiston et al., 2020] Battiston, F., Cencetti, G., Iacopini, I., Latora, V., Lucas, M., Patania, A., Young, J.-G., and Petri, G. (2020). Networks beyond pairwise interactions: structure and dynamics. *Physics Reports*, 874:1–92. arXiv: 2006.01764.

[Bayani et al., 2022] Bayani, A., Jafari, S., and Azarnoush, H. (2022). Explosive synchronization: From synthetic to real-world networks. *Chinese Physics B*, 31(2):020504.

[Bick, 2018] Bick, C. (2018). Heteroclinic switching between chimeras. *Physical Review E*, 97(5):050201.

[Bick, 2019] Bick, C. (2019). Heteroclinic Dynamics of Localized Frequency Synchrony: Heteroclinic Cycles for Small Populations. *Journal of Nonlinear Science*, 29(6):2547–2570.

[Bick and Ashwin, 2016] Bick, C. and Ashwin, P. (2016). Chaotic weak chimeras and their persistence in coupled populations of phase oscillators. *Nonlinearity*, 29(5):1468–1486.

[Bick et al., 2016] Bick, C., Ashwin, P. P., and Rodrigues, A. (2016). Chaos in generically coupled phase oscillator networks with nonpairwise interactions. *Chaos*, 26:094814.

[Bick et al., 2023a] Bick, C., Böhle, T., and Kuehn, C. (2023a). Higher-Order Interactions in Phase Oscillator Networks through Phase Reductions of Oscillators with Phase Dependent Amplitude.

[Bick et al., 2020] Bick, C., Goodfellow, M., Laing, C. R., and Martens, E. A. (2020). Understanding the dynamics of biological and neural oscillator networks through exact mean-field reductions: a review. *Journal of Mathematical Neuroscience*, 10(1).

[Bick et al., 2023b] Bick, C., Gross, E., Harrington, H. A., and Schaub, M. T. (2023b). What are higher-order networks? *SIAM Review*, 65(3):686–731.

[Bick et al., 2017] Bick, C., Sebek, M., and Kiss, I. Z. (2017). Robust Weak Chimeras in Oscillator Networks with Delayed Linear and Quadratic Interactions. *Physical Review Letters*, 119(16):168301.

[Boyett et al., 2000] Boyett, M. R., Honjo, H., and Kodama, I. (2000). The sinoatrial node, a heterogeneous pacemaker structure. *Cardiovascular Research*, 47(4):658–687.

[Broer and Takens, 2011] Broer, H. and Takens, F. (2011). *Dynamical Systems and Chaos*, volume 172 of *Applied Mathematical Sciences*. Springer.

[Brown et al., 2004] Brown, E., Moehlis, J., and Holmes, P. (2004). On the Phase Reduction and Response Dynamics of Neural Oscillator Populations. *Neural Computation*, 16(4):673–715.

[Cestnik et al., 2022] Cestnik, R., Mau, E. T. K., and Rosenblum, M. (2022). Inferring oscillator's phase and amplitude response from a scalar signal exploiting test stimulation. *New Journal of Physics*, 24(12):123012.

[Cestnik and Rosenblum, 2018] Cestnik, R. and Rosenblum, M. (2018). Inferring the phase response curve from observation of a continuously perturbed oscillator. *Scientific Reports*, 8(1):1–10.

[Daido, 1993] Daido, H. (1993). A solvable model of coupled limit-cycle oscillators exhibiting partial perfect synchrony and novel frequency spectra. *Physica D: Nonlinear Phenomena*, 69(3-4):394–403.

[Efimov et al., 2009] Efimov, D., Sacré, P., and Sepulchre, R. (2009). Controlling the phase of an oscillator: A phase response curve approach. *Proceedings of the IEEE Conference on Decision and Control*, pages 7692–7697.

[Engelborghs et al., 2000] Engelborghs, K., Luzyanina, T., and Roose, D. (2000). Numerical bifurcation analysis of delay differential equations. *Journal of Computational and Applied Mathematics*, 125(1-2):265–275.

[Epstein, 2014] Epstein, I. R. (2014). Coupled chemical oscillators and emergent system properties. *Chemical Communications*, 50(74):10758–10767.

[Ermentrout, 2007] Ermentrout, B. (2007). XPPAUT. *Scholarpedia*, 2(1):1399.

[Gad, 2022] Gad, A. G. (2022). Particle Swarm Optimization Algorithm and Its Applications: A Systematic Review. *Archives of Computational Methods in Engineering*, 29(5):2531–2561.

[Galán et al., 2010] Galán, R., Ermentrout, B., and Urban, N. (2010). Efficient Estimation of Phase-Resetting Curves in Real Neurons and its Significance for Neural-Network Modeling Roberto. *Physical Review Letters*, 5(3):379–390.

[Gambuzza et al., 2019] Gambuzza, L. V., Frasca, M., and Latora, V. (2019). Distributed Control of Synchronization of a Group of Network Nodes. *IEEE Transactions on Automatic Control*, 64(1):365–372.

[Gao and Wang, 2017] Gao, H. and Wang, Y. (2017). On phase response function based decentralized phase desynchronization. *IEEE Transactions on Signal Processing*, 65(21):5564–5577.

[Gendreau and Potvin, 2019] Gendreau, M. and Potvin, J.-Y., editors (2019). *Handbook of Metaheuristics*, volume 272 of *International Series in Operations Research & Management Science*. Springer International Publishing.

[Gengel et al., 2021] Gengel, E., Teichmann, E., Rosenblum, M., and Pikovsky, A. (2021). High-order phase reduction for coupled oscillators. *Journal of Physics: Complexity*, 2(1):015005.

[Gill et al., 1997] Gill, P. E., Murray, W., and Wright, M. H. (1997). *Practical Optimization*. Academic Press.

[Guckenheimer and Holmes, 1983] Guckenheimer, J. and Holmes, P. (1983). *Nonlinear Oscillations, Dynamical Systems, and Bifurcations of Vector Fields*, volume 42 of *Applied Mathematical Sciences*. Springer Science+Business Media, LLC.

[Hirsch et al., 2013] Hirsch, M. W., Smale, S., and Devaney, R. L. (2013). *Differential Equations, Dynamical Systems, and an Introduction to Chaos*. Elsevier.

[Holmes and Shea-Brown, 2006] Holmes, P. and Shea-Brown, E. (2006). Stability. *Scholarpedia*, 1(10):1838.

[Holt et al., 2016] Holt, A. B., Wilson, D., Shinn, M., Moehlis, J., and Netoff, T. I. (2016). Phasic Burst Stimulation: A Closed-Loop Approach to Tuning Deep Brain Stimulation Parameters for Parkinson's Disease. *PLoS Computational Biology*, 12(7):1–14.

[Izhikevich, 1998] Izhikevich, E. M. (1998). Phase models with explicit time delays. *Physical Review E*, 58(1):905–908.

[Izhikevich, 2005] Izhikevich, E. M. (2005). *Dynamical Systems in Neuroscience: The Geometry of Excitability and Bursting*. The MIT Press.

[Izhikevich and Kuramoto, 2006] Izhikevich, E. M. and Kuramoto, Y. (2006). Weakly Coupled Oscillators. In *Encyclopedia of Mathematical Physics*, pages 448–453. Academic Press, Oxford.

[Kiss, 2018] Kiss, I. Z. (2018). Synchronization engineering. *Current Opinion in Chemical Engineering*, 21:1–9.

[Kiss et al., 2007a] Kiss, I. Z., Rusin, C. G., Kori, H., and Hudson, J. L. (2007a). Engineering complex dynamical structures: Sequential patterns and desynchronization. *Science*, 316(5833):1886–1889.

[Kiss et al., 2007b] Kiss, I. Z., Rusin, C. G., Kori, H., and Hudson, J. L. (2007b). Engineering Complex Dynamical Structures: Sequential Patterns and Desynchronization. *Science*.

[Kori and Kuramoto, 2001] Kori, H. and Kuramoto, Y. (2001). Slow switching in globally coupled oscillators: Robustness and occurrence through delayed coupling. *Physical Review E - Statistical Physics, Plasmas, Fluids, and Related Interdisciplinary Topics*.

[Kori et al., 2008] Kori, H., Rusin, C. G., Kiss, I. Z., and Hudson, J. L. (2008). Synchronization engineering: Theoretical framework and application to dynamical clustering. *Chaos*, 18(2):1–13.

[Kuramoto, 1984] Kuramoto, Y. (1984). Chemical Oscillations, Waves and Turbulence.

[Lanford and Mintchev, 2015] Lanford, O. E. and Mintchev, S. M. (2015). Stability of a family of travelling wave solutions in a feedforward chain of phase oscillators. *Nonlinearity*, 28(1):237–261.

[Letson and E. Rubin, 2020] Letson, B. and E. Rubin, J. (2020). Local orthogonal rectification: Deriving natural coordinates to study flows relative to manifolds. *Discrete & Continuous Dynamical Systems - B*, 25(9):3725–3747.

[Letson and Rubin, 2018] Letson, B. and Rubin, J. E. (2018). A New Frame for an Old (Phase) Portrait: Finding Rivers and Other Flow Features in the Plane. *SIAM Journal on Applied Dynamical Systems*, 17(4):2414–2445.

[Letson and Rubin, 2020] Letson, B. and Rubin, J. E. (2020). LOR for Analysis of Periodic Dynamics: A One-Stop Shop Approach. *SIAM Journal on Applied Dynamical Systems*, 19(1):58–84. _eprint: https://doi.org/10.1137/19M1258529.

[Li et al., 2013] Li, J. S., Dasanayake, I., and Ruths, J. (2013). Control and synchronization of neuron ensembles. *IEEE Transactions on Automatic Control*, 58(8):1919–1930.

[Martens et al., 2016] Martens, E. A., Bick, C., and Panaggio, M. J. (2016). Chimera states in two populations with heterogeneous phase-lag. *Chaos*, 26(9):094819.

[Mihaliuk et al., 2002] Mihaliuk, E., Sakurai, T., Chirila, F., and Showalter, K. (2002). Experimental and theoretical studies of feedback stabilization of propagating wave segments. *Faraday Discussions*, 120(1):383–394.

[Mikhailov and Showalter, 2006] Mikhailov, A. S. and Showalter, K. (2006). Control of waves, patterns and turbulence in chemical systems. *Physics Reports*, 425(2-3):79–194.

[Moehlis et al., 2006] Moehlis, J., Josic, K., and Shea-Brown, E. T. (2006). Periodic orbit. *Scholarpedia*, 1(7):1358.

[Monga et al., 2019] Monga, B., Wilson, D., Matchen, T., and Moehlis, J. (2019). Phase reduction and phase-based optimal control for biological systems: a tutorial. *Biological Cybernetics*, 113(1-2):11–46.

[Mori and Kori, 2022] Mori, F. and Kori, H. (2022). Noninvasive inference methods for interaction and noise intensities of coupled oscillators using only spike time data. *Proceedings of the National Academy of Sciences*, 119(6):e2113620119.

[Nabi et al., 2013] Nabi, A., Stigen, T., Moehlis, J., and Netoff, T. (2013). Erratum: Minimum energy control for in vitro neurons. *Journal of Neural Engineering*, 10(4):036005.

[Nagumo et al., 1962] Nagumo, J., Arimoto, S., and Yoshizawa, S. (1962). An Active Pulse Transmission Line Simulating Nerve Axon. *Proceedings of the IRE*, 50(10):2061–2070.

[Nakao, 2016] Nakao, H. (2016). Phase reduction approach to synchronisation of nonlinear oscillators. *Contemporary Physics*, 57(2):188–214.

[Newman et al., 2001] Newman, M. E., Strogatz, S. H., and Watts, D. J. (2001). Random graphs with arbitrary degree distributions and their applications. *Physical Review E - Statistical Physics, Plasmas, Fluids, and Related Interdisciplinary Topics*, 64(2):17.

[Okuda, 1993] Okuda, K. (1993). Variety and generality of clustering in globally coupled oscillators. *Physica D: Nonlinear Phenomena*, 63(3-4):424–436.

[Ota et al., 2009] Ota, K., Nomura, M., and Aoyagi, T. (2009). Weighted Spike-Triggered Average of a Fluctuating Stimulus Yielding the Phase Response Curve. *Physical Review Letters*, 103(2):024101.

[Pietras and Daffertshofer, 2019] Pietras, B. and Daffertshofer, A. (2019). Network dynamics of coupled oscillators and phase reduction techniques. *Physics Reports*, 819:1–105.

[Pikovsky, 2015] Pikovsky, A. (2015). Comment on "Asymptotic Phase for Stochastic Oscillators". *Physical Review Letters*, 115(6):069401.

[Pikovsky et al., 2001] Pikovsky, A., Rosenblum, M., and Kurths, J. (2001). *Synchronization: A Universal Concept in Nonlinear Sciences*. Number 12 in Cambridge Nonlinear Science Series. Cambridge University Press.

[Porter, 2020] Porter, M. A. (2020). Nonlinearity + Networks: A 2020 Vision. In *Emerging Frontiers in Nonlinear Science*, volume 32 of *Nonlinear Systems and Complexity*, pages 131–159. Springer.

[Proskurnikov and Cao, 2017] Proskurnikov, A. V. and Cao, M. (2017). Synchronization of Pulse-Coupled Oscillators and Clocks under Minimal Connectivity Assumptions. *IEEE Transactions on Automatic Control*, 62(11):5873–5879.

[Pérez-Cervera et al., 2023] Pérez-Cervera, A., Gutkin, B., Thomas, P. J., and Lindner, B. (2023). A universal description of stochastic oscillators. *Proceedings of the National Academy of Sciences*, 120(29):e2303222120.

[Rodrigues et al., 2016] Rodrigues, F. A., Peron, T. K. D., Ji, P., and Kurths, J. (2016). The Kuramoto model in complex networks. *Physics Reports*, 610:1–98.

[Rohden et al., 2012] Rohden, M., Sorge, A., Timme, M., and Witthaut, D. (2012). Self-Organized Synchronization in Decentralized Power Grids. *Physical Review Letters*, 109(6):064101.

[Rusin et al., 2016] Rusin, C. G., Johnson, S. E., Kapur, J., and Hudson, J. L. (2016). Engineering the synchronization of neuron action potentials using global time-delayed feedback stimulation. *Phys Rev E Stat Nonlin Soft Matter Phys.*, 118(24):6072–6078.

[Rusin et al., 2009] Rusin, C. G., Kiss, I. Z., Kori, H., and Hudson, J. L. (2009). Framework for engineering the collective behavior of complex rhythmic systems. *Industrial and Engineering Chemistry Research*, 48(21):9416–9422.

[Rusin et al., 2010] Rusin, C. G., Kori, H., Kiss, I. Z., and Hudson, J. L. (2010). Synchronization engineering: Tuning the phase relationship between dissimilar oscillators using nonlinear feedback. *Philosophical Transactions: Mathematical, Physical and Engineering Sciences*, 368(1918):2189–2204.

[Rusin et al., 2011] Rusin, C. G., Tokuda, I., Kiss, I. Z., and Hudson, J. L. (2011). Engineering of synchronization and clustering of a population of chaotic chemical oscillators. *Angewandte Chemie - International Edition*, 50(43):10212–10215. ISBN: 4349822658.

[Sakurai et al., 2002] Sakurai, T., Mihaliuk, E., Chirila, F., and Showalter, K. (2002). Design and Control of Wave Propagation Patterns in Excitable Media. *Science*, 296:2009–2013.

[Sanders et al., 2007] Sanders, J., Verhulst, F., and Murdock, J. (2007). *Averaging methods in nonlinear dynamical systems*, volume 59. Springer. Publication Title: Applied Mathematical Sciences (Switzerland) ISSN: 2196968X.

[Schiff, 2010] Schiff, S. J. (2010). Towards model-based control of parkinson's disease. *Philosophical Transactions of the Royal Society A: Mathematical, Physical and Engineering Sciences*, 368(1918):2269–2308.

[Schuepbach et al., 2013] Schuepbach, W., Rau, J., Knudsen, K., Volkmann, J., Krack, P., Timmermann, L., Hälbig, T., Hesekamp, H., Navarro, S., Meier, N., Falk, D., Mehdorn, M., Paschen, S., Maarouf, M., Barbe, M., Fink, G., Kupsch,

A., Gruber, D., Schneider, G.-H., Seigneuret, E., Kistner, A., Chaynes, P., Ory-Magne, F., Brefel Courbon, C., Vesper, J., Schnitzler, A., Wojtecki, L., Houeto, J.-L., Bataille, B., Maltête, D., Damier, P., Raoul, S., Sixel-Doering, F., Hellwig, D., Gharabaghi, A., Krüger, R., Pinsker, M., Amtage, F., Régis, J.-M., Witjas, T., Thobois, S., Mertens, P., Kloss, M., Hartmann, A., Oertel, W., Post, B., Speelman, H., Agid, Y., Schade-Brittinger, C., and Deuschl, G. (2013). Neurostimulation for Parkinson's Disease with Early Motor Complications. *New England Journal of Medicine*, 368(7):610–622.

[Schwabedal and Pikovsky, 2010] Schwabedal, J. and Pikovsky, A. (2010). Effective phase description of noise-perturbed and noise-induced oscillations. *The European Physical Journal Special Topics*, 187(1):63–76.

[Smeal et al., 2010] Smeal, R. M., Ermentrout, G. B., and White, J. A. (2010). Phase-response curves and synchronized neural networks. *Philosophical Transactions of the Royal Society B: Biological Sciences*, 365(1551):2407–2422.

[Strogatz, 2003] Strogatz, S. (2003). *Sync - How order emerges from chaos in the universe, nature, and daily life*. Hyperion New York.

[Strogatz, 1994] Strogatz, S. H. (1994). *Nonlinear dynamics and chaos: with applications to physics, biology, chemistry, engineering*. Perseus Books. ISSN: 0009-4978.

[Strogatz, 2000] Strogatz, S. H. (2000). From Kuramoto to Crawford: exploring the onset of synchronization in populations of coupled oscillators. *Physica D: Nonlinear Phenomena*, 143(1-4):1–20.

[Thomas and Lindner, 2014] Thomas, P. J. and Lindner, B. (2014). Asymptotic Phase for Stochastic Oscillators. *Physical Review Letters*, 113(25):254101.

[Torres et al., 2021] Torres, L., Blevins, A. S., Bassett, D. S., and Eliassi-Rad, T. (2021). The why, how, and when of representations for complex systems. *SIAM Review*, 63(3):435–485.

[von der Gracht et al., 2023] von der Gracht, S., Nijholt, E., and Rink, B. (2023). A parametrisation method for high-order phase reduction in coupled oscillator networks. arXiv:2360:03320v1 [math.DS].

[Wang and Doyle, 2012] Wang, Y. and Doyle, F. J. (2012). Optimal phase response functions for fast pulse-coupled synchronization in wireless sensor networks. *IEEE Transactions on Signal Processing*, 60(10):5583–5588.

[Wang et al., 2013] Wang, Y., Nunez, F., and Doyle, F. J. (2013). Increasing sync rate of pulse-coupled oscillators via phase response function design: Theory and application to wireless networks. *IEEE Transactions on Control Systems Technology*, 21(4):1455–1462.

[Wedgwood et al., 2013] Wedgwood, K. C., Lin, K. K., Thul, R., and Coombes, S. (2013). Phase-Amplitude Descriptions of Neural Oscillator Models. *The Journal of Mathematical Neuroscience*, 3(1):2.

[Whitley, 1994] Whitley, D. (1994). A genetic algorithm tutorial. *Statistics and Computing*, 4:65–85.

[Wiedemann and Lüthi, 2003] Wiedemann, U. A. and Lüthi, A. (2003). Timing of Network Synchronization By Refractory Mechanisms. *Journal of Neurophysiology*, 90(6):3902–3911.

[Wiesenfeld and Moss, 1995] Wiesenfeld, K. and Moss, F. (1995). Stochastic resonance and the benefits of noise: From ice ages to crayfish and SQUIDs. *Nature*, 373(6509):33–36.

[Wilson, 2022] Wilson, D. (2022). An Adaptive Phase-Amplitude Reduction Framework without \mathcalO(\epsilon)\ Constraints on Inputs. *SIAM Journal on Applied Dynamical Systems*, 21(1):204–230. _eprint: https://doi.org/10.1137/21M1391791.

[Wilson and Moehlis, 2016] Wilson, D. and Moehlis, J. (2016). Isostable reduction of periodic orbits. *Physical Review E*, 94(5):052213.

[Winfree, 2002] Winfree, A. T. (2002). *The Geometry of Biological Time*. Springer.